UC Berkeley
UC Berkeley Electronic Theses and Dissertations

Title
Metabolic Regulation by Lipid Activated Receptors

Permalink
https://escholarship.org/uc/item/2h35n6fm

Author
Ruby, Maxwell A.

Publication Date
2010

Peer reviewed|Thesis/dissertation

eScholarship.org Powered by the California Digital Library
University of California

Metabolic Regulation by Lipid Activated Receptors

By

Maxwell A Ruby

A dissertation submitted in partial satisfaction of the
requirements for the degree of

Doctor of Philosophy

In

Molecular & Biochemical Nutrition

In the

Graduate Division

Of the University of California, Berkeley

Committee in charge:

Professor Marc K. Hellerstein, Chair
Professor Ronald M. Krauss
Professor George A. Brooks
Professor Andreas Stahl

Fall 2010

Abstract

Metabolic Regulation by Lipid Activated Receptors

By

Maxwell Alexander Ruby

Doctor of Philosophy in Molecular & Biochemical Nutrition

University of California, Berkeley

Professor Marc K. Hellerstein, Chair

Obesity and related metabolic disorders have reached epidemic levels with dire public health consequences. Efforts to stem the tide focus on behavioral and pharmacological interventions. Several hypolipidemic pharmaceutical agents target endogenous lipid receptors, including the peroxisomal proliferator activated receptor α (PPAR α) and cannabinoid receptor 1 (CB1). To further the understanding of these clinically relevant receptors, we elucidated the biochemical basis of PPAR α activation by lipoprotein lipolysis products and the metabolic and transcriptional responses to elevated endocannabinoid signaling.

PPAR α is activated by fatty acids and their derivatives *in vitro*. While several specific pathways have been implicated in the generation of PPAR α ligands, we focused on lipoprotein lipase mediated lipolysis of triglyceride rich lipoproteins. Fatty acids activated PPAR α similarly to VLDL lipolytic products. Unbound fatty acid concentration determined the extent of PPAR α activation. Lipolysis of VLDL, but not physiological unbound fatty acid concentrations, created the fatty acid uptake necessary to stimulate PPAR α. Consistent with a role for vascular lipases in the activation of PPAR α, administration of a lipase inhibitor (p-407) prevented PPAR α dependent induction of target genes in fasted mice. Apolipoprotein CIII, an endogenous inhibitor of lipoprotein lipase, regulated access to the lipoprotein pool of PPAR α ligands. Our results support a role for the local generation of PPAR α ligands by lipase activity.

The endocannabinoid system regulates diverse physiological functions, including energy balance. While loss of CB1 signaling has more pronounced effects on lipid parameters than expected based on weight loss alone, direct demonstration of endocannabinoid regulation of lipid metabolism is lacking. To test the effects of endogenously produced cannabinoids on lipid metabolism, independent of alterations in food intake, we analyzed tissues from mice treated with IDFP, an organophosphorus inhibitor of endocannabinoid breakdown. IDFP administration inhibited hepatic monoacylglycerol lipase leading to elevated levels of 2-arachidonylglycerol. We found that IDFP administration caused accumulation of apoE depleted VLDL. HDL particles accumulated apoE and failed to transfer it to VLDL *in vitro*. Importantly, these effects were prevented by pharmacological inhibition of CB1 and absent in plasma from CB1 mice. IDFP also caused a CB1-dependent increase in hepatic triglycerides. Thus, endocannabinoids inhibit the transfer of apoE from HDL to VLDL leading to apoE depletion of triglyceride rich lipoproteins.

Microarray analysis allowed us to determine the effects of IDFP on expression of genes involved in lipid metabolism and to discover novel cannabinoid responsive genes. IDFP increased expression of lipogenic and SREBP2 target genes in a CB1-dependent fashion. On a global scale, pre-administration of a CB1 antagonist prevented many of the IDFP induced alterations in gene expression. IDFP decreased expression of genes involved in amino acid metabolism and inflammation. PCR analysis of selected mRNAs confirmed several of the key array findings. Our work indicates that endocannabinoids exert a large influence on hepatic lipid metabolism independent of food intake and suggest that peripherally restricted CB1 antagonists

may be of therapeutic value.

Overall, these findings shed light on the endogenous mechanisms of PPAR α activation and the hepatic responses to Cb1 activation. This information may help guide the continuing effort to develop treatments for metabolic disease.

Acknowledgments

First and foremost, I'd like to thank my graduate advisor Dr. Ronald Krauss. His constant support and patience has allowed me to grow as a scientist and as a person. Discussing science with Dr. Krauss reminds me of my reasons for coming to graduate school. His contiguous enthusiasm for science fueled all of the research I've done and will do.

The collection of amazing individuals that make up the Krauss lab are a reflection of Dr. Krauss himself. Every member of the Krauss lab has been incredibly supportive and kind throughout these five years. I'd especially like to acknowledge Dr. Sally Chiu, Myra Gloria, Casey Geany and Katie Wojnoonski for their constant friendship. A special thanks to my office-mate, Dr. Lara Mangravite. You were a professional and personal compass when I was lost. Thanks to the entire lab!

I feel very fortunate to have worked with many amazing collaborators during my time at Berkeley. Thanks to Dr. Daniel Nomura. Carolyn Hudak, Roger Issa, and Dr. John Casida for making "work" such a pleasant experience. Daniel you were a true mentor in the daily life of a scientist. Thanks to Dr. Jorge Plutzky for hosting me in Boston and allowing me to learn several novel techniques. Thanks to Dr. Thomas Johnston for all the conversations, scientific and otherwise.

I also owe a debt of gratitude to my friends and family who have helped me navigate the occasionally rocky emotional terrain of graduate school. You guys are my heart and everything I do is yours.

TABLE OF CONTENTS

CHAPTER 1
Review of the Literature

Introduction

One of life's most amazing feats is the maintenance of homeostasis in the face of constant flux. Consider that over the past year I have consumed over a million calories, and yet my body weight has shifted less than a pound, representing only a few thousand calories. However, it would be a mistake to assume my body has remained the same. The body is in constant flux, with perpetual turnover of nutrients and cells. For example, while my body fat mass may have remained constant, its composition has undoubtedly shifted to reflect the increase in dairy-derived saturated fatty acid induced by the introduction of a gourmet ice cream parlor in my neighborhood. Homeostatic mechanisms disguise the reality of flux so seamlessly that mass spectrometry is necessary to uncover it.

What constitutes an acceptable error rate in biological homeostasis can best be judged by function. Many humans are experiencing a breakdown in their ability to maintain metabolic homeostasis that has serious functional consequences. Children today are not expected to outlive their parents for the first time in two centuries(1). This is largely attributed to increased prevalence of obesity and its associated diseases, which include two of the three leading causes of death, type II diabetes and heart disease.

Has the marvelous machinery of our body been fundamentally modified in the past few decades? Probably not, even if epigenetic effects are considered. More likely the current environment, characterized by excess consumption of calories and lack of physical activity, overwhelms the regulatory mechanisms that are in place. Although chronic caloric excess likely did not exert large evolutionary pressure, the organism still displays remarkable ability to adapt to this environmental condition. For example, energy expenditure will increase in response to overfeeding. Similarly, pancreatic β-cell mass will increase in response to insulin resistance. The current epidemic of metabolic diseases, in spite of these adaptations, is testimony to the extreme conditions under which we have placed our bodies. Efforts to combat metabolic disease focus on altering these conditions and exploring the homeostatic mechanisms that they are assaulting. Driven by curiosity, I have chosen the latter for the past half decade.

Aberrant lipid accumulation plays a crucial role in the pathogenesis of metabolic disease. For example, retention of lipoproteins in the sub-endothelial space is necessary for the development of atherosclerotic lesions. This knowledge, combined with a firm understanding of the homeostatic mechanisms governing cholesterol metabolism, improved prevention of cardiovascular disease by the advent of statins. High plasma concentrations of fatty acids and triglycerides are associated with insulin resistance and atherosclerosis, respectively. While many overlapping regulatory circuits govern fatty acid metabolism, several that respond to fatty acids, and related lipids, have successfully been pharmacologically targeted. Better understanding of metabolic regulation by these fatty acid sensors may further improve therapeutics in the treatment of cardiovascular disease and diabetes.

This dissertation focuses on the upstream generation of lipid signals and the downstream responses of several regulatory circuits in lipid metabolism at the level of molecular biology and biochemistry. In 1990, two novel lipid sensors, PPAR α and CB1, were cloned. My work focuses on the generation of PPAR α ligands and determination of downstream responses to CB1 activation. The review of literature will briefly outline the discovery, background, and pharmacologic application of each receptor to prepare the

reader for what follows.

PEROXISOMAL PROLIFERATOR ACTIVATED RECEPTOR α

Background & Discovery

In 1990, Issemann and Green reported the cloning of a novel member of the steroid receptor super family(2). As the newest member was responsive to peroxisome proliferators, a diverse set of compounds including herbicides, hypolipidemic drugs, and plasticizers that cause peroxisomal proliferation in the liver, it was termed the peroxisomal proliferator activated receptor (PPAR). The Xenopus ortholouge of PPAR α and two related genes (PPAR γ and PPAR β) were identified shortly thereafter(3). PPAR δ was identified in humans, but was determined to be highly homologous to PPAR β in Xenopus(4). Among researchers working in mammalian systems PPAR β/δ is commonly referred to simply as PPAR δ.

Today, upwards of 48 nuclear hormone receptors have been identified in the human genome and can be classified by type of ligand or sub-cellular localization and binding partners(5). PPARs belong to the adopted orphan receptor family and share similar functional domain structure with other nuclear hormone receptors. Foreshadowing the difficulty of identifying the endogenous ligand or ligands for PPAR, the ligand-binding domain was found to be unusually large (1300 cubic A)(6, 7). Like most class II nuclear hormone receptors, PPAR functions as a heterodimer with RXR and resides almost exclusively in the nucleus bound to its inverted repeat response element in DNA. PPARs possess ligand dependent trans-activating and repressive functions, depending on the recruitment of co-activators or repressors. Additionally, the mere presence of PPARs bound to DNA in the absence of ligand can influence the expression of target genes. With the novel receptors identified, work began to better understand their biological role. The identification of fibrates, a class of hypolipidemic agents, as PPAR α ligands helped to direct research efforts.

Pharmacology

Fibrates have been used as hypolipidemic agents for several decades before the discovery of PPAR α, and remain one of the frontline treatments for hypertriglyceridemia. In a fortunate example of species-specific differences in PPAR α function, fibrates do not promote peroxisomal or hepatocyte proliferation, and subsequent liver tumors, in humans(8). In several clinical trials, fibrates have been shown to significantly lower circulating triglyceride levels and have modest beneficial effects on HDL levels. Importantly, gemfibrozil, bezafibrate, and fenofibrate have all been shown to decrease the progression of atherosclerosis(9-11). The effect of fibrates on overall cardiovascular morbidity and mortality has been more difficult to demonstrate(12-14). Of interest, the cardiovascular risk reduction provided by fibrate treatment appears to be greatest in pre-diabetics or diabetics with dyslipidemia(15-17). However, in the recent ACCORD trial addition of fibrates to statin monotherapy did not provide any protective effects in diabetics (18). The benefits of fibrates may extend beyond lipid lowering, as fenofibrate has been shown to improve endothelial dysfunction in diabetics(19). Fibrates are relatively weak PPAR α ligands and stronger, next generation PPAR α ligands are a major focus of pharmacological research. The hypolipidemic effects of fibrates focused attention on the interaction between PPAR α and lipid metabolism.

Downstream Effects

PPAR α is highly expressed in tissues engaged in fatty acid metabolism, such as the liver, heart, and kidney. In the liver, PPAR α controls the expression of many the enzymes involved in β-oxidation (CPT1a, acyl-coa synthetase, very long and medium chain acyl CoA dehydrogenase, 3-ketoacyl-CoA thiolase), peroxisomal breakdown of long-chain fatty acids (acyl-CoA oxidase, thiolase), and ketone body synthesis (mitochondrial HMGCoA synthase)(20, 21). Likewise PPAR α simulates expression of fatty acid transport protein and the putative fatty acid transporter, CD36(22). PPAR α promotion of fatty acid uptake and oxidation may contribute to the hypolipidemic of fibrates. Indeed, fibrate treatment decreases triglyceride secretion by cultured hepatocytes. PPAR α also increases expression of lipoprotein lipase and decreases expression of its endogenous inhibitor apo CIII (23, 24).

A similar role for PPAR α has been elucidated in the heart. PPAR α agonist treatment stimulates fatty acid oxidation in cardiomyocytes(25). Overexpression of PPAR α leads to upregulation of genes involved in fatty acid oxidation, and decreases expression of those involved in glucose metabolism, leading to cardiac hypertrophy and dysfunction(26). Conversely, PPAR α deficiency decreases expression of mitochondrial β-oxidation genes, forcing the heart to rely primary on glucose for fuel(27).

PPAR α is also expressed in cells of the vessel wall and plays an important role in inflammatory and atherosclerotic pathways. In endothelial cells PPAR α limits monocyte recruitment by decreasing expression of adhesion molecules and regulates enzymes involved in redox responses and nitric oxide signaling (28-30). Some of these effects may be secondary to PPAR α induced expression of iKB, which limits Nf-KB signaling(31, 32). PPAR α activation in macrophages promotes cholesterol efflux, while limiting inflammation and thrombogenicity(33-38). PPAR α stimulation is anti-inflammatory and prevents proliferation and migration of smooth muscle cells(39-42). These pleitropic effects in the vessel wall may contribute to the cardioprotective effects of fibrates.

Surprisingly, initial studies on PPAR α knockout mice failed to produce a striking phenotype, showing only that fibrates failed to promote peroxisomal proliferation(43). As is often the case, environmental manipulation was necessary to reveal profound effects of the genetic alteration. In 1997, David Kelly's and Bart Stael's groups reported that PPAR α knockout mice responded poorly to fasting (44, 45). Knockout mice quickly became hypoglycemic, accumulated fat in the liver, and failed to generate ketone bodies as well as expression of several fasting-inducible genes involved in fatty acid oxidation(44, 45). Thus, PPAR α functions as a necessary starvation signal that regulates fatty acid utilization.

Regulation

The influential role of PPAR α begs the question as to its regulation. As is true of most important signaling pathways, multiple inputs control PPAR α activity. Protein levels of PPAR α are regulated by its expression, translation, and stability. Expression of PPAR α is controlled in a circadian fashion by glucocorticoids and Bmal1(46-49). Other hormonal signals such as leptin, insulin, and growth hormone can also alter expression of PPAR α(47, 50, 51). PPAR α regulates its own expression, which may contribute to increased PPAR α expression observed during fasting(44, 45, 52). Alternative splicing of PPAR α in humans leads to a truncated dominant negative isoform(53). Synthetic PPAR α ligands extend the half-life of PPAR α protein by preventing ubiquitination(54). PPAR

α can also be phosphorylated by PKC, an event which enhances its trans-repressive activity(55). As PPAR α functions as a heterodimer with RXR and requires the presence of co-activators and repressors, the levels of these binding partners may also influence its activity. While all these layers of control influence PPAR α function, the ligation of PPAR α is of paramount importance.

Unlike classical type 1 nuclear hormone receptors, a single nanomolar affinity ligand may not exist for PPAR α and other orphan hormone receptors. The observation that dietary polyunsaturated fatty acids possess hypolipidemic effects similar to fibrates raised the possibility that they may be PPAR α activators(56). This held particular appeal as a regulatory feedback loop whereby PPAR α regulates fatty acid levels and vice versa. Indeed, fatty acids, especially unsaturated fatty acids, were shown to stimulate the transcriptional activity of PPAR α (57, 58). While compelling, these studies relied upon trans-activation assays that do not directly demonstrate ligation of PPAR α, leading to the suggestion that fatty acids may influence PPAR α activity indirectly(59). Attempts to demonstrate ligation were limited by the unavailability of specific radiolabeled ligands. Similarly, attempts to use an electrophoretic mobility shift assay to demonstrate ligand-induced binding to DNA were fruitless, as at high levels the nuclear hormone receptors form heterodimers and bind DNA in the absence of ligand.

In 1997, two groups simultaneously overcame these technical difficulties to demonstrate that a variety of fatty acids and FA metabolites bind to PPAR α. Steven Kliewer developed a novel radio labeled fibrate, GW2331, which was a high affinity ligand for PPAR α and γ, suitable for use in classical competition binding assays(60). Micromolar concentrations of fatty acids were able to displace GW2331 in a cell-free system, demonstrating that FAs are bona fide PPAR ligands. Ronald Evans' group successfully titrated the levels of PPAR α and RXR until ligation of PPAR α became necessary to promote RXR binding and subsequent DNA binding(61). Similar to the findings from the competition assays, fatty acids were able to induce heterodimer formation and promote DNA binding. These reports were further validated by the development of a co-activator dependent receptor ligand assay. Walter Wahli and colleagues demonstrated that fatty acids and derivatives stimulated co-activator binding to the ligand-binding domain of PPAR(62). While both saturated and unsaturated fatty acids stimulate PPAR α in trans activation assays, ligand-binding assays showed a preference for unsaturated fatty acids, with limited binding of saturated fatty acids. A potential explanation for this discrepancy was offered by the finding that fatty acyl CoAs, regardless of degree of saturation, can bind to and induce conformational changes in PPAR α(63). Thus, it is possible that in cell based trans-activation assays saturated fatty acids, which themselves do not bind PPAR α, are converted to downstream metabolites, such as saturated fatty acyl CoAs, that bind PPAR α.

Together the *in vitro* studies have led to the view of PPARs as general lipid sensors; despite this, the upstream factors determining generation and delivery of the lipid ligands under physiological condition remains unclear. Several groups have taken a "pathway" approach to identify important means of generating endogenous PPAR ligands. Intracellular fatty acids can be generated by de novo lipogenesis, enzymatic hydrolysis, or uptake from exogenous sources. Each of these pathways has been implicated in the generation of PPAR α ligand generation.

The "New Fat" Hypothesis

Recent data from Clay Semenkovich's group suggest that products of the de novo lipogenesis pathway are physiologically relevant endogenous PPAR α ligands. This hypothesis has its origin in the generation of a mouse with hepatocyte specific deficiency of fatty acid synthase (FASKOL)(64). The FASKOL mouse has reduced insulin, and hepatic and plasma cholesterol levels but is otherwise similar to wild-type littermates when fed a chow diet. However on a zero-fat diet the FASKOL mice developed hypoglycemia, severe hepatic steatosis, and depleted glycogen stores, phenotypes characteristic of PPAR α deficiency. Similarly, FASKOL mice had normal expression of a cassette of PPAR α target genes (ACOX, HS-2, L-FABP, TRB3) on a chow diet, but greatly reduced expression compared to WT mice on a zero-fat diet. Importantly, these physiological and molecular phenotypes were reversed by administration of either synthetic (WY13643), or natural, (dietary fat) PPAR α ligands. Prolonged fasting of FASKOL mice recapitulated the phenotype observed on a zero-fat diet causing hypoglycemia, hepatic steatosis, hepatic glycogen depletion, and decreased expression of PPAR α target genes. Administration of WY-14643 at the onset of the fast prevented this phenotype. The ability of PPAR α ligands to prevent and reverse the metabolic abnormalities observed in the FASKOL mice led the investigators to conclude that the abnormalities were caused by failure to generate endogenous PPAR α ligands. From these data it appears that the relevant PPAR α ligand can be obtained from the diet or synthesized de novo, but is not present or cannot be delivered from lipid stored within the liver or adipose tissues. Similar results were obtained in mice with FAS deficiency in pancreatic β-cells and the hypothalamus(65). These mice were lean and hypophagic with increased physical activity and impaired hypothalamic PPAR α signaling. Again administration of a synthetic PPAR α agonist reversed the phenotype produced by FAS deficiency.

Interestingly, hepatocyte specific deficiency of acetyl CoA carboxylase 1failed to produce any of the phenotypes observed in the FASKOL mice(66). However, these mice retained more activity in the de novo lipogenesis pathway, likely due to compensatory up-regulation of ACC2(66, 67). Another potentially important difference is that FASKOL mice accumulate high levels of cytosolic malonyl CoA while the ACC1 knockout is depleted.

In a technological tour de force, Chakravarthy et al. identified the de novo lipogenesis product binding to PPAR α as 1-palmitoyl-2-oleoyl-sn-glycerol-3-phosphocholine (16:0/18:1-GPC)(68). FLAG-tagged PPAR α isolated from FASKOL mice was depleted in 16:0/18:1-GPC and Wy-14643 readily displaced 16:0/18:1 GPC bound to PPAR α. The synthesis of 16:0/18:1-GPC occurs through the Kennedy pathway. In the nucleus and ER, choline-ethanolamine phosphtransferase-1 (CEPT1) performs the final step in GPC synthesis, combining diacylglycerol and CDP-choline. Overexpression of CEPT1 in mouse hepatoma cells caused increased expression of PPAR α target genes, while knockdown of CEPT1 deceased expression of PPAR α target genes in mouse hepatoma cells and in whole animals. Portal vein infusion of 16:0/18:1-GPC decreased hepatic triglyceride and increased expression of PPAR α target genes in a PPAR α dependent manner.

Taken together this body of work implicates that FAS produces a precursor to the necessary PPAR α ligand 16:0/18:1-GPC, which is synthesized by CETP1. This work

identified the first nanomolar affinity endogenous PPAR α ligand and provided sound evidence that it functions in vivo. Nevertheless, several questions remain regarding the relationship between 16:0/18:1-GPC and PPAR α activation. FAS activity is increased in response to high-carbohydrate feeding and insulin, while PPAR α has a circadian regulation with high and low expression during fasting and feeding respectively(61, 69, 70). Given the antiphasic relationship between the machinery necessary to generate the ligands and the activity of their receptor, a more complex regulation must exist to deliver 16:0/18:1-GPC to PPAR α at the proper time. Alternatively, other PPAR α ligands, known or unknown, may play important roles during different spatiotemporal and physiological contexts.

Lipolysis of Stored TG

While the "new fat" hypothesis proposes that fatty acids liberated from intracellular lipid droplets cannot serve as PPAR α ligands, other evidence suggests lipid droplets can function as a rich supply of PPAR α ligands. This was most directly demonstrated by genetic manipulation of lipid droplet proteins in cultured hepatocytes(71). Adipose triglyceride lipase (ATGL) is a triglyceride lipase implicated in the breakdown of lipid droplets, while adipocyte differentiation related protein (ADRP) is a lipid droplet protein that promotes triglyceride storage. Overexpression of ATGL or siRNA meditated knockdown of ADRP increased PPAR α activity and expression of target genes. Conversely, overexpression of ADRP decreased PPAR α activity and expression of target genes. This straightforward experiment supports the role of lipid droplet derived PPAR α ligands. Furthermore, genetic manipulations in vivo have yielded similar results. PPAR α target genes are down regulated in animals null for the lipases responsible for lipid droplet catabolism (72). Loss of lipid droplet proteins or overexpression of hormone sensitive and adipose triglyceride lipase increase expression of PPAR α target genes (73-76). Thus, the pool of fatty acids liberated from stored TG may function as PPAR α ligands.

Lipolytic PPAR Activation

Non-esterified fatty acids circulate bound to albumin or are generated by vascular lipases acting on esterified fatty acids in lipoproteins. Vascular lipases include lipoprotein lipase, endothelial lipase, and hepatic lipase. Lipoprotein lipase possesses predominantly triglyceride lipase activity, while endothelial lipase is primarily a phospholipase, and hepatic lipase possesses both triglyceride and phospholipid lipase activities. In 2003, Jorge Plutzky's and Ronald Evans' groups highlighted the role that vascular lipases play in the generation of PPAR ligands.

The initial focus centered on lipolysis products of triglyceride-rich lipoproteins generated by the action of lipoprotein lipase. Lipoprotein lipase mediated lipolysis of VLDL, and to a much lesser extent LDL and HDL, potently activates PPAR α in endothelial cells(77). VLDL/LPL lipolysis products also activate PPAR α, although to a much lesser extent than PPAR δ. Furthermore, VLDL/LPL lipolysis products readily displace synthetic PPAR α agonists. Conversely, in macrophages PPAR δ seems to be the preferential isotype targeted by VLDL/LPL(78). In both cell types, VLDL/LPL fails to activate PPAR γ. In both endothelial cells and macrophages, the VLDL/LPL combination recapitulated the effects of synthetic PPAR agonists, in a PPAR α and δ dependent manner, respectively. In endothelial cells, VLDL lipolysis products inhibited TNF-α induced increases in VCAM expression. In vivo, over expression of LpL in muscle leads

to PPAR α dependent peroxisomal proliferation. In macrophages, VLDL treatment increases fat oxidation, concurrent with increased expression of PPAR δ target genes involved with β-oxidation, carnitine biosynthesis and lipid mobilization(79).

HDL particles are also capable of creating PPAR α ligands. Given the high phospholipid content of HDL, it is not surprising that endothelial lipase treatment generates PPAR α ligands. HDL/EL treatment increased expression of the canonical PPAR α target gene, ACO, and inhibited leukocyte adhesion to endothelial cells in a PPAR α dependent manner(80). Similarly, the electronegative fraction of LDL, which is increased in diabetes and implicated in accelerating atherosclerosis, has been identified as a potential store of PPAR α ligands. Interestingly, LDL(-) potentiates TNF-α induced VCAM expression through nf-kb and AP1 signaling when taken up by the LDL receptor, but inhibits the same process in a PPAR α dependent manner when incubated with LPL(81). LDL(-)/LPL displaces synthetic PPAR α ligands, indicating generation of PPAR α ligands, an effect attributed to the generation of hydroxy-octadecadienoic acids, known potent PPAR α activators.

Thus, lipoproteins function as circulating reservoirs of PPAR ligands that are accessible by lipase activity. The reason that lipoprotein derived lipids may play a role in activating PPAR α is unclear. One possibility is that a specific chemical species, such hydroxy-octadecadienoic acids in LDL(-), may underlie the preferential activation of PPAR α by lipolysis products. Another is that differential modes of delivery of lipid ligands produce alternate, or even opposing, outcomes. Thus, differences in chemical composition or routes of delivery may explain the observation that lipoprotein derived lipids stimulate PPAR α. In my work, I explored the biochemical basis of PPAR α activation by VLDL/LPL treatment.

CANNABINOID RECEPTOR 1

Background & Discovery

While humans were pharmacologically stimulating PPAR α decades before its discovery, the use of cannabis predates knowledge of its receptor by several millennia. Indeed, the Chinese emperor Huang Ti advised cannabis use for relief of rheumatic pain and relief of cramps in 2600 BC. The major psychoactive component of Cannabis, δ-9-tetrahyrdocannabinol, was isolated in 1964. Shortly thereafter, synthetic THC analogues, such as nabilone, began being used as anti-emetics and appetite stimulants to cancer patients. However the mechanism of THC action remained uncertain until the 1990's. While the hydrophobic nature of THC led to the hypothesis that it disrupted membrane fluidity, specific membrane binding sites for highly potent THC analogues, such as HU-210 and CP-55,245, were demonstrated in 1988(82). The first cannabinoid receptor, termed CB1, was cloned in 1990(83). Three years latter, a second G protein coupled cannabinoid receptor (CB2) was identified in blood cells and immune tissue(84). Despite the historical cultural use of cannabis, it is extremely unlikely that these receptors evolved to respond to THC. Nematodes, onychonphornas, and crustaceans appear to have cannabinoid receptors underscoring the ancient evolutionary history of the endocannabinoid system(85). In 1992, arachidonyl-ethanolamine, termed anandamide after the Sanskrit word for bliss, was the first endogenous cannabinoid receptor ligand, or endocannabinoid, to be identified(86). Three years later, 2-arachidonyl glycerol (2-AG) was shown to stimulate the cannabinoid receptors(87, 88). Although several other arachidonic acid containing lipids have attracted attention as possible endocannabinoids,

including noladin ether, virodhamine, and N-arachidonoyldopamine, 2-AG and anandamide are the best characterized and be the focus of this review(89-91).

CB1 is the most abundant G protein coupled receptor in the central nervous system(92). Both cannabinoid receptors function as classical G-protein coupled receptors, mostly coupled to Gi/o proteins. In neurons, CB1 transmits its signal by decreasing adenylate cyclase, and thus cAMP levels, stimulating mitogen-activated protein kinases, and K+ channels while inhibiting voltage-activated Ca2+ channels(93). Of note, these findings in the central nervous system may not be applicable throughout the body, as several examples of opposite regulation of downstream signaling molecules exist. For example, in the hypothalamus CB1 activation stimulates AMP kinase, while in the liver it inhibits AMP kinase(94).

Regulation

Anandamide is a partial CB1 agonist with high affinity and has been found at relevant concentrations within the central nervous system. 2-Ag is a full Cb1 agonist with lesser affinity and is present at much higher concentrations that anandamide. Whether there are distinct pools of 2-AG within the cell remains to be determined. The specific chemical agonist also may determine which of the intracellular signaling pathways follows CB1 activation. For example, whereas THC stimulates drug discrimination behavior, neither 2-AG nor AEA alone mimics this effect(95, 96). Interestingly, the combination of 2-AG and AEA is sufficient to stimulate this behavior, indicating crosstalk between the endocannabinod signals(95). Differential response to different agonists, and potentially antagonists, may allow for pharmacological exploitation while limiting adverse side effects.

Anandamide and 2-Ag levels are regulated by the complex enzymatic machinery responsible for their synthesis and degradation. Fatty acid amide hydrolase (FAAH) degrades anandamide to arachidonic acid and ethanolamine. FAAH is an intracellular membrane-bound serine hydrolyase with a broad specificity for amide and ester substrates(97-99).and is highly expressed throughout the brain. Generation of FAAH -/- mice definitively demonstrated that FAAH was responsible for the majority of anandamide breakdown(100). Tissue extracts from FAAH knockout mice had greatly reduced anandamide hydrolysis rates. When administered to wild-type mice, anandamide produces very weak and transient behavioral effects, likely due to its very short half-life(101). In contrast, when anandamide is administered to FAAH -/- mice they develop characteristic CB1 behavioral effects, including hypomobility, analgesia, hypothermia, and catalepsy. FAAH -/- mice also have raised endogenous levels of many fatty acid amides. Pharmacological inhibitors of FAAH, most notably URB597, raise brain anandamide levels and induce behavioral effects(102).

The enzymes responsible for the generation of anandamide are less clear. The classical pathway has two steps(103-105). First, N-acyltransferase transfers arachidonic acid to phosphatidylethanolamine to form n-archidonoyl-phoshophatylethanolamine (NAPE). NAPE-Phospholipase D then cleaves NAPE forming anandamide and phosphatidic acid. Both steps are stimulated by calcium and anandamide production is accompanied by synthesis of its precursor, NAPE. However, while NAPE-PLD -/- mice have increased levels of long chain saturated and monounsaturated n-acyl-ethanolamines, levels of polyunsaturated n-acyl ethanolamines, including anandamide, are unaltered(106). Thus, although NAPE PLD contributes to anandamide synthesis, other

routes surely exist. An alternative route of anandamide generation may be the double-O-deacylation of NAPE followed by phosphodiesterase action(107). Neither knockout of PDE1, a candidate phosphodiesterase, alone nor in combination with NAPE PLD changed anandamide levels(108, 109). This points to the existence of alternative routes of anandamide synthesis involving different enzymatic machinery and/or precursors.

Likewise, the synthesis of 2-AG is stimulated by calcium and may take place by multiple routes sharing phosphatidylinositol as a common precursor. Phospholipase C cleavage of the inositol head group yields diacylglycerol, which can be further hydrolyzed to monoacylglycerol by DAG lipase. Calcium induced 2-AG accumulation in neurons can be prevented by administration of synthetic inhibitors of PLC or DAG lipase(110). Sequential hydrolysis of the acyl group at the Sn1 position by phospholipase A1 and the phosphohead group by lysophospholipase C also may be able to generate 2-AG from phosphatidylinositol(111). Hydrolysis of triglycerides by the sequential action of adipose triglyceride lipase and hormone sensitive lipase also yields monoglycerides, but these enzymes show preference for saturated and monounsaturated fatty acids, making the generation of 2-AG by this route unlikely.

2-AG is predominantly degraded by monoacylglycerol lipase. MAG lipase is a cytosolic serine hydrolase originally characterized in adipose tissue that is also extensively expressed within the brain, mainly in nerve endings(112, 113). 2-AG hydrolytic activity is increased by overexpression and decreased by siRNA knockdown. of MAG lipase(114, 115). Treatment of rat brain membranes with an irreversible MAG lipase inhibitor, 2-arachidonylmaleimide, decreases 2-AG hydrolytic activity by upwards of 85%(116). Importantly, in vivo administration of JL184, a MAG lipase inhibitor, increases brain 2-AG levels 8 fold and induces cannabinoid like behavior, including analgesia, hypothermia, and hypomotility(117). Although, MAG lipase is the predominant 2-AG hydrolase in the brain, several other proteins, including α/β hydrolase 6 and 12, have been shown to contribute(118). Interestingly, the three proteins reside in different subcellular locations and may regulate different pools of 2-AG.

The pharmacological effects of THC, as well as genetic and epidemiological data, provide clues as to the physiologic role of the endocannabinoid system. As my work focuses on metabolic disease, the review will be limited to the metabolic actions of cannabinoids. In a hospital-based study, THC increased food intake, but the effect subsided within several days, while weight gain persisted for three weeks(119). THC also was found to decrease glucose tolerance in humans(120). In epidemiological studies, chronic THC users were reported to be more likely to develop hepatic steatosis and have increased plasma concentrations of apolipoprotein CIII, which is linked to hypertriglyceridmeia.(121, 122) Obese individuals have been found to have increased plasma anandamide and 2-AG concentrations(123). Correlative studies in human adipose samples have shown an inverse relationship between adipose FAAH activity and amount of visceral fat(124). Finally, polymorphisms in FAAH and CB1 have been linked to increased body mass index and waist circumference(125-127).

Pharmacology

The strongest evidence for the role of the endocannabioid system in human obesity and metabolic disease comes from the trials of the CB1 antagonist rimonabant. Four large-scale trials of rimonabant in obese individuals have yielded highly consistent results(128-131). Rimonabant (20 mg/day) resulted in clinically significant and

prolonged reductions in body weight and waist circumference and improved cardiometabolic risk factors associated with obesity. Rimonabant increased HDL cholesterol and mean LDL size, while decreasing triglyceride levels. In fact, statistical analysis showed significant (~50%) weight loss-independent effects of rimonabant in reducing plasma triglyceride as well as increasing HDL. Polymorphisms in CB1 have been linked to lipoprotein levels, independent of body mass index, supporting a weight-independent role for endocannabinoid signaling(132). Rimonabant increased adiponectin levels more than would be expected based on weight loss alone(133). In type II diabetics, rimonabant significantly improved fasting blood glucose and glycosylated hemoglobin, as well as body weight and lipid parameters(130). Despite the encouraging effects of plasma lipids, the STRAVIDARIUS trial failed to show an effect of rimonabant on atherosclerosis progression, as assessed by percent atheroma volume(134). However, the improvements on lipoprotein metabolism beyond those accounted for by weight loss suggest a direct and potentially beneficial effect of CB1 blockade on cardiovascular disease risk.

Downstream effects.

Many preclinical studies with CB1 antagonists and cb1 knockout mice demonstrate the powerful regulatory effects of the endocannabinoid system. It not only regulates food consumption, but also plays an anabolic role by increasing the storage and decreasing the expenditure of energy. Rimonabant reduces food intake, especially of "palatable" food, and this effect is absent in CB1 -/- mice(11, 135-137). Hypothalamic endocannabinoid content is decreased by leptin and increased in ob/ob mice(11). However, the hypophagic effect is transient in both diet and genetic induced models of obesity. Interestingly, the weight loss, change in adiposity, and normalization of metabolic parameters persist(137). The generation of CB1 knockout mice reinforced the food intake- independent effects of the cannabinoid system. CB1 knockout mice are leaner than wild-type littermates, a phenotype that persists even during pair-feeding experiments(138). Similarly, CB1-/-mice are resistant to diet-induced obesity despite maintaining caloric intake similar to CB1+/+ littermates(139). Studies with CB1 antagonists and CB1 null mice have demonstrated peripheral effects of CB1 activation. Levels of endocanniboids in the liver and adipose tissue are comparable to those in the brain(139-141). Furthermore, CB1 is expressed in both tissues, as well as the enzymatic machinery necessary for the synthesis and breakdown of the endocannabinoids.

CB1 stimulation in adipocytes increases LPL expression and inhibits adiponectin production(138, 142, 143). Thus, both the increased delivery of LPL-derived fatty acids and the decrease in their oxidation due to reduced adiponectin may contribute to triglyceride accumulation. On a more global scale, microarray analysis indicates that rimonabant reverses obesity-induced changes in adipose gene expression(144). More recently, reduced levels of anandamide in adipose tissue have been proposed to underlie the lipolytic effects of leptin(145). Overall, the evidence suggests that adipose CB1 inhibits lipolysis and promotes storage of triglycerides.

The laboratory of George Kunos has clearly demonstrated a role for hepatic CB1 in the pathogenesis of hepatic steatosis. High fat diet administration increases hepatic anandamide concentrations and CB1 receptor density in conjunction with decreased FAAH activity(139). CB1 KO mice are resistant to high-fat diet induced increases in de novo lipogenesis and hepatic steatosis. Administration of the synthetic CB1 agonist,

Hu210, increased expression of srebp1c and its target genes (fas, acc) and increased de novo lipogenesis in wild-type, but not CB1 KO mice. Similar results were obtained in primary hepatocytes implicating hepatic CB1 as the site of action. The generation of hepatocyte specific knockout mice further highlights the role of hepatic CB1. Hepatocyte specific knockout mice gain weight normally on a high fat diet, but do not develop the characteristic diet-induced steatosis, dyslipidemia, or leptin resistance(146). In addition to stimulating SREBP1c and subsequent lipogenesis, hepatic Cb1 inhibits AMP kinase. Consistent with this, THC decreases hepatic AMP kinase activity(94). AMP kinase phosphorylates and inactivates key enzymes in fatty acid and cholesterol biosynthesis, decreases lipogenic gene expression, and increases fatty acid oxidation.

Chronic alcohol consumption also promotes hepatic de novo lipogenesis and steatosis. Recently, chronic alcohol consumption has been shown to stimulate production of 2-AG from hepatic stellate cells by increasing expression of DAG lipase β(147). Again rimonabant treatment or genetic loss of CB1 prevented development of hepatic steatosis and accompanying metabolic abnormalities. Genetic deletion of CB1 in hepatocytes was sufficient to prevent alcohol induced hepatic steatosis. The CB1 signaling in hepatocytes caused by production of 2-AG in stellate cells demonstrates that paracrine CB1 signaling exists outside of the central nervous system.

A direct role in regulation of glucose metabolism has also been described for the EC system. Hepatocyte specific knockout mice are immune to diet induced insulin resistance(146). Rimonabant increases skeletal muscle basal oxygen consumption and glucose uptake(148). Administration of a synthetic CB1 agonist causes glucose intolerance and insulin resistance in wild-type mice, but not in CB1 germline or hepatocyte-specific knockout mice(146). Alterations in adiponectin levels have been proposed to mediate a portion of the effect of CB1 on insulin sensitivity(149).

While loss of CB1 function clearly prevents, and even reverses, obesity and disorders of lipid and glucose metabolism, the evidence that stimulation of CB1 causes metabolic abnormalities derives exclusively from the use of synthetic agonists. Furthermore, until the generation of hepatocyte specific knockout mice the effects of endocannabinoids on food intake and body weight had not been disassociated from the peripheral metabolic effects. In my work, a synthetic inhibitor of endocannabinoid breakdown was used to acutely increase levels of endocannabinoids. This approach enabled the demonstration that endogenously produced cannabinoids influence metabolic parameters independent of effects on food intake, and provided insight into the responsible mechanisms.

References

1. Olshansky, S.J., Passaro, D.J., Hershow, R.C., Layden, J., Carnes, B.A., Brody, J., Hayflick, L., Butler, R.N., Allison, D.B., and Ludwig, D.S. 2005. A potential decline in life expectancy in the United States in the 21st century. *N Engl J Med* 352:1138-1145.
2. Issemann, I., and Green, S. 1990. Activation of a member of the steroid hormone receptor superfamily by peroxisome proliferators. *Nature* 347:645-650.
3. Dreyer, C., Krey, G., Keller, H., Givel, F., Helftenbein, G., and Wahli, W. 1992. Control of the peroxisomal beta-oxidation pathway by a novel family of nuclear hormone receptors. *Cell* 68:879-887.
4. Schmidt, A., Endo, N., Rutledge, S.J., Vogel, R., Shinar, D., and Rodan, G.A. 1992. Identification of a new member of the steroid hormone receptor superfamily that is activated by a peroxisome proliferator and fatty acids. *Mol Endocrinol* 6:1634-1641.
5. Chawla, A., Repa, J.J., Evans, R.M., and Mangelsdorf, D.J. 2001. Nuclear receptors and lipid physiology: opening the X-files. *Science* 294:1866-1870.
6. Cronet, P., Petersen, J.F., Folmer, R., Blomberg, N., Sjoblom, K., Karlsson, U., Lindstedt, E.L., and Bamberg, K. 2001. Structure of the PPARalpha and -gamma ligand binding domain in complex with AZ 242; ligand selectivity and agonist activation in the PPAR family. *Structure* 9:699-706.
7. Xu, H.E., Stanley, T.B., Montana, V.G., Lambert, M.H., Shearer, B.G., Cobb, J.E., McKee, D.D., Galardi, C.M., Plunket, K.D., Nolte, R.T., et al. 2002. Structural basis for antagonist-mediated recruitment of nuclear co-repressors by PPARalpha. *Nature* 415:813-817.
8. Gonzalez, F.J., and Shah, Y.M. 2008. PPARalpha: mechanism of species differences and hepatocarcinogenesis of peroxisome proliferators. *Toxicology* 246:2-8.
9. Ruotolo, G., Ericsson, C.G., Tettamanti, C., Karpe, F., Grip, L., Svane, B., Nilsson, J., de Faire, U., and Hamsten, A. 1998. Treatment effects on serum lipoprotein lipids, apolipoproteins and low density lipoprotein particle size and relationships of lipoprotein variables to progression of coronary artery disease in the Bezafibrate Coronary Atherosclerosis Intervention Trial (BECAIT). *J Am Coll Cardiol* 32:1648-1656.
10. Frick, M.H., Syvanne, M., Nieminen, M.S., Kauma, H., Majahalme, S., Virtanen, V., Kesaniemi, Y.A., Pasternack, A., and Taskinen, M.R. 1997. Prevention of the angiographic progression of coronary and vein-graft atherosclerosis by gemfibrozil after coronary bypass surgery in men with low levels of HDL cholesterol. Lopid Coronary Angiography Trial (LOCAT) Study Group. *Circulation* 96:2137-2143.
11. Di Marzo, V., Goparaju, S.K., Wang, L., Liu, J., Batkai, S., Jarai, Z., Fezza, F., Miura, G.I., Palmiter, R.D., Sugiura, T., et al. 2001. Leptin-regulated endocannabinoids are involved in maintaining food intake. *Nature* 410:822-825.
12. 2000. Secondary prevention by raising HDL cholesterol and reducing triglycerides in patients with coronary artery disease: the Bezafibrate Infarction Prevention (BIP) study. *Circulation* 102:21-27.

13. Rubins, H.B., Robins, S.J., Collins, D., Fye, C.L., Anderson, J.W., Elam, M.B., Faas, F.H., Linares, E., Schaefer, E.J., Schectman, G., et al. 1999. Gemfibrozil for the secondary prevention of coronary heart disease in men with low levels of high-density lipoprotein cholesterol. Veterans Affairs High-Density Lipoprotein Cholesterol Intervention Trial Study Group. *N Engl J Med* 341:410-418.
14. Frick, M.H., Elo, O., Haapa, K., Heinonen, O.P., Heinsalmi, P., Helo, P., Huttunen, J.K., Kaitaniemi, P., Koskinen, P., Manninen, V., et al. 1987. Helsinki Heart Study: primary-prevention trial with gemfibrozil in middle-aged men with dyslipidemia. Safety of treatment, changes in risk factors, and incidence of coronary heart disease. *N Engl J Med* 317:1237-1245.
15. Tenkanen, L., Manttari, M., and Manninen, V. 1995. Some coronary risk factors related to the insulin resistance syndrome and treatment with gemfibrozil. Experience from the Helsinki Heart Study. *Circulation* 92:1779-1785.
16. Manninen, V., Tenkanen, L., Koskinen, P., Huttunen, J.K., Manttari, M., Heinonen, O.P., and Frick, M.H. 1992. Joint effects of serum triglyceride and LDL cholesterol and HDL cholesterol concentrations on coronary heart disease risk in the Helsinki Heart Study. Implications for treatment. *Circulation* 85:37-45.
17. Robins, S.J., Rubins, H.B., Faas, F.H., Schaefer, E.J., Elam, M.B., Anderson, J.W., and Collins, D. 2003. Insulin resistance and cardiovascular events with low HDL cholesterol: the Veterans Affairs HDL Intervention Trial (VA-HIT). *Diabetes Care* 26:1513-1517.
18. Ginsberg, H.N., Elam, M.B., Lovato, L.C., Crouse, J.R., 3rd, Leiter, L.A., Linz, P., Friedewald, W.T., Buse, J.B., Gerstein, H.C., Probstfield, J., et al. Effects of combination lipid therapy in type 2 diabetes mellitus. *N Engl J Med* 362:1563-1574.
19. Playford, D.A., Watts, G.F., Best, J.D., and Burke, V. 2002. Effect of fenofibrate on brachial artery flow-mediated dilatation in type 2 diabetes mellitus. *Am J Cardiol* 90:1254-1257.
20. Lefebvre, P., Chinetti, G., Fruchart, J.C., and Staels, B. 2006. Sorting out the roles of PPAR alpha in energy metabolism and vascular homeostasis. *J Clin Invest* 116:571-580.
21. Rodriguez, J.C., Gil-Gomez, G., Hegardt, F.G., and Haro, D. 1994. Peroxisome proliferator-activated receptor mediates induction of the mitochondrial 3-hydroxy-3-methylglutaryl-CoA synthase gene by fatty acids. *J Biol Chem* 269:18767-18772.
22. Brown, J.D., and Plutzky, J. 2007. Peroxisome proliferator-activated receptors as transcriptional nodal points and therapeutic targets. *Circulation* 115:518-533.
23. Schoonjans, K., Peinado-Onsurbe, J., Lefebvre, A.M., Heyman, R.A., Briggs, M., Deeb, S., Staels, B., and Auwerx, J. 1996. PPARalpha and PPARgamma activators direct a distinct tissue-specific transcriptional response via a PPRE in the lipoprotein lipase gene. *Embo J* 15:5336-5348.
24. Haubenwallner, S., Essenburg, A.D., Barnett, B.C., Pape, M.E., DeMattos, R.B., Krause, B.R., Minton, L.L., Auerbach, B.J., Newton, R.S., Leff, T., et al. 1995. Hypolipidemic activity of select fibrates correlates to changes in hepatic apolipoprotein C-III expression: a potential physiologic basis for their mode of action. *J Lipid Res* 36:2541-2551.

25. Gilde, A.J., van der Lee, K.A., Willemsen, P.H., Chinetti, G., van der Leij, F.R., van der Vusse, G.J., Staels, B., and van Bilsen, M. 2003. Peroxisome proliferator-activated receptor (PPAR) alpha and PPARbeta/delta, but not PPARgamma, modulate the expression of genes involved in cardiac lipid metabolism. *Circ Res* 92:518-524.
26. Finck, B.N., Lehman, J.J., Leone, T.C., Welch, M.J., Bennett, M.J., Kovacs, A., Han, X., Gross, R.W., Kozak, R., Lopaschuk, G.D., et al. 2002. The cardiac phenotype induced by PPARalpha overexpression mimics that caused by diabetes mellitus. *J Clin Invest* 109:121-130.
27. Aoyama, T., Peters, J.M., Iritani, N., Nakajima, T., Furihata, K., Hashimoto, T., and Gonzalez, F.J. 1998. Altered constitutive expression of fatty acid-metabolizing enzymes in mice lacking the peroxisome proliferator-activated receptor alpha (PPARalpha). *J Biol Chem* 273:5678-5684.
28. Inoue, I., Goto, S., Matsunaga, T., Nakajima, T., Awata, T., Hokari, S., Komoda, T., and Katayama, S. 2001. The ligands/activators for peroxisome proliferator-activated receptor alpha (PPARalpha) and PPARgamma increase Cu2+,Zn2+-superoxide dismutase and decrease p22phox message expressions in primary endothelial cells. *Metabolism* 50:3-11.
29. Teissier, E., Nohara, A., Chinetti, G., Paumelle, R., Cariou, B., Fruchart, J.C., Brandes, R.P., Shah, A., and Staels, B. 2004. Peroxisome proliferator-activated receptor alpha induces NADPH oxidase activity in macrophages, leading to the generation of LDL with PPAR-alpha activation properties. *Circ Res* 95:1174-1182.
30. Marx, N., Sukhova, G.K., Collins, T., Libby, P., and Plutzky, J. 1999. PPARalpha activators inhibit cytokine-induced vascular cell adhesion molecule-1 expression in human endothelial cells. *Circulation* 99:3125-3131.
31. Delerive, P., Gervois, P., Fruchart, J.C., and Staels, B. 2000. Induction of IkappaBalpha expression as a mechanism contributing to the anti-inflammatory activities of peroxisome proliferator-activated receptor-alpha activators. *J Biol Chem* 275:36703-36707.
32. Delerive, P., De Bosscher, K., Vanden Berghe, W., Fruchart, J.C., Haegeman, G., and Staels, B. 2002. DNA binding-independent induction of IkappaBalpha gene transcription by PPARalpha. *Mol Endocrinol* 16:1029-1039.
33. Chinetti, G., Gbaguidi, F.G., Griglio, S., Mallat, Z., Antonucci, M., Poulain, P., Chapman, J., Fruchart, J.C., Tedgui, A., Najib-Fruchart, J., et al. 2000. CLA-1/SR-BI is expressed in atherosclerotic lesion macrophages and regulated by activators of peroxisome proliferator-activated receptors. *Circulation* 101:2411-2417.
34. Chinetti, G., Lestavel, S., Bocher, V., Remaley, A.T., Neve, B., Torra, I.P., Teissier, E., Minnich, A., Jaye, M., Duverger, N., et al. 2001. PPAR-alpha and PPAR-gamma activators induce cholesterol removal from human macrophage foam cells through stimulation of the ABCA1 pathway. *Nat Med* 7:53-58.
35. Gbaguidi, F.G., Chinetti, G., Milosavljevic, D., Teissier, E., Chapman, J., Olivecrona, G., Fruchart, J.C., Griglio, S., Fruchart-Najib, J., and Staels, B. 2002. Peroxisome proliferator-activated receptor (PPAR) agonists decrease lipoprotein

lipase secretion and glycated LDL uptake by human macrophages. *FEBS Lett* 512:85-90.
36. Chinetti, G., Lestavel, S., Fruchart, J.C., Clavey, V., and Staels, B. 2003. Peroxisome proliferator-activated receptor alpha reduces cholesterol esterification in macrophages. *Circ Res* 92:212-217.
37. Marx, N., Mackman, N., Schonbeck, U., Yilmaz, N., Hombach, V., Libby, P., and Plutzky, J. 2001. PPARalpha activators inhibit tissue factor expression and activity in human monocytes. *Circulation* 103:213-219.
38. Neve, B.P., Corseaux, D., Chinetti, G., Zawadzki, C., Fruchart, J.C., Duriez, P., Staels, B., and Jude, B. 2001. PPARalpha agonists inhibit tissue factor expression in human monocytes and macrophages. *Circulation* 103:207-212.
39. Staels, B., Koenig, W., Habib, A., Merval, R., Lebret, M., Torra, I.P., Delerive, P., Fadel, A., Chinetti, G., Fruchart, J.C., et al. 1998. Activation of human aortic smooth-muscle cells is inhibited by PPARalpha but not by PPARgamma activators. *Nature* 393:790-793.
40. Delerive, P., De Bosscher, K., Besnard, S., Vanden Berghe, W., Peters, J.M., Gonzalez, F.J., Fruchart, J.C., Tedgui, A., Haegeman, G., and Staels, B. 1999. Peroxisome proliferator-activated receptor alpha negatively regulates the vascular inflammatory gene response by negative cross-talk with transcription factors NF-kappaB and AP-1. *J Biol Chem* 274:32048-32054.
41. Zahradka, P., Yurkova, N., Litchie, B., Moon, M.C., Del Rizzo, D.F., and Taylor, C.G. 2003. Activation of peroxisome proliferator-activated receptors alpha and gamma1 inhibits human smooth muscle cell proliferation. *Mol Cell Biochem* 246:105-110.
42. Nigro, J., Dilley, R.J., and Little, P.J. 2002. Differential effects of gemfibrozil on migration, proliferation and proteoglycan production in human vascular smooth muscle cells. *Atherosclerosis* 162:119-129.
43. Lee, S.S., Pineau, T., Drago, J., Lee, E.J., Owens, J.W., Kroetz, D.L., Fernandez-Salguero, P.M., Westphal, H., and Gonzalez, F.J. 1995. Targeted disruption of the alpha isoform of the peroxisome proliferator-activated receptor gene in mice results in abolishment of the pleiotropic effects of peroxisome proliferators. *Mol Cell Biol* 15:3012-3022.
44. Kersten, S., Seydoux, J., Peters, J.M., Gonzalez, F.J., Desvergne, B., and Wahli, W. 1999. Peroxisome proliferator-activated receptor alpha mediates the adaptive response to fasting. *J Clin Invest* 103:1489-1498.
45. Leone, T.C., Weinheimer, C.J., and Kelly, D.P. 1999. A critical role for the peroxisome proliferator-activated receptor alpha (PPARalpha) in the cellular fasting response: the PPARalpha-null mouse as a model of fatty acid oxidation disorders. *Proc Natl Acad Sci U S A* 96:7473-7478.
46. Lemberger, T., Saladin, R., Vazquez, M., Assimacopoulos, F., Staels, B., Desvergne, B., Wahli, W., and Auwerx, J. 1996. Expression of the peroxisome proliferator-activated receptor alpha gene is stimulated by stress and follows a diurnal rhythm. *J Biol Chem* 271:1764-1769.
47. Steineger, H.H., Sorensen, H.N., Tugwood, J.D., Skrede, S., Spydevold, O., and Gautvik, K.M. 1994. Dexamethasone and insulin demonstrate marked and opposite regulation of the steady-state mRNA level of the peroxisomal

proliferator-activated receptor (PPAR) in hepatic cells. Hormonal modulation of fatty-acid-induced transcription. *Eur J Biochem* 225:967-974.
48. Lemberger, T., Staels, B., Saladin, R., Desvergne, B., Auwerx, J., and Wahli, W. 1994. Regulation of the peroxisome proliferator-activated receptor alpha gene by glucocorticoids. *J Biol Chem* 269:24527-24530.
49. Oishi, K., Shirai, H., and Ishida, N. 2005. CLOCK is involved in the circadian transactivation of peroxisome-proliferator-activated receptor alpha (PPARalpha) in mice. *Biochem J* 386:575-581.
50. Zhou, Y.T., Shimabukuro, M., Wang, M.Y., Lee, Y., Higa, M., Milburn, J.L., Newgard, C.B., and Unger, R.H. 1998. Role of peroxisome proliferator-activated receptor alpha in disease of pancreatic beta cells. *Proc Natl Acad Sci U S A* 95:8898-8903.
51. Jalouli, M., Carlsson, L., Ameen, C., Linden, D., Ljungberg, A., Michalik, L., Eden, S., Wahli, W., and Oscarsson, J. 2003. Sex difference in hepatic peroxisome proliferator-activated receptor alpha expression: influence of pituitary and gonadal hormones. *Endocrinology* 144:101-109.
52. Pineda Torra, I., Jamshidi, Y., Flavell, D.M., Fruchart, J.C., and Staels, B. 2002. Characterization of the human PPARalpha promoter: identification of a functional nuclear receptor response element. *Mol Endocrinol* 16:1013-1028.
53. Gervois, P., Torra, I.P., Chinetti, G., Grotzinger, T., Dubois, G., Fruchart, J.C., Fruchart-Najib, J., Leitersdorf, E., and Staels, B. 1999. A truncated human peroxisome proliferator-activated receptor alpha splice variant with dominant negative activity. *Mol Endocrinol* 13:1535-1549.
54. Blanquart, C., Barbier, O., Fruchart, J.C., Staels, B., and Glineur, C. 2002. Peroxisome proliferator-activated receptor alpha (PPARalpha) turnover by the ubiquitin-proteasome system controls the ligand-induced expression level of its target genes. *J Biol Chem* 277:37254-37259.
55. Barger, P.M., Browning, A.C., Garner, A.N., and Kelly, D.P. 2001. p38 mitogen-activated protein kinase activates peroxisome proliferator-activated receptor alpha: a potential role in the cardiac metabolic stress response. *J Biol Chem* 276:44495-44501.
56. Hayes, K.C., and Khosla, P. 1992. Dietary fatty acid thresholds and cholesterolemia. *Faseb J* 6:2600-2607.
57. Gottlicher, M., Widmark, E., Li, Q., and Gustafsson, J.A. 1992. Fatty acids activate a chimera of the clofibric acid-activated receptor and the glucocorticoid receptor. *Proc Natl Acad Sci U S A* 89:4653-4657.
58. Keller, H., Dreyer, C., Medin, J., Mahfoudi, A., Ozato, K., and Wahli, W. 1993. Fatty acids and retinoids control lipid metabolism through activation of peroxisome proliferator-activated receptor-retinoid X receptor heterodimers. *Proc Natl Acad Sci U S A* 90:2160-2164.
59. Gottlicher, M., Demoz, A., Svensson, D., Tollet, P., Berge, R.K., and Gustafsson, J.A. 1993. Structural and metabolic requirements for activators of the peroxisome proliferator-activated receptor. *Biochem Pharmacol* 46:2177-2184.
60. Kliewer, S.A., Sundseth, S.S., Jones, S.A., Brown, P.J., Wisely, G.B., Koble, C.S., Devchand, P., Wahli, W., Willson, T.M., Lenhard, J.M., et al. 1997. Fatty acids and eicosanoids regulate gene expression through direct interactions with

peroxisome proliferator-activated receptors alpha and gamma. *Proc Natl Acad Sci U S A* 94:4318-4323.
61. Forman, B.M., Chen, J., and Evans, R.M. 1997. Hypolipidemic drugs, polyunsaturated fatty acids, and eicosanoids are ligands for peroxisome proliferator-activated receptors alpha and delta. *Proc Natl Acad Sci U S A* 94:4312-4317.
62. Krey, G., Braissant, O., L'Horset, F., Kalkhoven, E., Perroud, M., Parker, M.G., and Wahli, W. 1997. Fatty acids, eicosanoids, and hypolipidemic agents identified as ligands of peroxisome proliferator-activated receptors by coactivator-dependent receptor ligand assay. *Mol Endocrinol* 11:779-791.
63. Hostetler, H.A., Petrescu, A.D., Kier, A.B., and Schroeder, F. 2005. Peroxisome proliferator-activated receptor alpha interacts with high affinity and is conformationally responsive to endogenous ligands. *J Biol Chem* 280:18667-18682.
64. Chakravarthy, M.V., Pan, Z., Zhu, Y., Tordjman, K., Schneider, J.G., Coleman, T., Turk, J., and Semenkovich, C.F. 2005. "New" hepatic fat activates PPARalpha to maintain glucose, lipid, and cholesterol homeostasis. *Cell Metab* 1:309-322.
65. Chakravarthy, M.V., Zhu, Y., Lopez, M., Yin, L., Wozniak, D.F., Coleman, T., Hu, Z., Wolfgang, M., Vidal-Puig, A., Lane, M.D., et al. 2007. Brain fatty acid synthase activates PPARalpha to maintain energy homeostasis. *J Clin Invest* 117:2539-2552.
66. Mao, J., DeMayo, F.J., Li, H., Abu-Elheiga, L., Gu, Z., Shaikenov, T.E., Kordari, P., Chirala, S.S., Heird, W.C., and Wakil, S.J. 2006. Liver-specific deletion of acetyl-CoA carboxylase 1 reduces hepatic triglyceride accumulation without affecting glucose homeostasis. *Proc Natl Acad Sci U S A* 103:8552-8557.
67. Harada, N., Oda, Z., Hara, Y., Fujinami, K., Okawa, M., Ohbuchi, K., Yonemoto, M., Ikeda, Y., Ohwaki, K., Aragane, K., et al. 2007. Hepatic de novo lipogenesis is present in liver-specific ACC1-deficient mice. *Mol Cell Biol* 27:1881-1888.
68. Chakravarthy, M.V., Lodhi, I.J., Yin, L., Malapaka, R.R., Xu, H.E., Turk, J., and Semenkovich, C.F. 2009. Identification of a physiologically relevant endogenous ligand for PPARalpha in liver. *Cell* 138:476-488.
69. Gibson, D.M., Lyons, R.T., Scott, D.F., and Muto, Y. 1972. Synthesis and degradation of the lipogenic enzymes of rat liver. *Adv Enzyme Regul* 10:187-204.
70. Girard, J., Ferre, P., and Foufelle, F. 1997. Mechanisms by which carbohydrates regulate expression of genes for glycolytic and lipogenic enzymes. *Annu Rev Nutr* 17:325-352.
71. Sapiro, J.M., Mashek, M.T., Greenberg, A.S., and Mashek, D.G. 2009. Hepatic triacylglycerol hydrolysis regulates peroxisome proliferator-activated receptor alpha activity. *J Lipid Res* 50:1621-1629.
72. Pinent, M., Hackl, H., Burkard, T.R., Prokesch, A., Papak, C., Scheideler, M., Hammerle, G., Zechner, R., Trajanoski, Z., and Strauss, J.G. 2008. Differential transcriptional modulation of biological processes in adipocyte triglyceride lipase and hormone-sensitive lipase-deficient mice. *Genomics* 92:26-32.
73. Castro-Chavez, F., Yechoor, V.K., Saha, P.K., Martinez-Botas, J., Wooten, E.C., Sharma, S., O'Connell, P., Taegtmeyer, H., and Chan, L. 2003. Coordinated upregulation of oxidative pathways and downregulation of lipid biosynthesis

underlie obesity resistance in perilipin knockout mice: a microarray gene expression profile. *Diabetes* 52:2666-2674.
74. Saha, P.K., Kojima, H., Martinez-Botas, J., Sunehag, A.L., and Chan, L. 2004. Metabolic adaptations in the absence of perilipin: increased beta-oxidation and decreased hepatic glucose production associated with peripheral insulin resistance but normal glucose tolerance in perilipin-null mice. *J Biol Chem* 279:35150-35158.
75. Toh, S.Y., Gong, J., Du, G., Li, J.Z., Yang, S., Ye, J., Yao, H., Zhang, Y., Xue, B., Li, Q., et al. 2008. Up-regulation of mitochondrial activity and acquirement of brown adipose tissue-like property in the white adipose tissue of fsp27 deficient mice. *PLoS One* 3:e2890.
76. Reid, B.N., Ables, G.P., Otlivanchik, O.A., Schoiswohl, G., Zechner, R., Blaner, W.S., Goldberg, I.J., Schwabe, R.F., Chua, S.C., Jr., and Huang, L.S. 2008. Hepatic overexpression of hormone-sensitive lipase and adipose triglyceride lipase promotes fatty acid oxidation, stimulates direct release of free fatty acids, and ameliorates steatosis. *J Biol Chem* 283:13087-13099.
77. Ziouzenkova, O., Perrey, S., Asatryan, L., Hwang, J., MacNaul, K.L., Moller, D.E., Rader, D.J., Sevanian, A., Zechner, R., Hoefler, G., et al. 2003. Lipolysis of triglyceride-rich lipoproteins generates PPAR ligands: evidence for an antiinflammatory role for lipoprotein lipase. *Proc Natl Acad Sci U S A* 100:2730-2735.
78. Chawla, A., Lee, C.H., Barak, Y., He, W., Rosenfeld, J., Liao, D., Han, J., Kang, H., and Evans, R.M. 2003. PPARdelta is a very low-density lipoprotein sensor in macrophages. *Proc Natl Acad Sci U S A* 100:1268-1273.
79. Lee, C.H., Kang, K., Mehl, I.R., Nofsinger, R., Alaynick, W.A., Chong, L.W., Rosenfeld, J.M., and Evans, R.M. 2006. Peroxisome proliferator-activated receptor delta promotes very low-density lipoprotein-derived fatty acid catabolism in the macrophage. *Proc Natl Acad Sci U S A* 103:2434-2439.
80. Ahmed, W., Orasanu, G., Nehra, V., Asatryan, L., Rader, D.J., Ziouzenkova, O., and Plutzky, J. 2006. High-density lipoprotein hydrolysis by endothelial lipase activates PPARalpha: a candidate mechanism for high-density lipoprotein-mediated repression of leukocyte adhesion. *Circ Res* 98:490-498.
81. Ziouzenkova, O., Asatryan, L., Sahady, D., Orasanu, G., Perrey, S., Cutak, B., Hassell, T., Akiyama, T.E., Berger, J.P., Sevanian, A., et al. 2003. Dual roles for lipolysis and oxidation in peroxisome proliferation-activator receptor responses to electronegative low density lipoprotein. *J Biol Chem* 278:39874-39881.
82. Devane, W.A., Dysarz, F.A., 3rd, Johnson, M.R., Melvin, L.S., and Howlett, A.C. 1988. Determination and characterization of a cannabinoid receptor in rat brain. *Mol Pharmacol* 34:605-613.
83. Matsuda, L.A., Lolait, S.J., Brownstein, M.J., Young, A.C., and Bonner, T.I. 1990. Structure of a cannabinoid receptor and functional expression of the cloned cDNA. *Nature* 346:561-564.
84. Munro, S., Thomas, K.L., and Abu-Shaar, M. 1993. Molecular characterization of a peripheral receptor for cannabinoids. *Nature* 365:61-65.
85. McPartland, J.M., Agraval, J., Gleeson, D., Heasman, K., and Glass, M. 2006. Cannabinoid receptors in invertebrates. *J Evol Biol* 19:366-373.

86. Devane, W.A., Hanus, L., Breuer, A., Pertwee, R.G., Stevenson, L.A., Griffin, G., Gibson, D., Mandelbaum, A., Etinger, A., and Mechoulam, R. 1992. Isolation and structure of a brain constituent that binds to the cannabinoid receptor. *Science* 258:1946-1949.
87. Mechoulam, R., Ben-Shabat, S., Hanus, L., Ligumsky, M., Kaminski, N.E., Schatz, A.R., Gopher, A., Almog, S., Martin, B.R., Compton, D.R., et al. 1995. Identification of an endogenous 2-monoglyceride, present in canine gut, that binds to cannabinoid receptors. *Biochem Pharmacol* 50:83-90.
88. Sugiura, T., Kondo, S., Sukagawa, A., Nakane, S., Shinoda, A., Itoh, K., Yamashita, A., and Waku, K. 1995. 2-Arachidonoylglycerol: a possible endogenous cannabinoid receptor ligand in brain. *Biochem Biophys Res Commun* 215:89-97.
89. Hanus, L., Abu-Lafi, S., Fride, E., Breuer, A., Vogel, Z., Shalev, D.E., Kustanovich, I., and Mechoulam, R. 2001. 2-arachidonyl glyceryl ether, an endogenous agonist of the cannabinoid CB1 receptor. *Proc Natl Acad Sci U S A* 98:3662-3665.
90. Huang, S.M., Bisogno, T., Trevisani, M., Al-Hayani, A., De Petrocellis, L., Fezza, F., Tognetto, M., Petros, T.J., Krey, J.F., Chu, C.J., et al. 2002. An endogenous capsaicin-like substance with high potency at recombinant and native vanilloid VR1 receptors. *Proc Natl Acad Sci U S A* 99:8400-8405.
91. Porter, A.C., Sauer, J.M., Knierman, M.D., Becker, G.W., Berna, M.J., Bao, J., Nomikos, G.G., Carter, P., Bymaster, F.P., Leese, A.B., et al. 2002. Characterization of a novel endocannabinoid, virodhamine, with antagonist activity at the CB1 receptor. *J Pharmacol Exp Ther* 301:1020-1024.
92. Piomelli, D. 2003. The molecular logic of endocannabinoid signalling. *Nat Rev Neurosci* 4:873-884.
93. McAllister, S.D., and Glass, M. 2002. CB(1) and CB(2) receptor-mediated signalling: a focus on endocannabinoids. *Prostaglandins Leukot Essent Fatty Acids* 66:161-171.
94. Kola, B., Hubina, E., Tucci, S.A., Kirkham, T.C., Garcia, E.A., Mitchell, S.E., Williams, L.M., Hawley, S.A., Hardie, D.G., Grossman, A.B., et al. 2005. Cannabinoids and ghrelin have both central and peripheral metabolic and cardiac effects via AMP-activated protein kinase. *J Biol Chem* 280:25196-25201.
95. Long, J.Z., Nomura, D.K., Vann, R.E., Walentiny, D.M., Booker, L., Jin, X., Burston, J.J., Sim-Selley, L.J., Lichtman, A.H., Wiley, J.L., et al. 2009. Dual blockade of FAAH and MAGL identifies behavioral processes regulated by endocannabinoid crosstalk in vivo. *Proc Natl Acad Sci U S A* 106:20270-20275.
96. Balster, R.L., and Prescott, W.R. 1992. Delta 9-tetrahydrocannabinol discrimination in rats as a model for cannabis intoxication. *Neurosci Biobehav Rev* 16:55-62.
97. Schmid, P.C., Zuzarte-Augustin, M.L., and Schmid, H.H. 1985. Properties of rat liver N-acylethanolamine amidohydrolase. *J Biol Chem* 260:14145-14149.
98. Cravatt, B.F., Giang, D.K., Mayfield, S.P., Boger, D.L., Lerner, R.A., and Gilula, N.B. 1996. Molecular characterization of an enzyme that degrades neuromodulatory fatty-acid amides. *Nature* 384:83-87.

99. Bracey, M.H., Hanson, M.A., Masuda, K.R., Stevens, R.C., and Cravatt, B.F. 2002. Structural adaptations in a membrane enzyme that terminates endocannabinoid signaling. *Science* 298:1793-1796.
100. Cravatt, B.F., Demarest, K., Patricelli, M.P., Bracey, M.H., Giang, D.K., Martin, B.R., and Lichtman, A.H. 2001. Supersensitivity to anandamide and enhanced endogenous cannabinoid signaling in mice lacking fatty acid amide hydrolase. *Proc Natl Acad Sci U S A* 98:9371-9376.
101. Smith, P.B., Compton, D.R., Welch, S.P., Razdan, R.K., Mechoulam, R., and Martin, B.R. 1994. The pharmacological activity of anandamide, a putative endogenous cannabinoid, in mice. *J Pharmacol Exp Ther* 270:219-227.
102. Kathuria, S., Gaetani, S., Fegley, D., Valino, F., Duranti, A., Tontini, A., Mor, M., Tarzia, G., La Rana, G., Calignano, A., et al. 2003. Modulation of anxiety through blockade of anandamide hydrolysis. *Nat Med* 9:76-81.
103. Di Marzo, V., Fontana, A., Cadas, H., Schinelli, S., Cimino, G., Schwartz, J.C., and Piomelli, D. 1994. Formation and inactivation of endogenous cannabinoid anandamide in central neurons. *Nature* 372:686-691.
104. Sugiura, T., Kondo, S., Sukagawa, A., Tonegawa, T., Nakane, S., Yamashita, A., Ishima, Y., and Waku, K. 1996. Transacylase-mediated and phosphodiesterase-mediated synthesis of N-arachidonoylethanolamine, an endogenous cannabinoid-receptor ligand, in rat brain microsomes. Comparison with synthesis from free arachidonic acid and ethanolamine. *Eur J Biochem* 240:53-62.
105. Cadas, H., di Tomaso, E., and Piomelli, D. 1997. Occurrence and biosynthesis of endogenous cannabinoid precursor, N-arachidonoyl phosphatidylethanolamine, in rat brain. *J Neurosci* 17:1226-1242.
106. Leung, D., Saghatelian, A., Simon, G.M., and Cravatt, B.F. 2006. Inactivation of N-acyl phosphatidylethanolamine phospholipase D reveals multiple mechanisms for the biosynthesis of endocannabinoids. *Biochemistry* 45:4720-4726.
107. Simon, G.M., and Cravatt, B.F. 2006. Endocannabinoid biosynthesis proceeding through glycerophospho-N-acyl ethanolamine and a role for alpha/beta-hydrolase 4 in this pathway. *J Biol Chem* 281:26465-26472.
108. Simon, G.M., and Cravatt, B.F. Characterization of mice lacking candidate N-acyl ethanolamine biosynthetic enzymes provides evidence for multiple pathways that contribute to endocannabinoid production in vivo. *Mol Biosyst*.
109. Simon, G.M., and Cravatt, B.F. 2008. Anandamide biosynthesis catalyzed by the phosphodiesterase GDE1 and detection of glycerophospho-N-acyl ethanolamine precursors in mouse brain. *J Biol Chem* 283:9341-9349.
110. Stella, N., Schweitzer, P., and Piomelli, D. 1997. A second endogenous cannabinoid that modulates long-term potentiation. *Nature* 388:773-778.
111. Higgs, H.N., and Glomset, J.A. 1994. Identification of a phosphatidic acid-preferring phospholipase A1 from bovine brain and testis. *Proc Natl Acad Sci U S A* 91:9574-9578.
112. Dinh, T.P., Carpenter, D., Leslie, F.M., Freund, T.F., Katona, I., Sensi, S.L., Kathuria, S., and Piomelli, D. 2002. Brain monoglyceride lipase participating in endocannabinoid inactivation. *Proc Natl Acad Sci U S A* 99:10819-10824.
113. Karlsson, M., Contreras, J.A., Hellman, U., Tornqvist, H., and Holm, C. 1997. cDNA cloning, tissue distribution, and identification of the catalytic triad of

monoglyceride lipase. Evolutionary relationship to esterases, lysophospholipases, and haloperoxidases. *J Biol Chem* 272:27218-27223.
114. Dinh, T.P., Freund, T.F., and Piomelli, D. 2002. A role for monoglyceride lipase in 2-arachidonoylglycerol inactivation. *Chem Phys Lipids* 121:149-158.
115. Dinh, T.P., Kathuria, S., and Piomelli, D. 2004. RNA interference suggests a primary role for monoacylglycerol lipase in the degradation of the endocannabinoid 2-arachidonoylglycerol. *Mol Pharmacol* 66:1260-1264.
116. Saario, S.M., Salo, O.M., Nevalainen, T., Poso, A., Laitinen, J.T., Jarvinen, T., and Niemi, R. 2005. Characterization of the sulfhydryl-sensitive site in the enzyme responsible for hydrolysis of 2-arachidonoyl-glycerol in rat cerebellar membranes. *Chem Biol* 12:649-656.
117. Long, J.Z., Li, W., Booker, L., Burston, J.J., Kinsey, S.G., Schlosburg, J.E., Pavon, F.J., Serrano, A.M., Selley, D.E., Parsons, L.H., et al. 2009. Selective blockade of 2-arachidonoylglycerol hydrolysis produces cannabinoid behavioral effects. *Nat Chem Biol* 5:37-44.
118. Blankman, J.L., Simon, G.M., and Cravatt, B.F. 2007. A comprehensive profile of brain enzymes that hydrolyze the endocannabinoid 2-arachidonoylglycerol. *Chem Biol* 14:1347-1356.
119. Greenberg, I., Kuehnle, J., Mendelson, J.H., and Bernstein, J.G. 1976. Effects of marihuana use on body weight and caloric intake in humans. *Psychopharmacology (Berl)* 49:79-84.
120. Hollister, L.E., and Reaven, G.M. 1974. Delta-9-tetrahydrocannabinol and glucose tolerance. *Clin Pharmacol Ther* 16:297-302.
121. Hezode, C., Zafrani, E.S., Roudot-Thoraval, F., Costentin, C., Hessami, A., Bouvier-Alias, M., Medkour, F., Pawlostky, J.M., Lotersztajn, S., and Mallat, A. 2008. Daily cannabis use: a novel risk factor of steatosis severity in patients with chronic hepatitis C. *Gastroenterology* 134:432-439.
122. Jayanthi, S., Buie, S., Moore, S., Herning, R.I., Better, W., Wilson, N.M., Contoreggi, C., and Cadet, J.L. Heavy marijuana users show increased serum apolipoprotein C-III levels: evidence from proteomic analyses. *Mol Psychiatry* 15:101-112.
123. Engeli, S., Bohnke, J., Feldpausch, M., Gorzelniak, K., Janke, J., Batkai, S., Pacher, P., Harvey-White, J., Luft, F.C., Sharma, A.M., et al. 2005. Activation of the peripheral endocannabinoid system in human obesity. *Diabetes* 54:2838-2843.
124. Bluher, M., Engeli, S., Kloting, N., Berndt, J., Fasshauer, M., Batkai, S., Pacher, P., Schon, M.R., Jordan, J., and Stumvoll, M. 2006. Dysregulation of the peripheral and adipose tissue endocannabinoid system in human abdominal obesity. *Diabetes* 55:3053-3060.
125. Russo, P., Strazzullo, P., Cappuccio, F.P., Tregouet, D.A., Lauria, F., Loguercio, M., Barba, G., Versiero, M., and Siani, A. 2007. Genetic variations at the endocannabinoid type 1 receptor gene (CNR1) are associated with obesity phenotypes in men. *J Clin Endocrinol Metab* 92:2382-2386.
126. Benzinou, M., Chevre, J.C., Ward, K.J., Lecoeur, C., Dina, C., Lobbens, S., Durand, E., Delplanque, J., Horber, F.F., Heude, B., et al. 2008. Endocannabinoid receptor 1 gene variations increase risk for obesity and modulate body mass index in European populations. *Hum Mol Genet* 17:1916-1921.

127. Sipe, J.C., Waalen, J., Gerber, A., and Beutler, E. 2005. Overweight and obesity associated with a missense polymorphism in fatty acid amide hydrolase (FAAH). *Int J Obes (Lond)* 29:755-759.
128. Despres, J.P., Golay, A., and Sjostrom, L. 2005. Effects of rimonabant on metabolic risk factors in overweight patients with dyslipidemia. *N Engl J Med* 353:2121-2134.
129. Pi-Sunyer, F.X., Aronne, L.J., Heshmati, H.M., Devin, J., and Rosenstock, J. 2006. Effect of rimonabant, a cannabinoid-1 receptor blocker, on weight and cardiometabolic risk factors in overweight or obese patients: RIO-North America: a randomized controlled trial. *Jama* 295:761-775.
130. Scheen, A.J., Finer, N., Hollander, P., Jensen, M.D., and Van Gaal, L.F. 2006. Efficacy and tolerability of rimonabant in overweight or obese patients with type 2 diabetes: a randomised controlled study. *Lancet* 368:1660-1672.
131. Van Gaal, L.F., Rissanen, A.M., Scheen, A.J., Ziegler, O., and Rossner, S. 2005. Effects of the cannabinoid-1 receptor blocker rimonabant on weight reduction and cardiovascular risk factors in overweight patients: 1-year experience from the RIO-Europe study. *Lancet* 365:1389-1397.
132. Baye, T.M., Zhang, Y., Smith, E., Hillard, C.J., Gunnell, J., Myklebust, J., James, R., Kissebah, A.H., Olivier, M., and Wilke, R.A. 2008. Genetic variation in cannabinoid receptor 1 (CNR1) is associated with derangements in lipid homeostasis, independent of body mass index. *Pharmacogenomics* 9:1647-1656.
133. Van Gaal, L.F., Scheen, A.J., Rissanen, A.M., Rossner, S., Hanotin, C., and Ziegler, O. 2008. Long-term effect of CB1 blockade with rimonabant on cardiometabolic risk factors: two year results from the RIO-Europe Study. *Eur Heart J* 29:1761-1771.
134. Nissen, S.E., Nicholls, S.J., Wolski, K., Rodes-Cabau, J., Cannon, C.P., Deanfield, J.E., Despres, J.P., Kastelein, J.J., Steinhubl, S.R., Kapadia, S., et al. 2008. Effect of rimonabant on progression of atherosclerosis in patients with abdominal obesity and coronary artery disease: the STRADIVARIUS randomized controlled trial. *Jama* 299:1547-1560.
135. Arnone, M., Maruani, J., Chaperon, F., Thiebot, M.H., Poncelet, M., Soubrie, P., and Le Fur, G. 1997. Selective inhibition of sucrose and ethanol intake by SR 141716, an antagonist of central cannabinoid (CB1) receptors. *Psychopharmacology (Berl)* 132:104-106.
136. Colombo, G., Agabio, R., Diaz, G., Lobina, C., Reali, R., and Gessa, G.L. 1998. Appetite suppression and weight loss after the cannabinoid antagonist SR 141716. *Life Sci* 63:PL113-117.
137. Simiand, J., Keane, M., Keane, P.E., and Soubrie, P. 1998. SR 141716, a CB1 cannabinoid receptor antagonist, selectively reduces sweet food intake in marmoset. *Behav Pharmacol* 9:179-181.
138. Cota, D., Marsicano, G., Tschop, M., Grubler, Y., Flachskamm, C., Schubert, M., Auer, D., Yassouridis, A., Thone-Reineke, C., Ortmann, S., et al. 2003. The endogenous cannabinoid system affects energy balance via central orexigenic drive and peripheral lipogenesis. *J Clin Invest* 112:423-431.
139. Osei-Hyiaman, D., DePetrillo, M., Pacher, P., Liu, J., Radaeva, S., Batkai, S., Harvey-White, J., Mackie, K., Offertaler, L., Wang, L., et al. 2005.

Endocannabinoid activation at hepatic CB1 receptors stimulates fatty acid synthesis and contributes to diet-induced obesity. *J Clin Invest* 115:1298-1305.
140. Pagano, C., Pilon, C., Calcagno, A., Urbanet, R., Rossato, M., Milan, G., Bianchi, K., Rizzuto, R., Bernante, P., Federspil, G., et al. 2007. The endogenous cannabinoid system stimulates glucose uptake in human fat cells via phosphatidylinositol 3-kinase and calcium-dependent mechanisms. *J Clin Endocrinol Metab* 92:4810-4819.
141. Siegmund, S.V., Qian, T., de Minicis, S., Harvey-White, J., Kunos, G., Vinod, K.Y., Hungund, B., and Schwabe, R.F. 2007. The endocannabinoid 2-arachidonoyl glycerol induces death of hepatic stellate cells via mitochondrial reactive oxygen species. *Faseb J* 21:2798-2806.
142. Matias, I., Gonthier, M.P., Orlando, P., Martiadis, V., De Petrocellis, L., Cervino, C., Petrosino, S., Hoareau, L., Festy, F., Pasquali, R., et al. 2006. Regulation, function, and dysregulation of endocannabinoids in models of adipose and beta-pancreatic cells and in obesity and hyperglycemia. *J Clin Endocrinol Metab* 91:3171-3180.
143. Bensaid, M., Gary-Bobo, M., Esclangon, A., Maffrand, J.P., Le Fur, G., Oury-Donat, F., and Soubrie, P. 2003. The cannabinoid CB1 receptor antagonist SR141716 increases Acrp30 mRNA expression in adipose tissue of obese fa/fa rats and in cultured adipocyte cells. *Mol Pharmacol* 63:908-914.
144. Jbilo, O., Ravinet-Trillou, C., Arnone, M., Buisson, I., Bribes, E., Peleraux, A., Penarier, G., Soubrie, P., Le Fur, G., Galiegue, S., et al. 2005. The CB1 receptor antagonist rimonabant reverses the diet-induced obesity phenotype through the regulation of lipolysis and energy balance. *Faseb J* 19:1567-1569.
145. Buettner, C., Muse, E.D., Cheng, A., Chen, L., Scherer, T., Pocai, A., Su, K., Cheng, B., Li, X., Harvey-White, J., et al. 2008. Leptin controls adipose tissue lipogenesis via central, STAT3-independent mechanisms. *Nat Med* 14:667-675.
146. Osei-Hyiaman, D., Liu, J., Zhou, L., Godlewski, G., Harvey-White, J., Jeong, W.I., Batkai, S., Marsicano, G., Lutz, B., Buettner, C., et al. 2008. Hepatic CB1 receptor is required for development of diet-induced steatosis, dyslipidemia, and insulin and leptin resistance in mice. *J Clin Invest* 118:3160-3169.
147. Jeong, W.I., Osei-Hyiaman, D., Park, O., Liu, J., Batkai, S., Mukhopadhyay, P., Horiguchi, N., Harvey-White, J., Marsicano, G., Lutz, B., et al. 2008. Paracrine activation of hepatic CB1 receptors by stellate cell-derived endocannabinoids mediates alcoholic fatty liver. *Cell Metab* 7:227-235.
148. Liu, Y.L., Connoley, I.P., Wilson, C.A., and Stock, M.J. 2005. Effects of the cannabinoid CB1 receptor antagonist SR141716 on oxygen consumption and soleus muscle glucose uptake in Lep(ob)/Lep(ob) mice. *Int J Obes (Lond)* 29:183-187.
149. Watanabe, T., Kubota, N., Ohsugi, M., Kubota, T., Takamoto, I., Iwabu, M., Awazawa, M., Katsuyama, H., Hasegawa, C., Tokuyama, K., et al. 2009. Rimonabant ameliorates insulin resistance via both adiponectin-dependent and adiponectin-independent pathways. *J Biol Chem* 284:1803-1812.

CHAPTER 2
VLDL hydrolysis by LpL activates PPAR-α through generation of unbound fatty acids.

ABSTRACT

Recent evidence suggests that lipoproteins serve as circulating reservoirs of PPAR α ligands that are accessible through lipolysis. The present study was conducted to determine the biochemical basis of PPAR α activation by lipolysis products and their contribution to PPAR α function *in vivo*. PPAR-α activation was measured in bovine aortic endothelial cells (BAEC) following treatment with human plasma, VLDL lipolysis products, or oleic acid. While plasma failed to activate PPAR α, oleic acid performed similarly to VLDL lipolysis products. Therefore, fatty acids are likely to be the PPAR α ligands generated by VLDL lipolysis. Indeed, unbound fatty acid concentration determined PPAR-α activation regardless of fatty acid source, with PPAR α activation occurring only at unbound fatty acid concentrations that are unachievable under physiological conditions without lipase action. In mice, a synthetic lipase inhibitor (poloxamer-407) attenuated fasting-induced changes in expression of PPAR α target genes. Apolipoprotein CIII (apoCIII), an endogenous inhibitor of lipoprotein and hepatic lipase, regulated access to the lipoprotein pool of PPAR α ligands, since addition of exogenous apo CIII inhibited, and removal of endogenous apoCIII potentiated, lipolytic PPAR-α activation. These data suggest that the PPAR α response is generated by unbound fatty acids released locally by lipase activity and not by circulating plasma fatty acids.

INTRODUCTION

The peroxisomal proliferator activated receptor (PPAR) family of nuclear hormone receptors functions as transcriptional nodal points in the regulation of energy metabolism and inflammation (1). Three PPAR isotypes have been identified: PPAR α and PPAR δ, which stimulate fatty acid oxidation and share many target genes, but still differ in tissue distribution and functional effects, and PPAR-γ which activates lipid storage and adipogenesis. *In vitro* analyses demonstrate that PPARs are activated by high concentrations of fatty acids and their derivatives although the physiological context and relevance of these effects have remained unclear (2, 3). Together these data have led to the view of PPARs as lipid sensors; despite this, the upstream factors determining generation and delivery of the lipid ligands are poorly understood.

Intracellular fatty acids can be generated by three main sources: *de novo* lipogenesis, enzymatic hydrolysis, or uptake from extracellular sources. Plasma non-esterified fatty acids (NEFA) circulate bound to albumin or can be generated locally by vascular lipases acting on lipoproteins. Lipolytic processing of lipoproteins appears to be an important source of PPAR α and δ ligands as reported by us and others (4-6). *In vitro,* lipoprotein lipase (LpL) mediated lipolysis of VLDL stimulates PPAR α and PPAR δ activity and downstream responses, while similar quantities of NEFA from plasma fail to recapitulate these effects (4-6). Lipolysis of HDL by endothelial lipase also generates PPAR α ligands (7). In mouse models, transgenic LpL overexpression and treatment with a pharmacological LPL activator, NO-1886, indicate that LpL lipolytic products are sufficient to promote PPAR α dependent peroxisomal proliferation and induction of PPAR α target genes; likewise, cardiac specific LpL-deficient animals have reduced expression of PPAR α target genes (6, 8, 9). Together these data reveal that specific lipoproteins serve as circulating pools of PPAR α and δ ligands.

The unexplained observation that VLDL lipolysis products activate PPAR α while NEFA from plasma do not remains a key unresolved issue in understanding how FAs and their handling influence cellular responses. Differences in chemical composition could potentially account for the effective activation of PPAR α by triglyceride-rich lipoprotein lipolysis metabolites as opposed to plasma NEFA. For example, VLDLs contain retinoids, phospholipids, and other non-fatty acid compounds that may play a role in activating PPAR α. Alternatively, the source and delivery of the fatty acid may alter its cellular metabolism and signaling properties. For example, arachidonic acid released by phospholipase A2-mediated cleavage of phospholipids is preferentially channeled to eicosanoid biosynthesis. Therefore, it is possible that differences in chemistry or delivery of lipolysis products underlie their preferential activation of PPAR α. Moreover, the activity of LPL is under the control of multiple additional inputs, including the action of apoCIII, an endogenous LPL inhibitor. Whether regulators of LPL activity such as apoCIII modulate PPAR activity remains unknown. In the current study we assessed the biochemical basis of lipolytic PPAR α activation, the role of apoCIII in determining PPAR α activity, and the evidence for their contribution to PPAR α function *in vivo*.

MATERIALS AND METHODS

Cell culture, PPAR α Reporter, & Fatty Acid Uptake

Bovine aortic endothelial cells (BAEC) were transfected with a PPAR α transactivation assay as previously described (6). Briefly, BAEC were grown in Dulbecco's Modified Eagle's Medium (Invitrogen) supplemented with 10% fetal bovine serum (Omega

Scientific), penicillin/streptomycin (Invitrogen), and L-glutamine (Invitrogen). Cells were seeded in 24-well plates and transfected with three plasmids using Fugene HD transfection reagent (Roche Diagnostics): (1) PPAR α ligand binding domain fused to yeast Gal4 DNA binding domain, (2) a luciferase reporter under the control of a GAL4 promoter, and (3) constitutively expressed β-galactosidase (6). 24 hours after transfection, cells were treated as indicated for 18 hours. Cells were harvested and luciferase and β-galactosidase activity were measured by addition of substrate, luciferin (BD Biosciences) and chlorophenol red β-galactoside (Sigma) respectively, with quantification of resulting photoemission or absorbance. PPAR α activation was calculated as the ratio of luciferase activity to β-galactosidase activity (10). Cell culture medium was analyzed for NEFA content using an enzymatic colorimetric kit (Wako) (11). The equilibrium concentration of unbound oleate was calculated as described by Spector et al (12). To assess fatty acid uptake, BAEC were incubated with 90 μM unlabeled oleic acid spiked with 9,10-^{3}H oleic acid (1 μCi per well; 33.4 Ci/mmol; Perkin Elmer) or 10 μg/ml VLDL labelled, as previously described, with ^{3}H trioleate (Perkin Elmer) as indicated for 20 minutes (13). Cells were washed with ice-cold PBS and lysed with 0.1 M NaOH. Cell lysate was analyzed for protein concentration and cell associated CPM (5). All experiments were performed in triplicate.

Lipoprotein Isolation and Characterization

All plasma samples were obtained by the Cholesterol Research Center at Children's Hospital Oakland Research Institute. Blood was collected from healthy subjects after an overnight fast. The protocol was approved by the Institutional Review Board of Children's Hospital and Research Center Oakland, and informed consent was obtained from all volunteers. An aliquot of plasma was added to an immunoaffinity column prepared from purified goat anti-human apolipoprotein CIII sera (International Immunology Corp.) covalently linked to Affigel-10 (BioRad Laboratories) following manufacturer's instructions. Following overnight incubation at 4°C, the unbound fraction, depleted of apoCIII containing particles, was collected and concentrated (14). VLDLs were isolated from plasma or the unbound immunoaffinity column fraction by ultracentrifugation ($d<1.006$, 40,000 rpm, 24 hours). Apo B was measured by immunoturbidimetric assay (Bacton Assay Systems and Express 550 Plus analyzer). ApoCIII was measured in triplicate by sandwich-style enzyme-linked immunosorbent assay with purchased goat anti-human apo C-III (International Immunology Corp) (14). Triglyceride content was quantified by enzymatic end point assay (Sigma) (15).

In Vivo Experiments

Male C57BL6 mice were fasted for 2 hours prior to treatment and divided into three groups (n=5 per group). Group 1 (Fed) were injected with saline and returned to ad libidum feeding. Group 2 (Fasted) were injected with saline and fasted for 24 h. Group 3 (Fasted + P-407) were injected with poloxamer-407 (500 mg/kg, i.p.) and fasted for 24 h (16). Animals were sacrificed, and all harvested tissues and plasma samples were stored at -80°. The treatment protocol was approved by the Institutional Animal Care and Use Committee (IACUC) at the University of Missouri-Kansas City. RNA was isolated from homogenized tissue using the QAIGEN RNAeasy kit (Qiagen) (17). Relative quantitative PCR was performed on the ABI7900 system using SYBR green master mix in triplicate (Applied Biosystems) (18). All genes were normalized to an endogenous control gene (gusb). The primers used were: pmp70: 5'-TGTTCAGGACTGGATGGATG-3'

(forward), 5'-TGGCAAACTGGGGTTTATG -3'(reverse); cd36: 5'-GCTTGCAAATCCAAGAATG-3'(forward), 5'- CGGCTTTACCAAAGATGTAGC-3' (reverse); pparα: 5'-CCTGAACATCGAGTGTCGAA-3'(forward), 5'-CAGCTCCGATCACACTTGTC-3' (reverse); mlycd: 5'-CTCGGGACCTTCCTCATAAA-3'(forward), 5'- ATAGGCGACAGGCTTGAAAA-3' (reverse); cpt1a: 5'-ACGGAGTCCTGCAACTTTGT-3'(forward), 5'-GTACAGGTGCTGGTGCTTTTC-3' (reverse); mcad: 5'-GCCCAGAGAGCTCTAGACGA-3'(forward), 5'-GTTCAACCTTCATCGCCATT-3' (reverse); cpt1b: 5'-CCAGATCTGCATGTTTGACC-3'(forward), 5'-TGCTGGAGATGTGGAAGAA-3' (reverse); acox: 5'-CATGCGGATTAATGAGAGCA-3'(forward), 5'- TCCGACATTCTTCGATACCA-3' (reverse); lpl: 5'-CAAGAGAAGCAGCAAGAT-3'(forward), 5'-CACTGTGCCGTACAGAGAA-3' (reverse); gusb: 5'-CATGAGAGTGGTGTTGAG GATCA-3'(forward), 5'-CCCATTCACCCACACAACTG-3' (reverse)

Statistical Analysis

One-way ANOVA with post hoc analysis (Tukey's HSD) was used to test for differences in treatment effects. Paired two tailed t-tests were used to analyze differences in PPAR α activation between lipoprotein fractions isolated from the same donor. All analyses were performed using JMP version 7.0 (SAS institute Inc.). Data are presented as mean ± standard error.

RESULTS

Albumin inhibits PPAR α activation by VLDL lipolytic products.

To test if differences in chemistry explain the disparity in PPAR α activation observed with plasma and lipolysis products, the ability of LPL/VLDL, oleic acid, and plasma to stimulate PPAR α was evaluated on a molar basis in BAEC. Oleic acid activated PPAR α similarly to VLDL lipolytic products, while plasma failed to activate PPAR α despite the presence of fatty acids (Fig. 1A). Given that oleic acid is the major fatty acid in plasma, the ability of VLDL to activate PPAR α in preference to plasma likely results from differential delivery rather than chemistry. To test if LPL/VLDL mediated PPAR α activation depends on the generation of unbound fatty acids, BAEC were incubated with LPL/VLDL and increasing concentrations of albumin. Albumin in combination with LPL/VLDL decreased PPAR α activation in a concentration-dependent fashion with half-maximal inhibition at 0.014 mM albumin (Fig. 1B). To ensure that albumin inhibited delivery of FA and did not influence PPAR α activity directly, the effect of albumin on PPAR α activation by a synthetic ligand, WY14643. PPAR α activation by WY14643 was not altered by addition of 0.015 mM albumin (WY14643: 33.85 ±.78 vs WY14643 + albumin: 33.00 ± .57 fold, p=0.51).

Unbound fatty acid concentration determines fatty acid uptake and PPAR α activation.

While at low oleic acid levels (as in Fig 1a), fatty acid uptake is related to total concentration, at physiological NEFA levels the unbound fatty acid concentration becomes the major determinant of uptake (19). To determine the relationship between fatty acid uptake and PPAR α activation, fatty acid uptake and PPAR α reporter activity were measured in parallel in BAEC treated with varying concentrations of unbound oleic acid generated by varying the albumin content added to 90 μM oleic acid. As expected, both fatty acid uptake and PPAR α activation increased with unbound oleic acid

concentration (Fig. 2A); however, the two variables displayed markedly different kinetics with half-maximal values achieved at 21 nM for fatty acid uptake and 286 nM for PPAR α activation. Further experiments with varied unbound oleic acid concentrations revealed that fatty acid uptake above 300 pmol/mg protein/min displayed a linear relationship with PPAR α activation (Fig. 2B). Interestingly, fatty acid uptake above 300 pmol/mg protein/min was unachievable at physiological unbound fatty acids concentrations (~6-30 nM), explaining the failure of plasma NEFA to activate PPAR α (19, 20). Conversely, VLDL (10 μg/ml) treated with LpL (10 units/ml) generated fatty acid uptake (463 ± 2 pmol/mg protein/min) sufficient to activate PPAR α.

Lipase inhibition prevents fasting-induced increases in PPAR α target genes *in vivo*

To test the contribution of lipase action to the *in vivo* generation of PPAR α ligands, the transcriptional response of PPAR α target genes to fasting was quantified in mice treated with a lipase inhibitor, the nonionic detergent Poloxamer-407 (P-407), or vehicle control at the outset of a 24-hr fast. Fasting decreased triglyceride concentrations (75 ± 14 vs. 40 ± 6 mg/dl, $p<0.05$), while P-407 caused severe hypertriglyceridemia (3578 ± 798 mg/dl). In addition, fasting increased hepatic and cardiac expression of a PPAR α target gene cassette including *pparα, cd36, acox, mlycd, mcad, pmp70, cpt1a, and cpt1b* (Fig. 3A and 3B). In mice treated with P-407, hepatic transcriptional changes in response to fasting were absent for *mlycd and cd36*, diminished for *pmp70*, and unchanged for *mcad, pparα, acox and cpt1b* (Fig. 3A). P-407 treatment prevented the fasting response for all PPAR α target genes tested in the heart (Fig. 3B).

Apolipoprotein CIII inhibits the lipolytic generation of PPAR α ligands.

Since modifiers of lipolytic activity may also alter downstream PPAR α activation, the role of apoCIII, a natural inhibitor of LpL, in regulating lipolytic availability of PPAR α ligands was examined. Addition of apoCIII or orlistat, a synthetic lipase inhibitor, to VLDL decreased the resulting PPAR α activation, concurrent with decreased release of NEFA into the cell culture media (Fig. 4A). To determine if changes in endogenous apoCIII content alter lipolytic accessibility to PPAR α ligands, PPAR α activation in response to VLDL particles depleted of apoCIII by immunoaffinity chromatography was compared to activation in response to total VLDL isolated from the same plasma. Immunoaffinity chromatography depleted VLDL of the majority (86.2 ± 5.8%) of apoCIII. Transfected BAEC were incubated with VLDL or apoCIII depleted VLDL from the same donor. ApoCIII depleted VLDL particles activated PPAR α to a significantly greater extent than the VLDL particles derived from the same donor sample (Fig. 4B).

DISCUSSION

The data presented here demonstrate the biochemical basis for the activation of PPAR α by lipolysis of triglyceride-rich lipoproteins. On a molar basis, LPL lipolysis products activate PPAR α similarly to oleic acid, the most abundant plasma fatty acid. Thus more efficient delivery, rather than chemistry, likely accounts for preferential PPAR α activation by VLDL lipolysis products. Addition of albumin to the LPL/VLDL treatment abrogates PPAR α activation, indicating that lipolysis products activate PPAR α by generating unbound fatty acids. Since fatty acids must be liberated from albumin prior to becoming available for tissue uptake, the unbound fatty acid concentration is a major determinant of subsequent uptake (19). Our results show that significant fatty acid uptake must occur prior to activation of PPAR-α. In fact, PPAR α activation requires a threshold of fatty acid uptake that is unachievable at physiological plasma unbound fatty

acid concentrations. This offers a simple explanation for the failure of plasma to activate PPAR α despite the presence of ample fatty acids. Conversely, at physiological ratios of triglyceride to albumin, lipase action generates an unbound fatty acid concentration sufficient to drive fatty acid uptake beyond the PPAR α activation threshold. This is demonstrated by the ability of plasma exposed to lipase *in vivo* or *in vitro* to activate PPAR α (6). However, this work was done in an artificial gene reporter system and does not directly demonstrate PPAR α ligand binding.

The biphasic relationship between FA uptake and PPAR α activation may represent different routes of FA uptake. FA uptake is the sum of saturable and linear processes (21). FA uptake in the physiological range of unbound fatty acids is largely driven by the saturable process and, in the current study, failed to activate PPAR α. The saturable process likely represents the action of fatty acid transporters, such as CD36. Intriguingly, loss of CD36 *in vivo* or *in vitro* decreases lipid uptake without altering PPAR α activation (22, 23). Thus, plasma NEFA may fail to activate PPAR α because they are largely taken up by CD36. However, at the higher unbound fatty acid concentrations achieved in the lipolytic microenvironment, a CD36 independent route of FA uptake may become active and lead to PPAR α activation. This CD36 independent route of FA uptake may reflect the action of other FA transporters, such as the fatty acid transport proteins, or non-protein mediated fatty acid uptake. The nature of the alternate route of FA uptake and how it may target FAs to the nucleus for signaling requires further study.

These data suggest that VLDL can serve as a potent source of PPAR α ligands by generating high local concentrations of unbound fatty acids. Although tracer studies have shown that fatty acids derived from lipolysis of triglyceride-rich lipoproteins mix with plasma NEFAs, fatty acid uptake is regulated by the tissue specific activity of LpL, likely as a result of the high concentration of unbound fatty acids generated in the microenviroment surrounding active LpL (24). In fact, LpL activity has been shown to contribute a large portion of the FAs consumed by the heart and other tissues (25, 26).

Thus, increased lipase activity, and not the increased release of NEFA from adipose tissue, is likely to be responsible for increased PPAR α function in the fasted state. This is supported by our finding that injection of the nonionic detergent P-407 inhibits fasting-induced increases in PPAR α gene expression. As P-407 inhibits lipoprotein, endothelial and hepatic lipase, the resulting alterations in PPAR α signaling cannot be attributed to the action of a specific lipase. Although many hormonal signalling pathways are altered during the transition to the fasting state, fasting-induced increases in several genes (*mcad, acox, and cpt1b*) are known to be dependent on PPAR α (27). Increased hepatic expression of *mlycd, pmp70, and cd36* in response to fasting was substantially prevented by P-407 administration. The absence of an effect on *cpt1a* is consistent with data from studies in PPAR α deficient mice (27, 28). In the heart, we showed that P-407 attenuated fasting-induced increases in expression of the PPAR α target genes that were tested. Together with the *in vitro* data, these findings suggest that lipase activity is necessary to activate PPAR α. Although these data are consistent with our model, P-407 is not a specific inhibitor of lipase activity and other effects may confound our results. However, P-407 does not inhibit fatty acid uptake or intracellular lipase activity and has no direct effects on PPAR α function (29-31). Furthermore, LpL deficiency decreases expression of PPAR α target genes and mitigates cardiac myopathy induced by PPAR α

overexpression (22). The current study supports the importance of LpL in PPAR α activation *in vivo* and builds upon the genetic models to demonstrate that pharmacological inhibition of LpL limits PPAR α activation by endogenous mechanisms.

A number of other observations support a key role of lipase activities in the generation of PPAR ligands. Lipolysis of HDL by endothelial lipase increases *acox* expression and inhibits leukocyte adhesion in a PPAR α dependent manner (7). Cardiac specific LpL knockout animals display reduced cardiac expression of PPAR α target genes despite increased uptake of plasma NEFA (25, 32). Conversely, mice over-expressing lipoprotein lipase in skeletal muscle, but not those overexpressing CD36, display peroxisomal and mitochondrial proliferation, increased oxidative fibers, and cold-tolerance, hallmarks of PPAR α and δ activation (33, 34). Chronic exposure to heparin-releasable lipase activity also increases mitochondrial proliferation and binding of PPAR δ to the PPAR response element in the cpt1b promoter in skeletal muscle (35). NO-1886, a pharmacological LpL stimulator, activates fatty acid oxidation genes and protects against high-fat induced weight gain and hepatic steatosis, effects closely resembling those seen with PPAR α activation (9). Likewise, the activity of LpL in skeletal muscle has been shown to regulate uncoupling protein 3, a PPAR α and δ responsive gene, independent of NEFA levels (36). Taken together these findings in animal models support the role of lipolysis products as determinants of PPAR α and δ function irrespective of plasma NEFA levels.

While our results focus on the delivery of PPAR α ligands from extracellular sources, intracellular fatty acids generated by *de novo* lipogenesis or enzymatic hydrolysis may also activate PPAR α. Impaired PPAR α dependent gene expression in hepatocyte-specific fatty acid synthase-deficient mice suggests a specific role for *de novo* lipogenesis products as PPAR α ligands (37). The relevant FAS product bound to PPAR α was recently identified as 16:0/18:1-GPC (38). Hepatocyte specific knockout of another lipogenic enzyme, acetyl CoA carboxylase 1, had no effect on PPAR α dependent gene expression, suggesting that alternative sources of PPAR α ligands exist (39). Accordingly, recent *in vitro* work has shown that genetic manipulation of access to hepatic lipid droplets alters PPAR α activity (40). Given the potential for intracellular generation of PPAR α ligands, our findings may be particularly relevant to cells with low rates of lipogenesis and small TG stores.

The evidence for LPL-mediated PPAR α activation suggests that other parameters that determine LPL activity might also influence PPAR α activation. The biochemical function of apoCIII makes it a likely candidate for modulation of lipolytic PPAR α and δ activation. ApoCIII, an 8.8-kDa exchangeable apolipoprotein, is linked to metabolic and cardiovascular disease by strong epidemiological and genetic data, but the biology underlying these observations remains incompletely understood (41). *In vitro*, apoCIII inhibits lipoprotein lipase, hepatic lipase, heparin sulfate proteoglycan interactions, and hepatic receptor mediated clearance (42). Recently, apoCIII has been found to have a number of proinflammatory properties including activation of toll-like receptor 2 (43). The present findings demonstrate that apoCIII can play an additional role in PPAR α mediated metabolic and inflammatory functions by controlling lipolytic generation of PPAR α ligands. Since apoCIII expression is suppressed and LpL activity is stimulated by PPAR α, a positive feedback system may exist (44). Individuals with high apoCIII

levels may have impaired generation of endogenous PPAR α ligands and hence be particularly likely to benefit from synthetic PPAR α ligands.

In summary, our results demonstrate that lipolysis of VLDL provides the unbound fatty acid concentration required for activation of PPAR α by an extracellular source and that apoCIII is an important player in modulating this process. Future efforts will characterize the CD36-independent route of FA uptake activated at high-unbound FA concentrations that is responsible for PPAR α activation by extracellular sources.

REFERENCES

1. Brown, J.D., and Plutzky, J. 2007. Peroxisome proliferator-activated receptors as transcriptional nodal points and therapeutic targets. *Circulation* 115:518-533.
2. Kliewer, S.A., Sundseth, S.S., Jones, S.A., Brown, P.J., Wisely, G.B., Koble, C.S., Devchand, P., Wahli, W., Willson, T.M., Lenhard, J.M., et al. 1997. Fatty acids and eicosanoids regulate gene expression through direct interactions with peroxisome proliferator-activated receptors alpha and gamma. *Proc Natl Acad Sci U S A* 94:4318-4323.
3. Forman, B.M., Chen, J., and Evans, R.M. 1997. Hypolipidemic drugs, polyunsaturated fatty acids, and eicosanoids are ligands for peroxisome proliferator-activated receptors alpha and delta. *Proc Natl Acad Sci U S A* 94:4312-4317.
4. Chawla, A., Lee, C.H., Barak, Y., He, W., Rosenfeld, J., Liao, D., Han, J., Kang, H., and Evans, R.M. 2003. PPARdelta is a very low-density lipoprotein sensor in macrophages. *Proc Natl Acad Sci U S A* 100:1268-1273.
5. Lee, C.H., Kang, K., Mehl, I.R., Nofsinger, R., Alaynick, W.A., Chong, L.W., Rosenfeld, J.M., and Evans, R.M. 2006. Peroxisome proliferator-activated receptor delta promotes very low-density lipoprotein-derived fatty acid catabolism in the macrophage. *Proc Natl Acad Sci U S A* 103:2434-2439.
6. Ziouzenkova, O., Perrey, S., Asatryan, L., Hwang, J., MacNaul, K.L., Moller, D.E., Rader, D.J., Sevanian, A., Zechner, R., Hoefler, G., et al. 2003. Lipolysis of triglyceride-rich lipoproteins generates PPAR ligands: evidence for an antiinflammatory role for lipoprotein lipase. *Proc Natl Acad Sci U S A* 100:2730-2735.
7. Ahmed, W., Orasanu, G., Nehra, V., Asatryan, L., Rader, D.J., Ziouzenkova, O., and Plutzky, J. 2006. High-density lipoprotein hydrolysis by endothelial lipase activates PPARalpha: a candidate mechanism for high-density lipoprotein-mediated repression of leukocyte adhesion. *Circ Res* 98:490-498.
8. Augustus, A.S., Buchanan, J., Park, T.S., Hirata, K., Noh, H.L., Sun, J., Homma, S., D'Armiento, J., Abel, E.D., and Goldberg, I.J. 2006. Loss of lipoprotein lipase-derived fatty acids leads to increased cardiac glucose metabolism and heart dysfunction. *J Biol Chem* 281:8716-8723.
9. Doi, M., Kondo, Y., and Tsutsumi, K. 2003. Lipoprotein lipase activator NO-1886 (ibrolipim) accelerates the mRNA expression of fatty acid oxidation-related enzymes in rat liver. *Metabolism* 52:1547-1550.
10. Ziouzenkova, O., Asatryan, L., Sahady, D., Orasanu, G., Perrey, S., Cutak, B., Hassell, T., Akiyama, T.E., Berger, J.P., Sevanian, A., et al. 2003. Dual roles for lipolysis and oxidation in peroxisome proliferation-activator receptor responses to electronegative low density lipoprotein. *J Biol Chem* 278:39874-39881.
11. Yu, J.G., Javorschi, S., Hevener, A.L., Kruszynska, Y.T., Norman, R.A., Sinha, M., and Olefsky, J.M. 2002. The effect of thiazolidinediones on plasma adiponectin levels in normal, obese, and type 2 diabetic subjects. *Diabetes* 51:2968-2974.
12. Spector, A.A., Fletcher, J.E., and Ashbrook, J.D. 1971. Analysis of long-chain free fatty acid binding to bovine serum albumin by determination of stepwise equilibrium constants. *Biochemistry* 10:3229-3232.

13. Seo, T., Al-Haideri, M., Treskova, E., Worgall, T.S., Kako, Y., Goldberg, I.J., and Deckelbaum, R.J. 2000. Lipoprotein lipase-mediated selective uptake from low density lipoprotein requires cell surface proteoglycans and is independent of scavenger receptor class B type 1. *J Biol Chem* 275:30355-30362.
14. Olin-Lewis, K., Krauss, R.M., La Belle, M., Blanche, P.J., Barrett, P.H., Wight, T.N., and Chait, A. 2002. ApoC-III content of apoB-containing lipoproteins is associated with binding to the vascular proteoglycan biglycan. *J Lipid Res* 43:1969-1977.
15. Campos, E., Kotite, L., Blanche, P., Mitsugi, Y., Frost, P.H., Masharani, U., Krauss, R.M., and Havel, R.J. 2002. Properties of triglyceride-rich and cholesterol-rich lipoproteins in the remnant-like particle fraction of human blood plasma. *J Lipid Res* 43:365-374.
16. Millar, J.S., Cromley, D.A., McCoy, M.G., Rader, D.J., and Billheimer, J.T. 2005. Determining hepatic triglyceride production in mice: comparison of poloxamer 407 with Triton WR-1339. *J Lipid Res* 46:2023-2028.
17. Nomura, I., Goleva, E., Howell, M.D., Hamid, Q.A., Ong, P.Y., Hall, C.F., Darst, M.A., Gao, B., Boguniewicz, M., Travers, J.B., et al. 2003. Cytokine milieu of atopic dermatitis, as compared to psoriasis, skin prevents induction of innate immune response genes. *J Immunol* 171:3262-3269.
18. Yin, J.L., Shackel, N.A., Zekry, A., McGuinness, P.H., Richards, C., Putten, K.V., McCaughan, G.W., Eris, J.M., and Bishop, G.A. 2001. Real-time reverse transcriptase-polymerase chain reaction (RT-PCR) for measurement of cytokine and growth factor mRNA expression with fluorogenic probes or SYBR Green I. *Immunol Cell Biol* 79:213-221.
19. Sorrentino, D., Robinson, R.B., Kiang, C.L., and Berk, P.D. 1989. At physiologic albumin/oleate concentrations oleate uptake by isolated hepatocytes, cardiac myocytes, and adipocytes is a saturable function of the unbound oleate concentration. Uptake kinetics are consistent with the conventional theory. *J Clin Invest* 84:1325-1333.
20. Richieri, G.V., and Kleinfeld, A.M. 1995. Unbound free fatty acid levels in human serum. *J Lipid Res* 36:229-240.
21. Stump, D.D., Nunes, R.M., Sorrentino, D., Isola, L.M., and Berk, P.D. 1992. Characteristics of oleate binding to liver plasma membranes and its uptake by isolated hepatocytes. *J Hepatol* 16:304-315.
22. Duncan, J.G., Bharadwaj, K.G., Fong, J.L., Mitra, R., Sambandam, N., Courtois, M.R., Lavine, K.J., Goldberg, I.J., and Kelly, D.P. Rescue of cardiomyopathy in peroxisome proliferator-activated receptor-alpha transgenic mice by deletion of lipoprotein lipase identifies sources of cardiac lipids and peroxisome proliferator-activated receptor-alpha activators. *Circulation* 121:426-435.
23. Yang, J., Sambandam, N., Han, X., Gross, R.W., Courtois, M., Kovacs, A., Febbraio, M., Finck, B.N., and Kelly, D.P. 2007. CD36 deficiency rescues lipotoxic cardiomyopathy. *Circ Res* 100:1208-1217.
24. Teusink, B., Voshol, P.J., Dahlmans, V.E., Rensen, P.C., Pijl, H., Romijn, J.A., and Havekes, L.M. 2003. Contribution of fatty acids released from lipolysis of plasma triglycerides to total plasma fatty acid flux and tissue-specific fatty acid uptake. *Diabetes* 52:614-620.

25. Augustus, A., Yagyu, H., Haemmerle, G., Bensadoun, A., Vikramadithyan, R.K., Park, S.Y., Kim, J.K., Zechner, R., and Goldberg, I.J. 2004. Cardiac-specific knock-out of lipoprotein lipase alters plasma lipoprotein triglyceride metabolism and cardiac gene expression. *J Biol Chem* 279:25050-25057.
26. Voshol, P.J., Rensen, P.C., van Dijk, K.W., Romijn, J.A., and Havekes, L.M. 2009. Effect of plasma triglyceride metabolism on lipid storage in adipose tissue: studies using genetically engineered mouse models. *Biochim Biophys Acta* 1791:479-485.
27. Leone, T.C., Weinheimer, C.J., and Kelly, D.P. 1999. A critical role for the peroxisome proliferator-activated receptor alpha (PPARalpha) in the cellular fasting response: the PPARalpha-null mouse as a model of fatty acid oxidation disorders. *Proc Natl Acad Sci U S A* 96:7473-7478.
28. Kersten, S., Seydoux, J., Peters, J.M., Gonzalez, F.J., Desvergne, B., and Wahli, W. 1999. Peroxisome proliferator-activated receptor alpha mediates the adaptive response to fasting. *J Clin Invest* 103:1489-1498.
29. Johnston, T.P., and Waxman, D.J. 2008. The induction of atherogenic dyslipidaemia in poloxamer 407-treated mice is not mediated through PPARalpha. *J Pharm Pharmacol* 60:753-759.
30. Johnston, T.P., and Palmer, W.K. 1993. Mechanism of poloxamer 407-induced hypertriglyceridemia in the rat. *Biochem Pharmacol* 46:1037-1042.
31. Pillutla, P., Hwang, Y.C., Augustus, A., Yokoyama, M., Yagyu, H., Johnston, T.P., Kaneko, M., Ramasamy, R., and Goldberg, I.J. 2005. Perfusion of hearts with triglyceride-rich particles reproduces the metabolic abnormalities in lipotoxic cardiomyopathy. *Am J Physiol Endocrinol Metab* 288:E1229-1235.
32. Augustus, A.S., Kako, Y., Yagyu, H., and Goldberg, I.J. 2003. Routes of FA delivery to cardiac muscle: modulation of lipoprotein lipolysis alters uptake of TG-derived FA. *Am J Physiol Endocrinol Metab* 284:E331-339.
33. Ibrahimi, A., Bonen, A., Blinn, W.D., Hajri, T., Li, X., Zhong, K., Cameron, R., and Abumrad, N.A. 1999. Muscle-specific overexpression of FAT/CD36 enhances fatty acid oxidation by contracting muscle, reduces plasma triglycerides and fatty acids, and increases plasma glucose and insulin. *J Biol Chem* 274:26761-26766.
34. Levak-Frank, S., Radner, H., Walsh, A., Stollberger, R., Knipping, G., Hoefler, G., Sattler, W., Weinstock, P.H., Breslow, J.L., and Zechner, R. 1995. Muscle-specific overexpression of lipoprotein lipase causes a severe myopathy characterized by proliferation of mitochondria and peroxisomes in transgenic mice. *J Clin Invest* 96:976-986.
35. Garcia-Roves, P., Huss, J.M., Han, D.H., Hancock, C.R., Iglesias-Gutierrez, E., Chen, M., and Holloszy, J.O. 2007. Raising plasma fatty acid concentration induces increased biogenesis of mitochondria in skeletal muscle. *Proc Natl Acad Sci U S A* 104:10709-10713.
36. Kratky, D., Strauss, J.G., and Zechner, R. 2001. Tissue-specific activity of lipoprotein lipase in skeletal muscle regulates the expression of uncoupling protein 3 in transgenic mouse models. *Biochem J* 355:647-652.

37. Chakravarthy, M.V., Pan, Z., Zhu, Y., Tordjman, K., Schneider, J.G., Coleman, T., Turk, J., and Semenkovich, C.F. 2005. "New" hepatic fat activates PPARalpha to maintain glucose, lipid, and cholesterol homeostasis. *Cell Metab* 1:309-322.
38. Chakravarthy, M.V., Lodhi, I.J., Yin, L., Malapaka, R.R., Xu, H.E., Turk, J., and Semenkovich, C.F. 2009. Identification of a physiologically relevant endogenous ligand for PPARalpha in liver. *Cell* 138:476-488.
39. Mao, J., DeMayo, F.J., Li, H., Abu-Elheiga, L., Gu, Z., Shaikenov, T.E., Kordari, P., Chirala, S.S., Heird, W.C., and Wakil, S.J. 2006. Liver-specific deletion of acetyl-CoA carboxylase 1 reduces hepatic triglyceride accumulation without affecting glucose homeostasis. *Proc Natl Acad Sci U S A* 103:8552-8557.
40. Sapiro, J.M., Mashek, M.T., Greenberg, A.S., and Mashek, D.G. 2009. Hepatic triacylglycerol hydrolysis regulates peroxisome proliferator-activated receptor alpha activity. *J Lipid Res* 50:1621-1629.
41. Sacks, F.M., Alaupovic, P., Moye, L.A., Cole, T.G., Sussex, B., Stampfer, M.J., Pfeffer, M.A., and Braunwald, E. 2000. VLDL, apolipoproteins B, CIII, and E, and risk of recurrent coronary events in the Cholesterol and Recurrent Events (CARE) trial. *Circulation* 102:1886-1892.
42. Jong, M.C., Hofker, M.H., and Havekes, L.M. 1999. Role of ApoCs in lipoprotein metabolism: functional differences between ApoC1, ApoC2, and ApoC3. *Arterioscler Thromb Vasc Biol* 19:472-484.
43. Kawakami, A., Osaka, M., Aikawa, M., Uematsu, S., Akira, S., Libby, P., Shimokado, K., Sacks, F.M., and Yoshida, M. 2008. Toll-like receptor 2 mediates apolipoprotein CIII-induced monocyte activation. *Circ Res* 103:1402-1409.
44. Ziouzenkova, O., and Plutzky, J. 2004. Lipolytic PPAR activation: new insights into the intersection of triglycerides and inflammation? *Curr Opin Clin Nutr Metab Care* 7:369-375.

Figure 1

A.

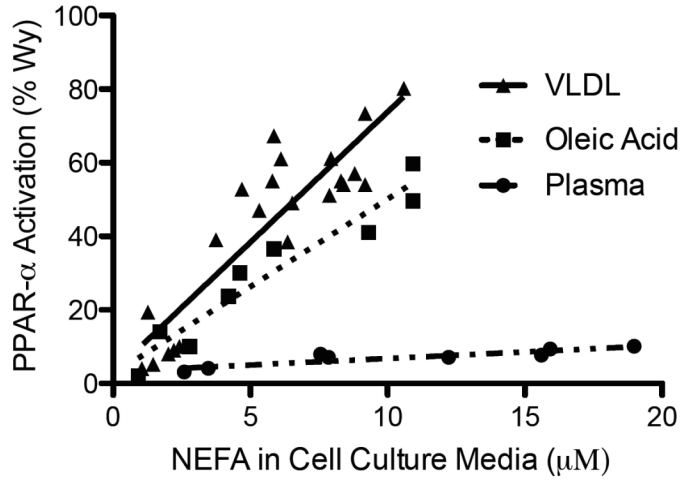

B.

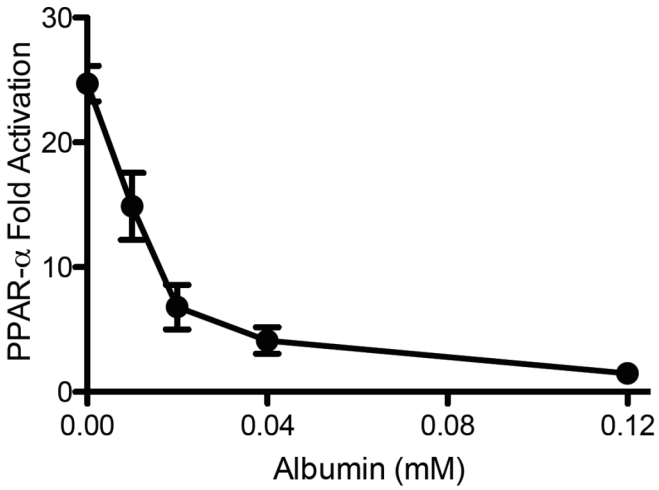

Figure 1: VLDL derived fatty acids serve as potent PPAR α ligands due to efficient delivery. BAEC were transfected with the PPAR α-LBD-GAL4 reporter system, as described in methods, treated for 18 hours and cell lysate assayed for luciferase and β-galoctosidase activity. A) BAEC were exposed to various concentrations of LPL (1, 3, or 10 units/ml) and VLDL (1, 3, 10, or 30 μg/ml), oleic acid (0, 5, 10, or 20 μM at an unbound oleic acid concentration of 2450 nM) or plasma (0-5% v/v). This produced a range of NEFA concentrations, as measured in the cell culture media at the end of treatment. For oleic acid, a linear relationship exists between oleic acid added and NEFA concentration in the cell culture media (data not shown), such that ~60% of NEFA added remains in the media following incubation with cells. PPAR α activity is presented as percentage of activation by 10 μM Wy14643, a synthetic PPAR α ligand. B) Transfected BAEC were incubated with VLDL (10 μg protein/ml) and LpL (10 units/ml) and increasing concentrations of albumin in triplicate. PPAR α activity is expressed as fold activation over control.

Figure 2

A.

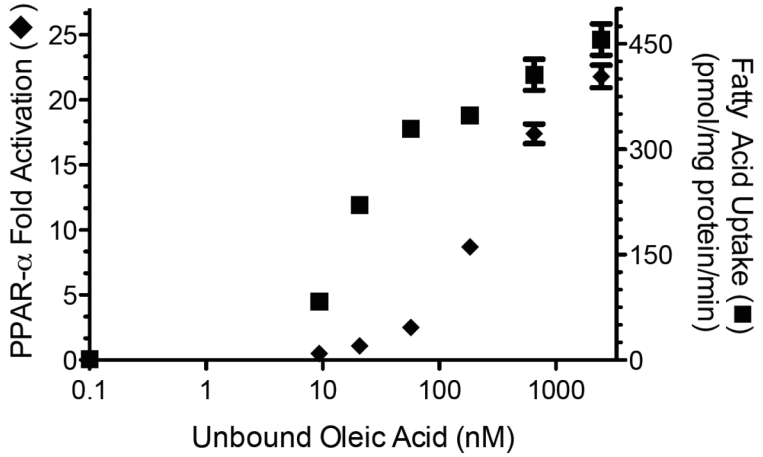

B.

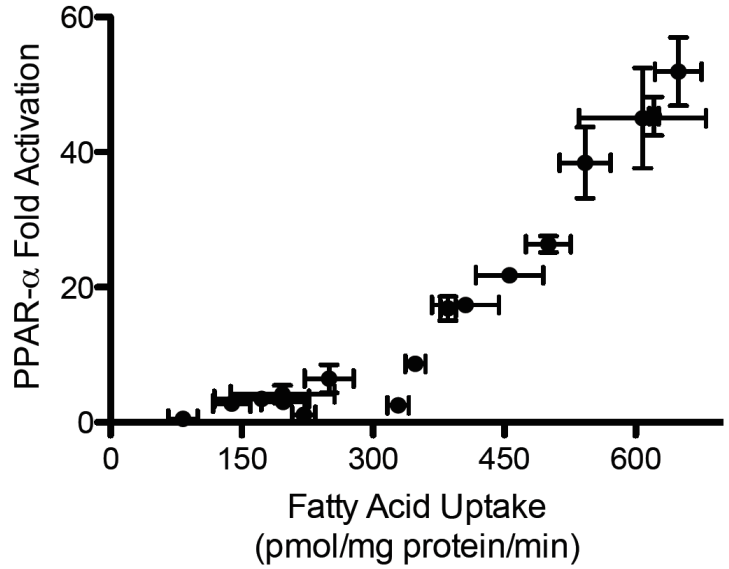

Figure 2: Fatty acid uptake determines PPAR α activation.
A) In parallel experiments, BAECs were treated with oleic acid (90 μM) and varying concentrations of albumin, and PPAR α activation and fatty acid uptake were determined as described in Methods. B. Varying total (0-180 μM) and unbound oleic acid concentrations (0-2450 nM) were used to generate a range of fatty acid uptake. Fatty acid uptake above 300 pmol/mg protein/min displayed a strong linear relationship with PPAR α activation (r^2=.98, $p<0.05$).

Figure 3

A.

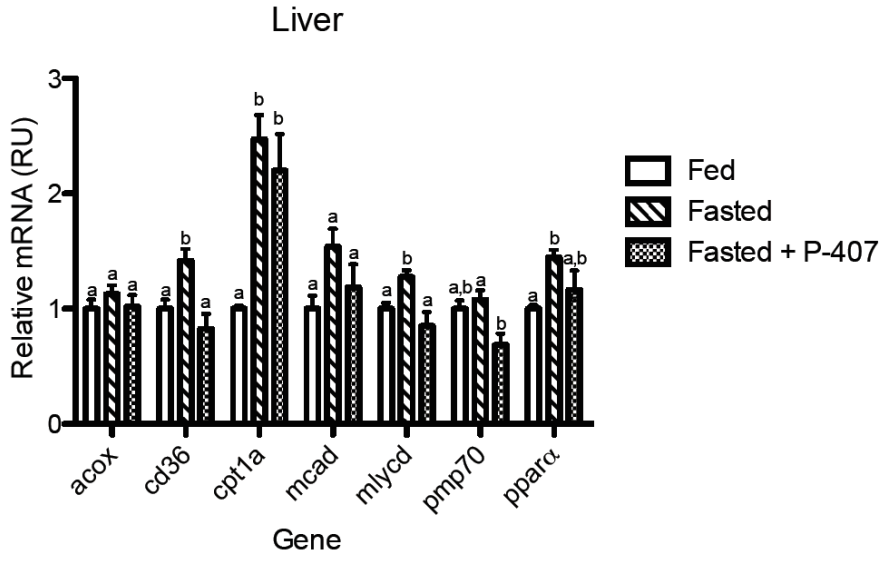

B.

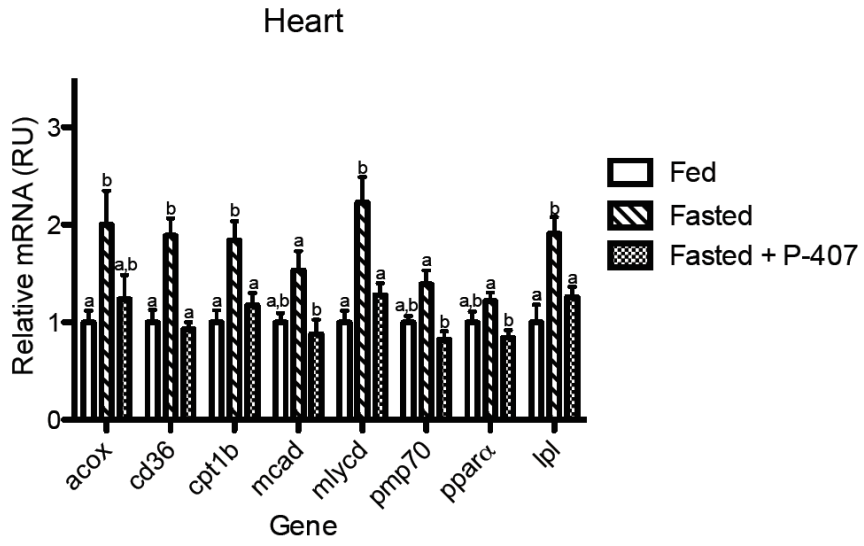

Figure 3: Poloxamer-407 inhibits the transcriptional response to fasting *in vivo*
Following an initial 2-hour fast, 9-week old male C57Bl6 mice were treated with saline or P-407 (500 mg/kg, i.p.) and fasted for an additional 24-hours. A group of saline injected animals was fed ad-lib for the 24-hour period. Abundance of mRNA for PPAR α target genes was determined by RT-PCR and normalized to a control gene (gusb) in the liver (A) and heart (B). Groups not sharing a common superscript letter are significantly different ($p<0.05$).

Figure 4

A.

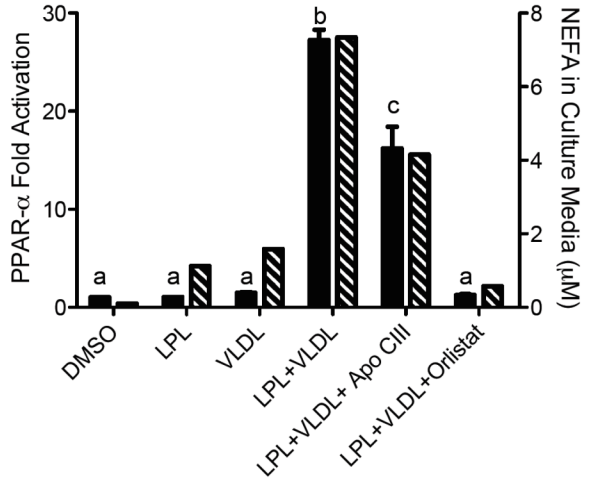

B.

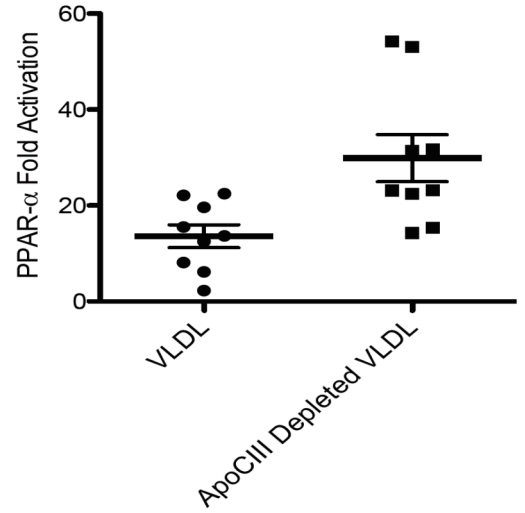

Figure 4: Apolipoprotein CIII regulates access to lipoprotein derived PPAR α ligands. A) PPAR α activation (solid bars) in BAEC were transfected as described in Figure 1 and treated with LpL (10 units/ml), VLDL (10 μg protein/ml), Orlistat (10 μM), ApoCIII (3 ug/ml) as indicated for 18 hours. Cell culture media was assayed for fatty acids. Groups not sharing a common superscript letter are significantly different ($p<0.05$). B) BAEC were transfected as described in Figure 1 and treated with total VLDL or apoCIII depleted VLDL (10 ug protein/ml) and LpL (3 units/ml). The difference between the VLDL treatments was significant ($p=0.002$) by paired two-tailed t-test.

CHAPTER 3
Overactive endocannabinoid signaling impairs apolipoprotein E mediated clearance of triglyceride rich lipoproteins

ABSTRACT
The endocannabinoid (EC) system regulates food intake and energy metabolism. Cannabinoid receptor type 1 (CB1) antagonists show promise in the treatment of obesity and its metabolic consequences. Although the reduction in adiposity resulting from therapy with CB1 antagonists may not fully account for the concomitant improvements in dyslipidemia, direct effects of overactive EC signaling on plasma lipoprotein metabolism have not been documented. The present study used a chemical approach to evaluate the direct effects of increased EC signaling in mice by inducing acute elevations of endogenously-produced cannabinoids through pharmacological inhibition of their enzymatic hydrolysis by isopropyl dodecylfluorophosphonate (IDFP). Acute IDFP treatment increased plasma levels of triglyceride (TG) (2.0-3.1 fold) and cholesterol (1.3-1.4 fold) in conjunction with an accumulation in plasma of apolipoprotein (apo)E-depleted TG-rich lipoproteins. These changes did not occur in CB1 null mice, were prevented by pretreatment with CB1 antagonists, and were not associated with reduced hepatic apoE gene expression. IDFP treatment increased hepatic mRNA levels of lipogenic genes (*Srebp1* and *Fas*). Therefore, overactive EC signaling elicits an increase in plasma triglyceride levels associated with an accumulation in plasma of apoE-depleted TG-rich lipoproteins**.** These findings suggest a role of CB1 activation in the pathogenesis of obesity-related hypertriglyceridemia and underscore the potential efficacy of CB1 antagonists in treating metabolic disease.

INTRODUCTION

Obesity elicits a cluster of interrelated disorders, termed the metabolic syndrome, that increases the risk of cardiovascular disease(1). Epidemiological and genetic data indicate that dysregulation of the endocannabinoid (EC) system increases adiposity in humans(2-4). Pharmacological or genetic ablation of the cannabinoid type 1 receptor (CB1) in normal mice and diet-induced and genetic mouse models of obesity results in a transient hypophagic response mediated through the hypothalamus but there are also prolonged effects on weight loss, adiposity, and normalization of metabolic parameters, including plasma lipids(5-11). This suggests that the improvement in adiposity-related measures with CB1 inactivation is not limited to reduced food intake, a major known effect of CB1 inactivation(5-11). CB1 activation in liver increases *de novo* lipogenesis and decreases fatty acid oxidation(12-14). High fat diet or chronic ethanol treatment increases cannabinoid signaling tone via increased hepatic CB1 receptor density and EC levels leading to CB1-mediated hepatic steatosis(12-14). These observations raise the possibility that aberrant EC signaling mediates development of obesity-related metabolic disturbances.

The EC system consists of the cannabinoid receptors, the endocannabinoids (ECs), and the enzymes responsible for their synthesis and breakdown(15, 16). CB1 is a G-protein coupled membrane receptor that transmits its response via $G_{i/o}$ protein-mediated reduction in adenylate cyclase activity(15). The ECs, anandamide and 2-arachidonoylglycerol (2-AG) are produced locally by *N*-acyl phosphatidylethanolamine phospholipase D and diacylglycerol lipase, respectively(15, 16). Signaling is terminated primarily by enzymatic breakdown of anandamide by fatty acid amide hydrolase (FAAH) and 2-AG by monoacylglycerol lipase (MAGL)(15-17).

Important specific CB1 antagonists are the pharmaceutical rimonabant, with a 4-chlorophenyl substituent, and its 4-iodophenyl analog AM251. In four large human trials, rimonabant at 20 mg/day resulted in clinically significant and prolonged reductions in body weight and waist circumference and improved cardiometabolic risk factors associated with obesity(18-22). There were significant improvements in plasma triglyceride (TG) and high-density lipoprotein (HDL) cholesterol concentrations that could not be fully accounted for by the expected effects of caloric restriction and weight loss, suggesting a direct and beneficial effect of CB1 blockade on lipid metabolism.

Inhibition of MAGL and/or FAAH offers an attractive approach to study the primary effects of elevated EC signaling on specific metabolic parameters. The organophosphorus (OP) compound isopropyl dodecylfluorophosphonate (IDFP) inhibits both MAGL and FAAH *in vivo* in mice, raises brain 2-AG and anandamide levels greater than 10-fold and elicits full-blown cannabinoid behavior(17). CB1-mediated effects of IDFP can be clearly differentiated from off-target actions by reversal with a specific CB1 antagonist and by their absence in CB1 -/- mice(17). This study determined the effects of IDFP-induced overactive EC signaling and CB1 agonism on lipid metabolism, independent of adiposity or food intake. We found that elevation of EC levels was sufficient to increase plasma TG levels in conjunction with apolipoprotein (apo)E depletion of TG-rich lipoproteins.

METHODS

Animals

Tissues were provided for sub-study by Dr. Daniel Nomura in the laboratory of Dr. John Casida(17). Swiss Webster mice were from Harlan Laboratories. CB1 +/+ and -/- breeding pairs were obtained from Andreas Zimmer and Carl Lupica(23). C57/Bl6 +/+ controls were obtained from Jackson Laboratories. All mice were 6-8 weeks of age, male, and weighed 18-23 g, with the exception of CB -/- mice (17 ± 2 g). They were treated ip at 1 μl/g with DMSO or test compounds dissolved in DMSO, and sacrificed at the indicated times. All experiments used Swiss Webster mice unless specifically stated otherwise, i.e. +/+ or -/-.

Chemicals

Sources for the chemicals were as follows: lipid standards from Alexis Biochemicals and Sigma; AM251 and WIN55212-2 from Tocris Cookson Inc.; IDFP was synthesized in the Berkeley laboratory(24).

MAGL activity and monoacylglycerol levels

MAGL activity was determined by measuring 2-AG hydrolysis using gas chromatography-mass spectrometry (GC-MS)(17). Tissue homogenates in 5 ml of 50 mM Tris buffer pH 8.0 containing 1 mM EDTA and 3 mM $MgCl_2$ were centrifuged at 1000 g. Supernatant protein (50 μg) was incubated with 100 μM 2-AG in Tris/EDTA/ $MgCl_2$ buffer (500 μl) for 1 h at 37^{o}C then extracted with 1 ml ethyl acetate containing 10 nmol of the internal standard 1-dodecylglycerol. After phase separation, 70 % of the upper organic layer was recovered, evaporated under nitrogen and derivatized by *N,O*-bis(trimethylsilyl)trifluoroacetamide (200 μl) for 30 min at room temperature with sonication. The trimethylsilyl derivatives (1 μl aliquot) were separated on a DB-XLB fused-silica capillary column (30 m × 0.25 mm × 25 μm) using a temperature program of 100 to 280 ^{o}C, and detected by electron impact ionization at 70 eV with an ion source temperature of 250 °C. A mass selective detector was used for single ion monitoring to quantitate individual lipids. MAGL activity was based on the formation of arachidonic acid (with endogenous arachidonic acid levels subtracted) normalized for tissue weight and internal standard. Monoacylglycerol levels in tissues were determined as described previously(17). Briefly, tissues were weighed and homogenized in a mixture of 3 ml 100 mM phosphate buffer pH 7.4 and 3 ml ethyl acetate containing 10 nmol of internal standard. The ethyl acetate phase was recovered and after workup the trimethylsilyl derivatives were analyzed by GC-MS as indicated above.

Plasma lipids and lipoproteins

Plasma was used for determination of lipid and lipoprotein profiles. Total TG and cholesterol were analyzed by enzymatic end-point measurements utilizing enzyme reagent kits (Sigma) with HDL-cholesterol concentration determined by measurement directly after polyethylene glycol-mediated precipitation of apoB(25). For ion mobility analysis of lipoprotein particle concentrations, 1 part plasma was incubated with 4 parts albumin-binding agent (reactive green 19 dextran), layering this mixture on top of deuterium oxide, and spinning in an ultracentrifuge to isolate the lipoproteins(26). The lipoprotein fraction was injected into the ion mobility instrument which utilizes an electrospray to create an aerosol. The particles were then passed through a differential mobility analyzer coupled to a condensation particle counter, where particle diameter and quantity were determined.

Lipoprotein fractionation

VLDL , IDL, LDL and HDL fractions were separated from pooled plasma by sequential density ultracentrifugation(27). ApoB100, B48, E and C in each fraction were quantified by measuring Coomassie band intensity after separation by denaturing gradient gel electrophoresis. Lipid compositions were determined as described above.

Determination of VLDL particle composition

Phospholipids were analyzed by enzymatic end-point measurements utilizing an enzyme reagent kit (Waco Diagnostics). Protein was determined by the method of Lowry *et al*.(28). Free cholesterol was measured by the method of Allain *et al* in the absence of cholesterol ester hydrolase(29). Cholesterol ester concentration was calculated as (total cholesterol – free cholesterol) x 1.68.

Measurement of lipogenic gene transcripts

Fresh liver was flash frozen with liquid nitrogen and stored at -80^{o}C until analyzed. RNA was isolated and cDNA synthesized. RTq-PCR was performed on the ABI 7900 Real Time PCR instrument using SYBR green gene expression assays. All values were adjusted to an appropriate control gene (GusB).

Western Blot, ELISA, and Exchange Assay

Lipoproteins were transferred to polyvinylidene difluoride (PVDF) membranes and probed with primary and secondary antibodies diluted in Tris-buffered saline with 0.05% Tween. HRP-conjugated secondary antibodies were detected using West Femto chemiluminescent substrate (Pierce). ApoE was quantified in triplicate by sandwich-style enzyme-linked immunosorbent assay. For the exchange assay, 27 micrograms of HDL total protein was incubated with 33 micrograms of apoE -/- VLDL in 1 ml of PBS for 18 h at 37°C. Following incubation, the VLDL was recovered as described above, and analyzed by western blot.

Statistical analyses

Results are presented as mean ± standard deviation. One-way and two-way analysis of variance was used to test significance of treatment effects and interactions with genotypes, respectively. Post-hoc analysis (Student's unpaired t-test) examined significance of individual treatment and/or genotype effects. Significance is given as *$p<0.05$, **$p<0.01$, and ***$p<0.001$. NS, not significant, ND, not detected. All analyses were performed using JMP version 7.0.

RESULTS

IDFP inhibits MAGL activity and elevates 2-AG levels in liver, muscle and adipose tissue

To test the ability of IDFP to inhibit MAGL in peripheral tissues, MAGL activity and 2-AG levels were determined in liver, skeletal muscle, white adipose tissue (WAT) and brown adipose tissue (BAT) from IDFP treated mice. IDFP (10 mg/kg, ip, 4 h) inhibited 2-AG hydrolytic activity in liver, skeletal muscle, white adipose tissue (WAT) and brown adipose tissue (BAT) by 78-97 % and raised 2-AG levels in liver, muscle and BAT by 5-13-fold (Fig. 1). 2-Oleoyl- and 2-palmitoylglycerol levels were also elevated in these tissues but 1-oleoyl- and 1-palmitoylglycerol were less affected (Table 1).

CB1-dependent effects of IDFP on plasma lipid levels and hepatic lipogenic gene expression

To test the effects of increased endocannabinoid levels of plasma lipids, triglycerides, cholesterol, and lipoprotein particle count were determined in plasma from mice

administered IDFP (10 mg/kg, ip, 4 h) or DMSO as a vehicle control. CB1 -/- mice and CB1 antagonist pre-administration were used to determine the CB1 dependence of IDFP effects. IDFP significantly increased plasma TG (2.0-3.1-fold) (Fig. 2A) and cholesterol (1.3-1.4-fold) levels (Fig. 2B) and very low density lipoprotein (VLDL) mass (2.1-fold) (Fig. 2C) 4 h after administration. Each of these effects was completely ablated by pretreatment with the CB1 antagonist AM251 and was absent in CB1 -/- mice (Fig. 2). HDL-cholesterol levels were unaffected (Table 2). The increased TG and cholesterol levels were largely in the plasma VLDL fraction, accompanied by small alterations in particle composition mainly due to reduced protein content (Table 3). To affirm the effect of acute CB1 stimulation to regulate plasma lipids levels, mice were treated with the synthetic CB1 agonist, WIN55212-2. WIN55212-2 recapitulated the hyperlipidemic effects of IDFP raising plasma TG levels and VLDL mass (Fig. 3). To gain insight into which endocannabinoid stimulates the increase in plasma lipids, mice were treated with a FAAH-selective inhibitor (URB597). URB597 had no significant effect on plasma lipids indicating that anandamide elevation alone was not responsible (Fig. 3). To confirm stimulation of hepatic CB1, the expression of known CB1 stimulated genes were determined in IDFP treated mice. IDFP increased hepatic expression of the genes for both sterol regulatory element binding protein-1c (SREBP-1c) and fatty acid synthase (FAS), changes which were prevented by AM251 and not found in CB1 -/- mice (Fig. 4.)

CB1-dependent effects of IDFP on apolipoprotein content of TG-rich-lipoproteins

As apolipoproteins are responsible for directing the metabolism of lipoproteins, the effects of IDFP on apolipoprotein content was determined. Consistent with the effects of IDFP treatment on plasma TG concentrations, there were substantial increases in VLDL apoB100 and apoB48 (Fig. 5). However, there was no concurrent increase in VLDL apoE with IDFP treatment, resulting in a reduced ratio of apoE to apoB. IDFP treatment also increased the apoAI content of the VLDL fractions. Similar changes in apolipoproteins, although of much lesser magnitude, were observed in the intermediate density lipoprotein (IDL) and low density lipoprotein (LDL) fractions (Fig. 6). Interestingly, HDL apoE content was increased by 3.1-fold in IDFP-treated mice, and this was negated by AM251 (Fig. 6). To determine if alterations in expression of the apolipoproteins contributed to changes in plasma concentrations, the effect of IDFP on hepatic mRNA levels of apoE, apoAI, apoAV, and apoCIII was determined. IDFP had no effect on hepatic transcript levels of apoE, apoAI, apoAV, and apoCIII (Table 4).

CB1-dependent effects of IDFP on apoE exchange

To further investigate the effects of IDFP on apoE partitioning an *in vitro* exchange assay was established. Isolated HDL from animals was used as an apo E source and incubated with VLDL particles isolated from apo E -/- mice. Western blot analysis confirmed that IDFP increases HDL apo E content in a CB1 dependent manner (Fig. 7a). Following an 18 h incubation, ultracentrifugation was performed to collect the d<1.006 mg/ml fraction. Western blot analysis demonstrated that an apo E donor, HDL, and a TG-rich apo E acceptor, apo E -/- VLDL, were necessary to recover apo E in the d<1.006 mg/ml fraction. Interestingly, while HDL isolated from DMSO and Am251/DMSO treated animals readily transferred apo E to the VLDL fraction, HDL from IDFP animals, despite a higher apo E content, failed to transfer apo E (Fig 7b). Interestingly, when examined by ELISA, plasma apoE content in IDFP treated animals was drastically reduced compared to the levels observed in DMSO and AM251/IDFP treatment (Fig 8).

Discussion

The involvement of the EC system in regulation of plasma lipid and lipoprotein metabolism has been demonstrated in several clinical trials by the effects of treating obese patients with the CB1 antagonist rimonabant(18-22). These effects include reductions in plasma TG and small LDL particles and increases in HDL cholesterol. A major determinant of these changes is the weight loss resulting from reduced caloric intake, but post-hoc analysis suggests that this is not sufficient to explain the full magnitude of the drug's effects(22). To determine the contribution of elevated EC signaling to plasma lipid and lipoprotein metabolism, independent of food intake or adiposity, we used IDFP to acutely raise systemic levels of 2-AG by inhibiting its hydrolysis.

The present study establishes that overactive EC signaling is sufficient to acutely elicit hypertriglyceridemia in a CB1-dependent manner characterized by accumulation of TG-rich lipoproteins. Hepatic *de novo* lipogenic gene transcript levels were elevated upon overactive EC signaling as also observed under chronic ethanol or high-fat diet administration(13, 14). Hypertriglyceridemia can result from increased hepatic production or decreased catabolism of TG-rich lipoproteins, which undergo lipolytic processing to remnant particles that can be cleared from plasma through apoE-mediated receptor endocytosis.

We propose that defective clearance of TG-rich lipoproteins in IDFP-treated mice results from decreased apoE-mediated whole particle uptake. This might explain previous reports that CB1 -/- mice have reduced TG levels despite the stimulatory effect of CB1 activation on adipose tissue lipoprotein lipase activity(6, 12). Indeed, IDFP-induced CB1 signaling resulted in both apoE depletion and apoAI enrichment of VLDL particles. ApoAI is normally associated with HDL particles, but has been observed on TG-rich lipoproteins in the genetic absence of apoE. ApoE plays a multifunctional role in intravascular and cellular lipid metabolism, primarily as a ligand for the seven identified members of the LDL receptor family and for cell surface heparin proteoglycans(30, 31). Although apoE is expressed throughout the body, circulating apoE largely originates from the liver, where both newly-synthesized and recycled apoE is secreted(30, 31). It is interesting to note that IDFP-induced increases in plasma TG values in +/+ mice reached levels similar to those in apoE -/- mice(32, 33). As shown here for IDFP-treated wild-type mice, apoE -/- mice similarly have high concentrations of apoAI in native apoB-containing lipoproteins, and accumulation in plasma of apoB48 particles, which rely solely on apoE for receptor-mediated clearance. Additionally, TG-rich lipoproteins in apoE -/- mice turn over slowly and are enriched in sphingomyelin at the expense of phosphatidylcholine(32, 33).

IDFP-treated mice do not develop the severe hypercholesterolemia characteristic of apoE -/- mice. This might be due to the short treatment period coupled with the slower turnover of cholesterol-rich compared to TG-rich lipoproteins. Alternatively, depletion of apoE may not be sufficient to cause hypercholesterolemia; individuals with the apoE2/E3 genotype have decreased concentrations of apoE3 protein, but display decreased LDL cholesterol levels(34). The coupling of apoE depletion in TG-rich lipoproteins with increased apoE content of HDL particles suggests that CB1 activation may alter the

partitioning of secreted apoE or cause a conformational change in apoE on HDL or VLDL resulting in altered equilibration between these apoE pools.

The discordant results obtained by a denaturing gel and ELISA suggest a possible conformational change in apo E on VLDL. As the antibody used is polyclonal, stearic hindrance is more likely to account for the discrepancy than differential epitope exposure. A buried, and perhaps more structurally necessary conformation, of apo E is consistent with the failure of apoE to transfer between lipoproteins. The exchange assay suggests that the altered equilibration of apo E results from a failure of HDL to release apo E. A similar situation has been observed in a mouse model of kidney failure, where apoE rich HDL appear and apoE depleted VLDL accumulate causing hypertriglyceridemia(35). The resulting apoE made the VLDL a poor substrate for LPL and receptor binding, and importantly injection of normal HDL or apoE reversed binding defects. Altered equilibration of apo E also has been noted in humans and linked to disease. Even among VLDLs, there exist apo E positive and negative fractions. Apo E free VLDL has a higher half-life within plasma, and individuals with a greater proportion of this fraction DL higher triglyceride levels(36, 37). Conversely, apoE is enriched in HDL from individuals with cardiovascular disease(38). The mechanism by which CB1 activation alters apoE exchange and thus distribution remains to be elucidated.

Although hepatic CB1 activation is likely the target of our observed effects, we cannot exclude centrally-mediated actions upon peripheral tissues since brain EC levels are elevated as well(17). The development of peripheral CB1 antagonists that do not cross the blood-brain barrier and tissue-specific CB1 -/- mouse models will aid in addressing this issue.

IDFP effects on TG metabolism could result from its inhibition of MAGL and/or FAAH. Notably, fibrogenic stimuli elevate hepatic 2-AG whereas high-fat diet elevates anandamide levels and both ECs are implicated in pathogenesis of hepatic steatosis(12-14). Although we show here that FAAH inhibition alone (by URB597) is not sufficient to elicit acute hypertriglyceridemia, evaluation of the specific effects of 2-AG will require development of a selective MAGL inhibitor or a MAGL -/- mouse model. Moreover, IDFP off-targets, such as hormone-sensitive lipase, neuropathy target esterase, carboxylesterase-N and α/β hydrolases 3 and 6(17), may potentiate the EC actions observed here. However, the complete reversal of IDFP effects by pharmacological (AM251 and rimonabant) or genetic (CB1 -/- mice) ablation of CB1 unequivocally ascribes the metabolic abnormalities to the EC system.

Our short-term studies in fasted mice show that CB1-mediated reduction in plasma TG clearance does not require alterations in food intake or body weight. The findings, however, do not define the contribution of this mechanism to longer-term effects of CB1 activation, particularly in the context of changes in adiposity, or to its role in humans. It may be, for example, that increased hepatic secretion of TG-rich lipoproteins would result from chronic CB1-induced activation of hepatic lipogenic pathways with high fat diet or ethanol intake(12-14). Moreover, our studies do not identify direct impacts of CB1 activation on HDL metabolism, as might be expected given the weight-independent effects of rimonabant on HDL levels in humans(22). In view of the much greater turnover time of HDL than TG-rich lipoproteins, such effects may require a longer duration of CB1 activation. Other factors, such as cholesteryl ester transfer protein activity, which is absent in mice, may also be required(39). It is of

interest, however, that the apoE content of HDL was increased by CB1 activation, and this, coupled with VLDL enrichment of apoAI, might lead to changes in HDL production or clearance that would be apparent with a longer duration of IDFP treatment. Unfortunately long-term IDFP treatment is not an option because of probable delayed non-CB1 dependent central nervous system toxicity(24).

ECs are elevated prior to the onset of obesity, implicating hyperactive EC signaling as a cause of metabolic disease rather than a consequence(11). Despite encouraging clinical data, rimonabant failed to gain Food and Drug Administration approval due to psychiatric side effects, illustrating both the promise of targeting the EC system for treatment of obesity-related metabolic disturbances and the need to better understand the basic biology and pharmacology involved. It may then be possible to develop CB1 antagonists that limit adverse psychological side effects while achieving the desired metabolic endpoints.

Future work may also focus on understanding the mechanisms leading to apoE depletion of TG rich lipoproteins. Determining the prevalence of apoE depleted TG rich lipoproteins, and corresponding HDL apoE enrichment, in dyslipidemic individuals would be of great interest. If the mechanisms controlling apoE depletion are better understood it may be possible to favorably alter apoE distribution, and thus plasma lipid levels.

References

1. Lakka, H.M., Laaksonen, D.E., Lakka, T.A., Niskanen, L.K., Kumpusalo, E., Tuomilehto, J., and Salonen, J.T. 2002. The metabolic syndrome and total and cardiovascular disease mortality in middle-aged men. *Jama* 288:2709-2716.
2. Bluher, M., Engeli, S., Kloting, N., Berndt, J., Fasshauer, M., Batkai, S., Pacher, P., Schon, M.R., Jordan, J., and Stumvoll, M. 2006. Dysregulation of the peripheral and adipose tissue endocannabinoid system in human abdominal obesity. *Diabetes* 55:3053-3060.
3. Engeli, S., Bohnke, J., Feldpausch, M., Gorzelniak, K., Janke, J., Batkai, S., Pacher, P., Harvey-White, J., Luft, F.C., Sharma, A.M., et al. 2005. Activation of the peripheral endocannabinoid system in human obesity. *Diabetes* 54:2838-2843.
4. Sipe, J.C., Waalen, J., Gerber, A., and Beutler, E. 2005. Overweight and obesity associated with a missense polymorphism in fatty acid amide hydrolase (FAAH). *Int J Obes (Lond)* 29:755-759.
5. Colombo, G., Agabio, R., Diaz, G., Lobina, C., Reali, R., and Gessa, G.L. 1998. Appetite suppression and weight loss after the cannabinoid antagonist SR 141716. *Life Sci* 63:PL113-117.
6. Cota, D., Marsicano, G., Tschop, M., Grubler, Y., Flachskamm, C., Schubert, M., Auer, D., Yassouridis, A., Thone-Reineke, C., Ortmann, S., et al. 2003. The endogenous cannabinoid system affects energy balance via central orexigenic drive and peripheral lipogenesis. *J Clin Invest* 112:423-431.
7. Di Marzo, V., Goparaju, S.K., Wang, L., Liu, J., Batkai, S., Jarai, Z., Fezza, F., Miura, G.I., Palmiter, R.D., Sugiura, T., et al. 2001. Leptin-regulated endocannabinoids are involved in maintaining food intake. *Nature* 410:822-825.
8. Jbilo, O., Ravinet-Trillou, C., Arnone, M., Buisson, I., Bribes, E., Peleraux, A., Penarier, G., Soubrie, P., Le Fur, G., Galiegue, S., et al. 2005. The CB1 receptor antagonist rimonabant reverses the diet-induced obesity phenotype through the regulation of lipolysis and energy balance. *Faseb J* 19:1567-1569.
9. Ravinet Trillou, C., Arnone, M., Delgorge, C., Gonalons, N., Keane, P., Maffrand, J.P., and Soubrie, P. 2003. Anti-obesity effect of SR141716, a CB1 receptor antagonist, in diet-induced obese mice. *Am J Physiol Regul Integr Comp Physiol* 284:R345-353.
10. Ravinet Trillou, C., Delgorge, C., Menet, C., Arnone, M., and Soubrie, P. 2004. CB1 cannabinoid receptor knockout in mice leads to leanness, resistance to diet-induced obesity and enhanced leptin sensitivity. *Int J Obes Relat Metab Disord* 28:640-648.
11. Starowicz, K.M., Cristino, L., Matias, I., Capasso, R., Racioppi, A., Izzo, A.A., and Di Marzo, V. 2008. Endocannabinoid dysregulation in the pancreas and adipose tissue of mice fed with a high-fat diet. *Obesity (Silver Spring)* 16:553-565.
12. Osei-Hyiaman, D., DePetrillo, M., Pacher, P., Liu, J., Radaeva, S., Batkai, S., Harvey-White, J., Mackie, K., Offertaler, L., Wang, L., et al. 2005. Endocannabinoid activation at hepatic CB1 receptors stimulates fatty acid synthesis and contributes to diet-induced obesity. *J Clin Invest* 115:1298-1305.

13. Osei-Hyiaman, D., Liu, J., Zhou, L., Godlewski, G., Harvey-White, J., Jeong, W.I., Batkai, S., Marsicano, G., Lutz, B., Buettner, C., et al. 2008. Hepatic CB1 receptor is required for development of diet-induced steatosis, dyslipidemia, and insulin and leptin resistance in mice. *J Clin Invest* 118:3160-3169.
14. Jeong, W.I., Osei-Hyiaman, D., Park, O., Liu, J., Batkai, S., Mukhopadhyay, P., Horiguchi, N., Harvey-White, J., Marsicano, G., Lutz, B., et al. 2008. Paracrine activation of hepatic CB1 receptors by stellate cell-derived endocannabinoids mediates alcoholic fatty liver. *Cell Metab* 7:227-235.
15. Piomelli, D. 2003. The molecular logic of endocannabinoid signalling. *Nat Rev Neurosci* 4:873-884.
16. Ahn, K., McKinney, M.K., and Cravatt, B.F. 2008. Enzymatic pathways that regulate endocannabinoid signaling in the nervous system. *Chem Rev* 108:1687-1707.
17. Nomura, D.K., Blankman, J.L., Simon, G.M., Fujioka, K., Issa, R.S., Ward, A.M., Cravatt, B.F., and Casida, J.E. 2008. Activation of the endocannabinoid system by organophosphorus nerve agents. *Nat Chem Biol* 4:373-378.
18. Despres, J.P., Golay, A., and Sjostrom, L. 2005. Effects of rimonabant on metabolic risk factors in overweight patients with dyslipidemia. *N Engl J Med* 353:2121-2134.
19. Pi-Sunyer, F.X., Aronne, L.J., Heshmati, H.M., Devin, J., and Rosenstock, J. 2006. Effect of rimonabant, a cannabinoid-1 receptor blocker, on weight and cardiometabolic risk factors in overweight or obese patients: RIO-North America: a randomized controlled trial. *Jama* 295:761-775.
20. Scheen, A.J., Finer, N., Hollander, P., Jensen, M.D., and Van Gaal, L.F. 2006. Efficacy and tolerability of rimonabant in overweight or obese patients with type 2 diabetes: a randomised controlled study. *Lancet* 368:1660-1672.
21. Van Gaal, L.F., Rissanen, A.M., Scheen, A.J., Ziegler, O., and Rossner, S. 2005. Effects of the cannabinoid-1 receptor blocker rimonabant on weight reduction and cardiovascular risk factors in overweight patients: 1-year experience from the RIO-Europe study. *Lancet* 365:1389-1397.
22. Van Gaal, L.F., Scheen, A.J., Rissanen, A.M., Rossner, S., Hanotin, C., and Ziegler, O. 2008. Long-term effect of CB1 blockade with rimonabant on cardiometabolic risk factors: two year results from the RIO-Europe Study. *Eur Heart J* 29:1761-1771.
23. Zimmer, A., Zimmer, A.M., Hohmann, A.G., Herkenham, M., and Bonner, T.I. 1999. Increased mortality, hypoactivity, and hypoalgesia in cannabinoid CB1 receptor knockout mice. *Proc Natl Acad Sci U S A* 96:5780-5785.
24. Segall, Y., Quistad, G.B., Sparks, S.E., Nomura, D.K., and Casida, J.E. 2003. Toxicological and structural features of organophosphorus and organosulfur cannabinoid CB1 receptor ligands. *Toxicol Sci* 76:131-137.
25. Briggs, C.J., Anderson, D., Johnson, P., and Deegan, T. 1981. Evaluation of the polyethylene glycol precipitation method for the estimation of high-density lipoprotein cholesterol. *Ann Clin Biochem* 18:177-181.
26. Caulfield, M.P., Li, S., Lee, G., Blanche, P.J., Salameh, W.A., Benner, W.H., Reitz, R.E., and Krauss, R.M. 2008. Direct determination of lipoprotein particle sizes and concentrations by ion mobility analysis. *Clin Chem* 54:1307-1316.

27. Qiu, S., Bergeron, N., Kotite, L., Krauss, R.M., Bensadoun, A., and Havel, R.J. 1998. Metabolism of lipoproteins containing apolipoprotein B in hepatic lipase-deficient mice. *J Lipid Res* 39:1661-1668.
28. Lowry, O.H., Rosebrough, N.J., Farr, A.L., and Randall, R.J. 1951. Protein measurement with the Folin phenol reagent. *J Biol Chem* 193:265-275.
29. Allain, C.C., Poon, L.S., Chan, C.S., Richmond, W., and Fu, P.C. 1974. Enzymatic determination of total serum cholesterol. *Clin Chem* 20:470-475.
30. Ishibashi, S., Herz, J., Maeda, N., Goldstein, J.L., and Brown, M.S. 1994. The two-receptor model of lipoprotein clearance: tests of the hypothesis in "knockout" mice lacking the low density lipoprotein receptor, apolipoprotein E, or both proteins. *Proc Natl Acad Sci U S A* 91:4431-4435.
31. Meir, K.S., and Leitersdorf, E. 2004. Atherosclerosis in the apolipoprotein-E-deficient mouse: a decade of progress. *Arterioscler Thromb Vasc Biol* 24:1006-1014.
32. Conde-Knape, K., Bensadoun, A., Sobel, J.H., Cohn, J.S., and Shachter, N.S. 2002. Overexpression of apoC-I in apoE-null mice: severe hypertriglyceridemia due to inhibition of hepatic lipase. *J Lipid Res* 43:2136-2145.
33. Ebara, T., Ramakrishnan, R., Steiner, G., and Shachter, N.S. 1997. Chylomicronemia due to apolipoprotein CIII overexpression in apolipoprotein E-null mice. Apolipoprotein CIII-induced hypertriglyceridemia is not mediated by effects on apolipoprotein E. *J Clin Invest* 99:2672-2681.
34. Bennet, A.M., Di Angelantonio, E., Ye, Z., Wensley, F., Dahlin, A., Ahlbom, A., Keavney, B., Collins, R., Wiman, B., de Faire, U., et al. 2007. Association of apolipoprotein E genotypes with lipid levels and coronary risk. *Jama* 298:1300-1311.
35. Shearer, G.C., Couser, W.G., and Kaysen, G.A. 2004. Nephrotic livers secrete normal VLDL that acquire structural and functional defects following interaction with HDL. *Kidney Int* 65:228-237.
36. Campos, H., Perlov, D., Khoo, C., and Sacks, F.M. 2001. Distinct patterns of lipoproteins with apoB defined by presence of apoE or apoC-III in hypercholesterolemia and hypertriglyceridemia. *J Lipid Res* 42:1239-1249.
37. Fielding, P.E., and Fielding, C.J. 1986. An apo-E-free very low density lipoprotein enriched in phosphatidylethanolamine in human plasma. *J Biol Chem* 261:5233-5236.
38. Vaisar, T., Pennathur, S., Green, P.S., Gharib, S.A., Hoofnagle, A.N., Cheung, M.C., Byun, J., Vuletic, S., Kassim, S., Singh, P., et al. 2007. Shotgun proteomics implicates protease inhibition and complement activation in the antiinflammatory properties of HDL. *J Clin Invest* 117:746-756.
39. Jiao, S., Cole, T.G., Kitchens, R.T., Pfleger, B., and Schonfeld, G. 1990. Genetic heterogeneity of lipoproteins in inbred strains of mice: analysis by gel-permeation chromatography. *Metabolism* 39:155-160.

Figure 1

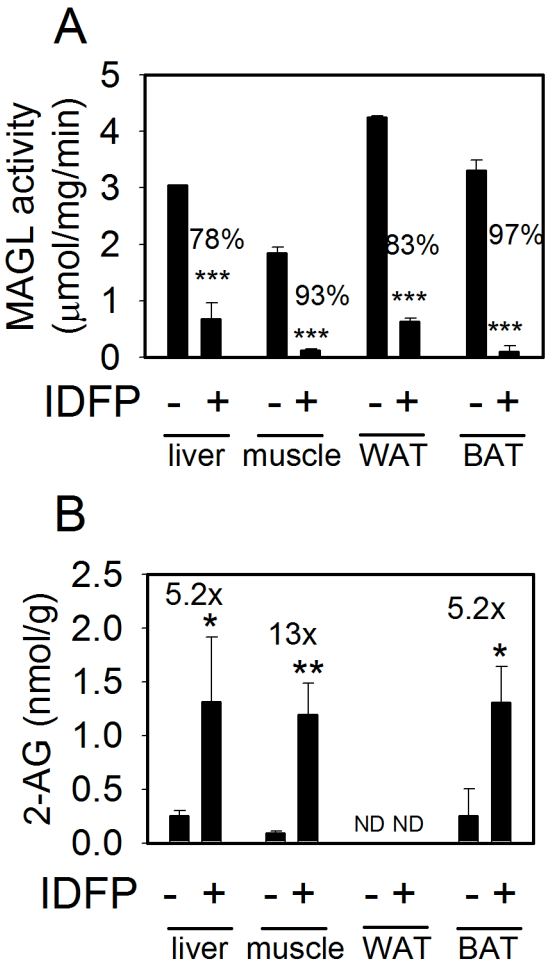

Figure 1: IDFP inhibition of MAGL activity (A) and elevation of 2-AG levels (B) in liver, muscle and adipose tissue (WAT and BAT). Mice were treated with dimethyl sulfoxide (DMSO) or IDFP (10 mg/kg, ip, 4 h). n=3-4.

Figure 2

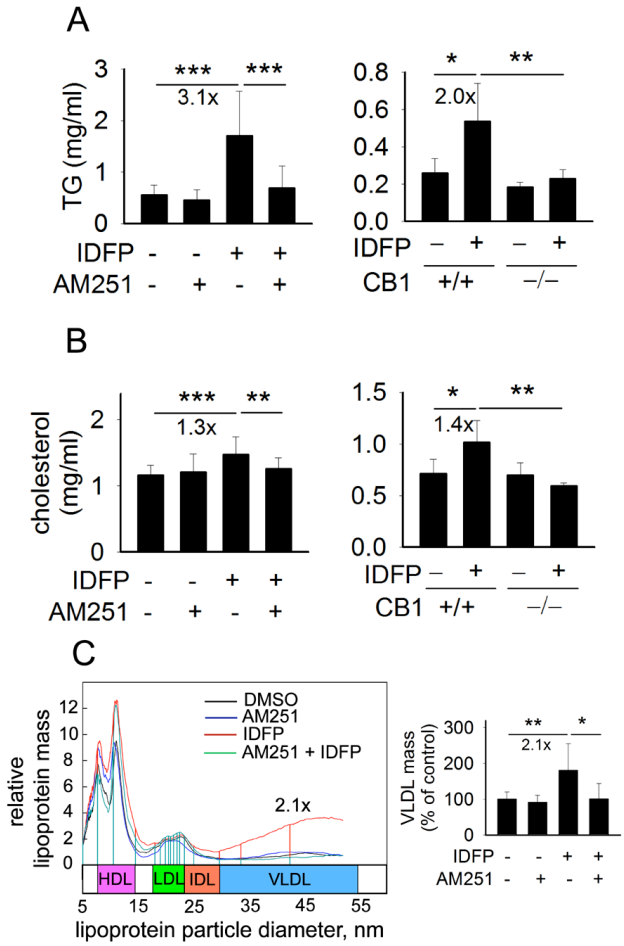

Figure 2: CB1-dependent effects of IDFP on plasma TG (A) and cholesterol (B) levels and lipoprotein profiles (C). Mice were treated with DMSO or IDFP (10 mg/kg, ip, 4 h) alone or 15 min following AM251 (10 mg/kg, ip). n=5-21.

Figure 3

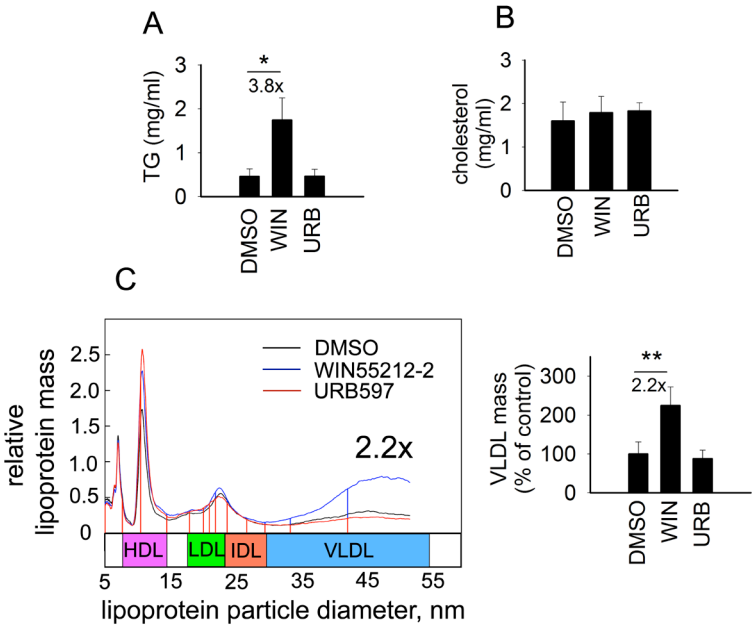

Figure 3: WIN55212-2 and URB597 effects on plasma TG (A) and cholesterol (B) levels and lipoprotein profiles (C). Mice were treated with DMSO or WIN55212-2 or URB597 (10 mg/kg, ip, 2 h). n=5.

Figure 4

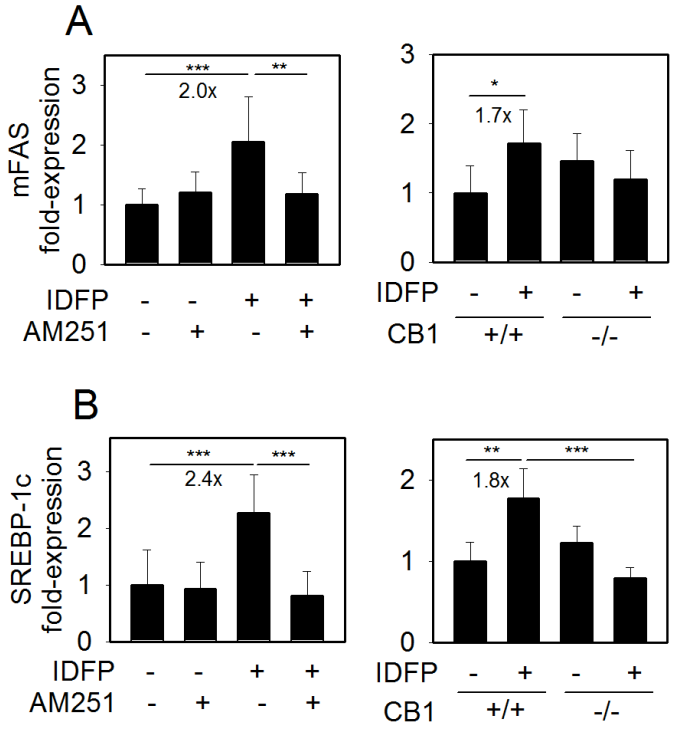

Figure 4: CB1-dependent effects of IDFP on hepatic expression of FAS (A) and SREBP-1c (B). RNA was isolated from the mice used for the experiment in Fig. 2.

Figure 5

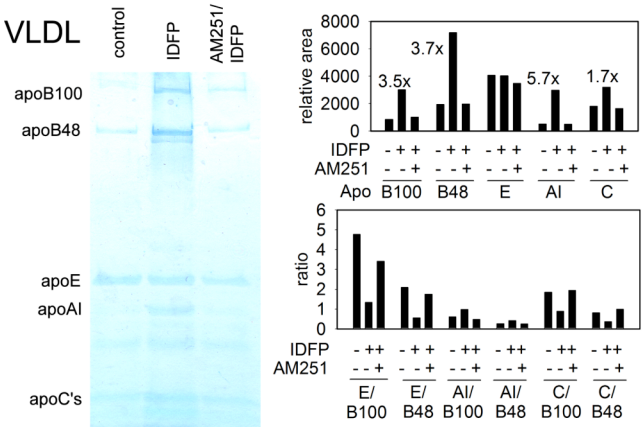

Figure 5. CB1-dependent effects of IDFP on apolipoproteins in the VLDL fraction. Mice were treated as in Fig. 2 and plasma from 10 mice was pooled for analysis. VLDL apolipoprotein composition was quantitated based on Commassie staining.

Figure 6

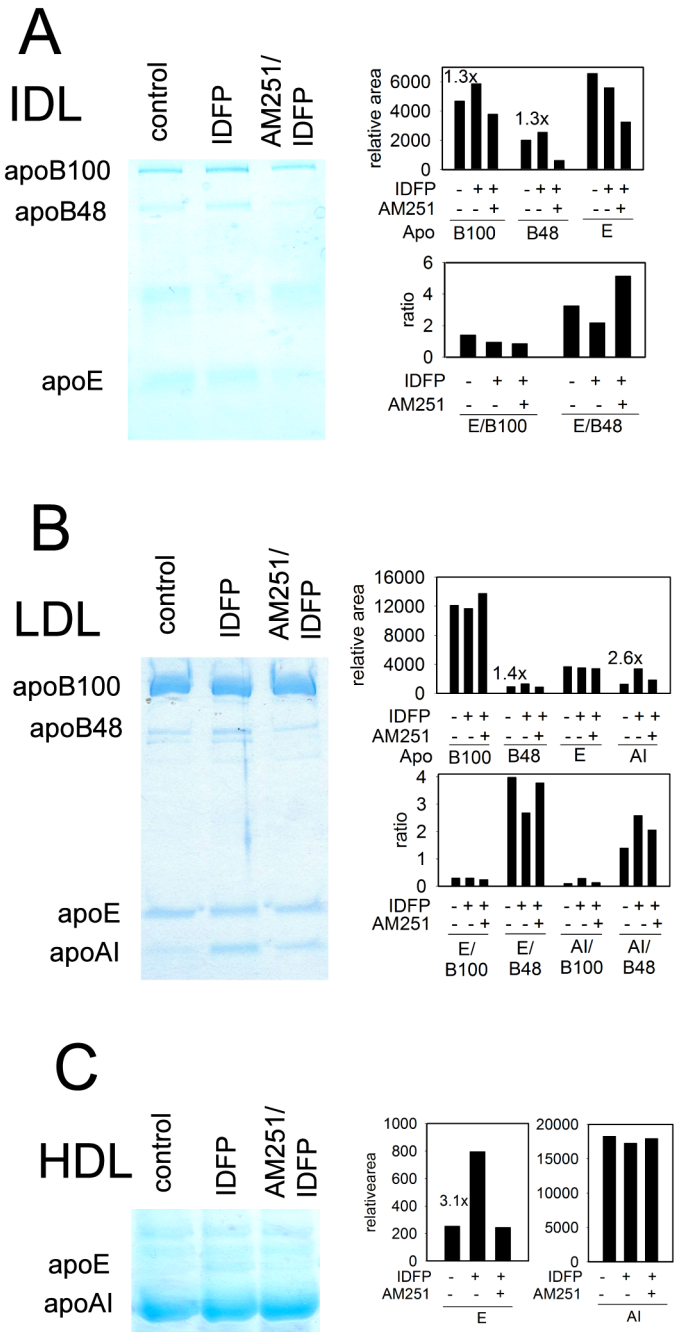

Figure 6: CB1-dependent effects of IDFP on apolipoproteins in IDL (A), LDL (B), and HDL (C) fractions. The experimental conditions and results for the VLDL fractions are given in Fig. 5.

Figure 7

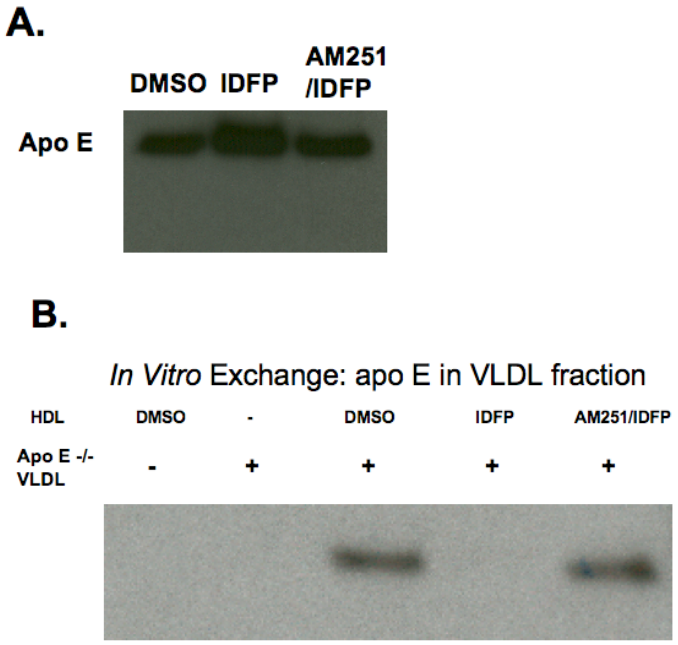

Figure 7: CB1-dependent effects of IDFP on ApoE HDL content (A) and exchange (B). HDL from Fig. 5 was subject to western blot analysis (A). HDL from animals treated as indicated was incubated with apoE -/- VLDL/IDL from Fig 8 for 18 hr and then the d<1.006 mg/ml fraction was collected and analyzed by western blot.

Figure 8

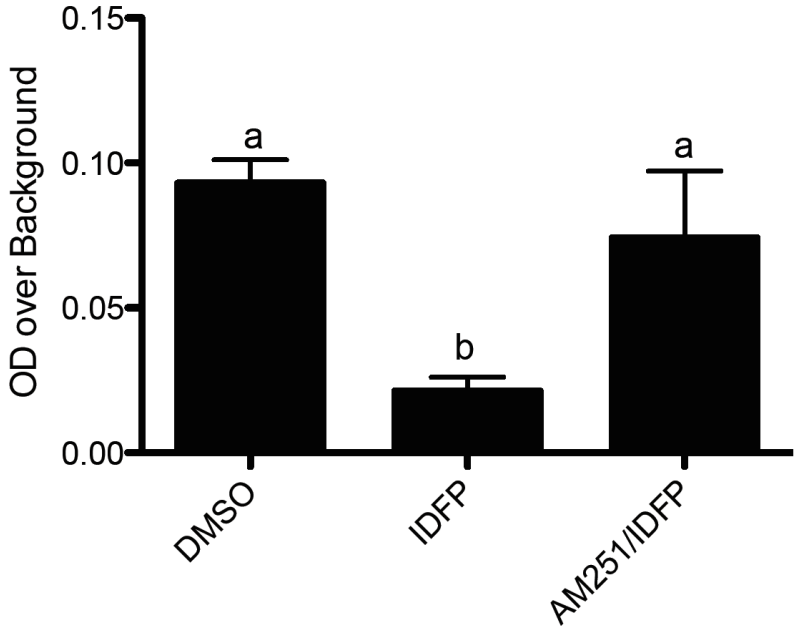

Figure 8: CB1-dependent effects of IDFP on plasma ApoE immunoreactivity. Plasma from animals in Fig 2 was analyzed by ELISA for apoE content. n=6-7.

Table 1. IDFP elevation of 2- and 1- palmitoylglycerol and 2- and 1-oleoylglycerol levels in liver, skeletal muscle, and adipose tissue[a]

Tissue and treatment	Monoacylglycerol (nmol/g)			
	2-palmitoyl	1-palmitoyl	2-oleoyl	1-oleoyl
Liver				
Control	0.39 ± 0.01	1.1 ± 0.2	3.8 ± 0.7	1.1 ± 0.1
IDFP	3.5 ± 1.6 *	3.0 ± 1.1 *	45 ± 15*	3.6 ± 1.5*
Skeletal Muscle				
Control	0.52 ± 0.03	4.0 ± 0.5	3.2 ± 2.2	2.6 ± 0.1
IDFP	6.3 ± 0.5***	4.7 ± 0.3	25 ± 4.3 **	2.5 ± 0.7
WAT				
Control	3.8 ± 0.4	6.2 ± 0.6	18 ± 3	14 ± 3
IDFP	6.7 ± 0.8**	7.1 ± 0.7	44 ± 12*	22 ± 6
BAT				
Control	4.7 ± 1.7	9.2 ± 3.2	18 ± 8.7	17 ± 10
IDFP	13 ± 4.2*	21 ± 7	66 ± 25*	22 ± 3

[a] The experimental conditions are given in Fig. 1 which also includes the data for 2-arachidonoylglycerol. n=3-4.

Table 2. Test for possible IDFP and AM251 effects on HDL cholesterol[a]

Mouse model and treatment	HDL cholesterol (mg/ml)
Swiss Webster	
DMSO	0.78 ± 0.39
AM251	0.81 ± 0.03
IDFP	0.84 ± 0.19
AM251/IDFP	0.79 ± 0.14
CB1 +/+	
DMSO	0.51 ± 0.15
IDFP	0.50 ± 0.14
CB1 -/-	
DMSO	0.47 ± 0.23
IDFP	0.38 ± 0.10

[a] Treatment protocols were as in Fig. 2. n=5-11.

Table 3. CB1-dependent effects of IDFP on VLDL composition[a]

Measurement	VLDL (mg/ml)
Triglycerides	
Control	0.26 (62)
IDFP	0.94 (68)
AM251/IDFP	0.35 (68)
Ratio (IDFP/control)	3.6
Free cholesterol	
Control	0.010 (2.5)
IDFP	0.033 (2.3)
AM251/IDFP	0.013 (2.6)
Ratio (IDFP/control)	3.3
Cholesterol ester	
Control	0.034 (8.0)
IDFP	0.077 (5.6)
AM251/IDFP	0.022 (4.4)
Ratio (IDFP/control)	2.3
Total phospholipids	
Control	0.053 (13)
IDFP	0.20 (14)
AM251/IDFP	0.063 (12)
Ratio (IDFP/control)	3.8
Protein	
Control	0.065 (15)
IDFP	0.13 (9.2)
AM251/IDFP	0.066 (13)
Ratio (IDFP/control)	2.0

Table 4. Test for possible IDFP effects on hepatic mRNA expression of apolipoproteins[a]

Lipoprotein	Fold-expression	
	Control	IDFP
Apo AI	1.0 ± 0.49	0.95 ± 0.17
Apo AV	1.0 ± 0.34	0.90 ± 0.25
Apo CIII	1.0 ± 0.28	1.08 ± 0.27
Apo E	1.0 ± 0.30	1.15 ± 0.29

[a] Treatment protocols for the Swiss Webster mice were as in Fig. 2**.** n=11.

CHAPTER 4
Overactive endocannabinoid signalling promotes hepatic steatosis and global transcriptional changes.

Abstract

Endocannabinoids regulate energy balance and lipid metabolism by stimulating the cannabinoid receptor type 1 (CB1). Genetic deletion and pharmacological antagonism have shown that CB1 signalling is necessary for the development of obesity and related metabolic disturbances. However, the sufficiency of endogenously produced endocannabinoids to cause hepatic lipid accumulation, independent of food intake, has not been demonstrated. Here, I show that administration of isopropoyl dodecyl fluorophosphonate (IDFP), a pharmacological inhibitor of endocannabinoid degradation, increases hepatic triglycerides in mice. These effects involve increased CB1 signaling, as they are mitigated by CB1 antagonist (AM251) pre-administration and in CB1 knockout mice. Despite the strong physiological effects of CB1 on hepatic lipid metabolism, little is known about the downstream targets responsible for these effects. To elucidate transcriptional targets of CB1 signaling, we performed microarrays on hepatic RNA isolated from DMSO (control), IDFP and AM251/IDFP treated mice. The expression pattern of IDFP mice segregated from DMSO in hierarchal cluster analysis and AM251 pre-administration reduced (>50%) most (303 out of 533) of the IDFP induced alterations. Pathway analysis revealed that IDFP altered expression of genes involved in lipid, fatty acid and steroid metabolism, the acute phase response, and amino acid metabolism in a CB1 dependent manner. PCR confirmed array results of most key target genes in multiple independent experiments. Overall, I show that IDFP creates hepatic TG accumulation, at least in part through the CB1 receptor, and identify novel cannabinoid responsive genes.

Introduction

Obesity elicits a cluster of interrelated disorders, termed the "metabolic syndrome", that increase the risk of cardiovascular disease(1). Dysregulation of the endocannabinoid (EC) system has been linked to increased adiposity in humans by epidemiological and genetic data(2-4). In four large human trials, 20 mg/day of the CB1 antagonist rimonabant resulted in clinically significant and prolonged reductions in body weight, waist circumference, and components of the metabolic syndrome(5-8)**.** The effects of rimonabant on plasma lipids and glycosylated hemoglobin appear to be partly independent of weight loss(9). Pharmacological or genetic ablation of the cannabinoid type 1 receptor (CB1) in diet-induced and genetic mouse models of obesity results in a transient hypophagic response, followed by prolonged effects on weight loss, adiposity, and normalization of metabolic parameters(10-15). These effects suggest that reduced food intake, a major known effect of CB1 inactivation, does not fully explain the improvement in adiposity-related measures with CB1 inactivation. Hepatic CB1 activation increases *de novo* lipogenesis through SREBP1c activation, and decreases fatty acid oxidation by inhibiting AMP kinase(16, 17). Furthermore, hepatocyte specific deletion of CB1 prevents hepatic steatosis, hyperlipidemia, and insulin resistance on a high-fat diet, despite normal weight gain(18). Similarly, ethanol-induced hepatic steatosis is absent in hepatocyte specific CB1 -/- animals(17). Together these observations raise the possibility that aberrant EC signaling mediates development of the metabolic syndrome, both by influencing body weight and direct regulation of metabolic processes.

While the necessity of CB1 signalling to the development of obesity and related metabolic disturbances has been demonstrated, it is uncertain if elevated endocannabinoids are sufficient to cause components of the metabolic syndrome. Furthermore, the molecular pathways underlying the powerful regulatory effects of CB1 on hepatic metabolism remain largely unclear. Here, I aimed to determine the ability of elevated endocannabinoid to stimulate hepatic steatosis and alter hepatic gene expression independent of food intake.

The EC system consists of the cannabinoid receptors, the endocannabinoids, and the enzymes responsible for their synthesis and breakdown. CB1 is a G-protein coupled membrane receptor that transmits its response via a $G_{i/o}$ protein mediated reduction in adenylate cyclase activity(19). The endocannabinoids, N-arachidonyl ethanolamine (AEA) and 2-arachidonoyl glycerol (2-AG), are arachidonic acid derivatives that are produced locally by phospholipases, N-acyl-phosphoatidylethanolamine-selective phospholipase D, and sn-1-selective diacylglycerol lipases, respectively(20). Anandamide is a partial CB1 agonist with moderate affinity for CB1, and 2-AG is a lower affinity complete CB1 agonist that is present at much higher concentrations than AEA. Signaling is terminated by enzymatic breakdown of AEA and 2-AG by fatty acid amide hydrolase (FAAH) and monoacylglycerol lipase (MAG-L), respectively(20).

To study the primary effects of elevated endocannabinoids, I chose to inhibit the enzymes responsible for endocannabinoid degradation since exogenously administered 2-AG and AEA are rapidly degraded(21). The organophosphorus compound isopropyl dodecylfluorophosphonate (IDFP) inhibits both MAGL and FAAH *in vivo* and raises 2-AG and anandamide levels(22). I have previously shown that IDFP increases circulating triglyceride concentrations in a CB1 dependent manner through the decreased clearance of TG-rich lipoproteins(23). CB1 antagonists and knockout mice can be used to assess

the contribution of CB1 signalling to IDFP effects. In the current study, I determined the CB1 dependent effects of IDFP on hepatic steatosis. In addition, to gain mechanistic insight into CB1 regulation of lipid metabolism, I also assayed global hepatic gene expression by microarray analysis of IDFP treated mice.

Materials and methods

Chemicals: AM251, the 4-iodophenyl analog of rimonabant which has a 4-chlorophenyl substituent, was obtained from Tocris Cookson Inc. IDFP was synthesized as previously described(24).

Animals: Tissues were provided for sub-study by Dr. Daniel Nomura in the laboratory of Dr. John Casida(22). Swiss Webster mice were from Harlan Laboratories. CB1 +/+ and -/- breeding pairs were obtained from Andreas Zimmer and Carl Lupica(25). All experiments used Swiss Webster mice unless specifically stated otherwise, i.e. +/+ or -/-. All mice were 6-8 weeks of age, male, and weighed 18-23 g. They were, treated i.p. at 1 µl/g with DMSO or test compounds dissolved in DMSO, and sacrificed at the indicated times.

Biochemical Analysis: Flash frozen liver samples were homogenized in radioimmunoprecipitation assay buffer and TG and cholesterol were analyzed by enzymatic end-point measurements utilizing enzyme reagent kits (Catalog # F6428 & T2449, Sigma & Catalog # EE3940, Siemens, respectively)(18). Protein concentration of the hepatic homogenate was determined by the bicinchoninic acid method(26).

Microarray Analysis: RNA was isolated from homogenized liver using the QAIGEN RNAeasy kit (Catalog # 74104, Qiagen) and cRNA synthesized using Illumina TotalPrep RNA amplification kit (Catalog # AMIL1791, Applied Biosystems) from isolated RNA(27). The cRNA was hybridized to mouseref-8 v2.0 beadchips and read on the iscan instrument according to manufactures instructions (Catalog # BD-202-0202, Illumina)(28). Data were processed using BeadStudio software 3.2 (Illumina) with quantile normalization, background subtraction, and multiple testing correction (Benjamini and Hochberg false discovery rate)(29). To quantify the effects of AM251 preadministration relative to IDFP induced alterations a reversal metric was calculated as follows with DMSO fold as 1.00:

reversal = (1 – ((DMSO fold – AM251/IDFP fold)/(DMSO fold– IDFP fold)))x100.

The web-based data analysis tools Panther (http://www.pantherdb.org) and FUNCASSOCIATE 2.0 ((http://llama.med.harvard.edu/funcassociate) were used with default settings(30, 31). The complete dataset is archived in the GEO database (accession # GSE22949).

PCR Conformation. Relative quantitative PCR was performed on the ABI7900 system using SYBR green master mix in triplicate (Applied Biosystems)(32). All genes were normalized to an endogenous control gene, gusb. The primers used are given in Table 1.

Statistical analyses. Results are presented as mean ± standard error. One-way analysis of variance was used to test significance of treatment effects. Post-hoc analysis (Student's unpaired t-test) examined significance ($p<0.05$) of individual treatment effects. All analyses were performed using JMP version 7.0.

RESULTS

1.1 IDFP produces CB1-dependent hepatic steatosis

To test the effects of elevated endocannabinoids on hepatic lipid levels, livers from mice treated with IDFP or vehicle control (DMSO) were analyzed for triglyceride and

cholesterol content. To determine the CB1-dependence of these effects, livers isolated from mice pretreated with the CB1 antagonist, AM251, were also analyzed. IDFP treatment significantly increased hepatic triglycerides levels (Fig. 1a), while AM251 pre-administration partially reversed this effect (Fig. 1a). IDFP had no significant effect on hepatic cholesterol content (Fig. 1b). The partially CB1 dependent increase in hepatic triglyceride levels was confirmed in CB1 -/- mice and wild-type littermates treated with IDFP (Fig. 2).

1.2 Global Gene Expression

To gain insight into the pathways activated by IDFP administration, specifically those dependent on CB1 activation, microarray analysis was performed on hepatic mRNA from DMSO, IDFP and AM251/IDFP treated animals. Of the 18,097 genes present on the array, 8,857 were detected in at least one of the groups at $p<0.05$. IDFP treated animals segregated well from DMSO treated animals in cluster analysis, while AM251/IDFP treated animals were intermingled with DMSO treated animals (fig 3). After correction for multiple testing, the expression of 533 genes was significantly altered by IDFP administration (Table 2). Of these, 230 were increased by IDFP, while 303 were decreased. To quantitate the ability of AM251 pre-administration to reverse IDFP induced changes in gene expression, the percent reversal (see methods for calculations) of the 533 significantly altered genes was determined. Although there was a large range (-128.3-310.5%), the average percent reversal (58.4 +/- 2.2%) was high, indicating that AM251 reversed a significant portion the IDFP effects on gene expression.

Two complementary approaches were used to identify functional categories within the data set. First, the Panther classification system was used to determine biological processes regulated within the dataset. This analysis accounts for the fold change of every gene detected, but is limited to differential analysis between two groups at a time. Lipid, fatty acid, and steroid metabolism was the only category to appear both when IDFP was compared with DMSO and when compared with Am251/IDFP (Table 3). To probe the CB1 dependent portion of significantly altered genes, upregulated (n=112) and downregulated (n=168) genes with >50% reversal and a nominal p value <0.05 between the IDFP and IDFP/AM251 groups were queried in Funcassociate 2.0. While the upregulated genes were not significantly enriched for any gene ontology attributes, the downregulated genes were enriched in genes with roles in translation, cellular amino acid metabolic processes, and the acute phase response (Table 4). The altered CB1 dependent genes represented within the enriched pathways and biological processes are shown in Table 5.

1.3 PCR Confirmation

To confirm and extend the results of IDFP effect on gene expression, quantitative PCR was performed on a larger set of samples representing three independent experiments, including the one used to generate the array data. The CB1 dependent effect of IDFP was confirmed for several key components of the lipid and cholesterol metabolism gene set including ldlr, insg1, pgc1β, acsl1 (Fig. 4). Although there were significant inter-sample correlations between the array and PCR data ($r=0.75$), in the larger sample set LPIN2 was not effectively reversed by AM251 pre-administration. Given the effects of IDFP on the srebp2 target genes, insig1 and ldlr, we also chose to probe the effect of IDFP on the rate-limiting enzyme in cholesterol biosynthesis, hmgcoA reductase, which was not represented on the array. IDFP increased expression hmgcoA

reductase, an effect that was completely prevented by AM251 pre-administration (Figure 4a).

The CB1 dependent inhibitory effect of IDFP was confirmed for several acute phase (saa2, orm2, stat3) and amino acid response genes (asns, aars, eef1e1, psat1, rars) (Fig. 4b,c). As stat3 is an essential transcription factor involved in the acute phase response, we tested the effect of IDFP on the canonical stat3 downstream targets apcs and lbp(33). IDFP decreased expression of both apcs and lbp in a CB1 dependent manner. We were not able to detect significant alterations in the phosphorylation status of tyrosine 709 in stat3 by western blot analysis (data not shown). There was good inter-sample correlation between the array and PCR data for all genes tested (r=0.7-1.0). The effect of IDFP on expression of genes involved in lipid metabolism and stat3 signaling were determined in CB1 -/- and wildtype littermates. There was a significant genotype-treatment interaction for several of the lipid metabolism genes tested, (ldlr, insig1, pgc1β, and acsl1), confirming the CB1 dependent effect of IDFP (Table 6). Stat3 and its targets, lbp and apcs, displayed the expected trend, but did not reach significance (Table 6).

Discussion

The data presented here demonstrate that IDFP induces hepatic steatosis partially through CB1 signaling. IDFP significantly increased hepatic triglyceride levels 4 hours after treatment. This effect was largely mediated by the CB1 receptor, as it was mitigated by AM251 pre-administration and deficient in CB1 -/- mice. As neither the effects of AM251 nor the genetic absence of CB1 in the animals used in the current study are confined to the periphery, the site of CB1 action responsible for observed effects cannot be addressed. However, all animals were fasted prior to and during the experimental period, eliminating differential energy intake as a confounding variable. Hepatic triglyceride content reflects the balance of secretion, uptake, synthesis, and oxidation. We have previously shown that IDFP decreases clearance of circulating triglycerides with no effect on hepatic TG secretion(23). Since CB1 antagonists increase adipose TG lipolysis, CB1 stimulated hepatic TG accumulation likely does not result from increased delivery of FA from adipose tissue(13, 34). Hepatic CB1 stimulates sprebp1c and inhibits AMP kinase, making both decreased oxidation and increased synthesis of fatty acids likely contributors to IDFP induced increase in hepatic triglyceride content(17, 18). Indeed, Ifound that IDFP increases expression of the lipogenic genes, fas and srebp1c, in a CB1 dependent manner(23). The CB1 independent effects of IDFP on hepatic triglycerides may result from inhibition of MAG lipase or other unknown effects. Further studies with specific MAG lipase inhibitors and knockout mice will be necessary to clarify the role of MAG lipase in the lipolytic cascade.

This work suggests that increased cannabinoid signaling can be considered a cause of hepatic steatosis rather than a consequence. As only a few genes have been identified as CB1 responsive in the liver, we aimed to identify novel CB1 targets stimulated by endocannabinoids. Although the microarrays detected ~9000 genes in at least one of the sample groups, some candidate genes were not represented on the chip, such as hmgcoA reductase. Comparison between the DMSO and IDFP groups yielded 533 significantly affected genes after multiple testing correction. The 533 genes had a skewed distribution of p-values for the IDFP vs. AM251/IDFP comparison, making the dataset ill-suited for FDR analysis including the generation of q-values. To quantify the CB1 dependence of the effect, a reversal metric and a nominal p-value were used to

screen the 533 genes. The 50% reversal cutoff for inclusion as CB1 dependent was by nature arbitrary, however stricter thresholds (80% cutoff) yielded similar results in the pathway analysis. PCR was used to validate several of the array findings in multiple independent experiments.

Hepatic CB1 has been shown to increase expression of the lipogenic genes fas, acc, and srebp1c. Here I identify pgc1β as a novel downstream target of CB1. This is of particular interest as pgc1β is a co-activator for srebp1c and is necessary for the development of diet-induced hyperlipidemia(35). Likewise expression of acsl1 was stimulated by CB1 activation. Acyl-coA synthetases activate fatty acids into acyl-CoAs, providing substrates for downstream fatty acid metabolic processing, such as esterification and β oxidation. Acsl1 is highly expressed in the liver and hepatocyte specific loss of acsl1 has been shown to decrease both fatty acid oxidation and incorporation into triglyceride(36). Acsl1 overexpression enhances incorporation of fatty acids in diacylglycerol, but does not cause TG accumulation(37). The effect of raising pgc1β and acsl1 expression in the setting of CB1 signalling requires further study.

Several of the key regulators of cholesterol homeostasis were increased by IDFP in CB1 dependent manner. This is of particular interest as CB1 signalling regulates plasma lipid and lipoprotein metabolism. In clinical trials, rimonabant had greater effects on triglyceride and HDL cholesterol than would be expected based on the basis of weight loss alone(9). Hepatocyte specific CB1 -/- mice are immune to diet induced alterations in plasma lipoproteins, and we have previously shown that IDFP causes hypertriglyceridemia secondary to decreased clearance of triglyceride-rich lipoproteins(18, 23). The coordinated regulation of several srebp2 target genes by IDFP in a CB1 dependent manner may result from direct regulation of this pathway by the CB1 signalling cascade. Alternatively, the IDFP induced decreased uptake of plasma lipoproteins may transiently decrease hepatic cholesterol content triggering srebp2 activity. Although we did not detect alterations in hepatic cholesterol content, the small magnitude and transience of changes required to stimulate srebp2 processing may not be detectable by the present methodology.

Previous work has uncovered a complex relationship between CB1 signaling and inflammation. Both activation and inhibition of CB1 have been shown to have anti-inflammatory outcomes in different contexts(38-41). In our study, IDFP decreased expression of acute phase proteins in a CB1 dependent manner. Interestingly, stat3 and several of its targets (apcs, lbp) were downregulated in IDFP treated livers. In neurons CB1 activation stimulates stat3(42). Consistent with a reversal of this system in the liver, rimonabant administration was recently shown to potentiate stat3 activation in response to LPS stimulation(38). While our results demonstrate that CB1 stimulation limits hepatic inflammation under basal conditions, the role of CB1 on systemic inflammation in response to various stimuli requires further study.

Interestingly, inflammatory signaling pathways, including stat3, influence metabolic regulation. Stat3 signaling mediates the hypophagic and hypoglycemic effects of leptin. Additionally, stat3 downregulates srebp1c, which was increased by IDFP in a CB1 dependent manner(43, 44). Hepatocyte specific loss of stat3 produces insulin resistance and increases susceptibility to ethanol-induced hepatic steatosis, lipogenic gene expression, and hypertriglyceridemia(43, 45). The current study raises the possibility that

CB1 mediated inhibition of hepatic stat3 signalling contributes to the metabolic disturbances caused by increased endocannabinoid signalling.

Although CB1 signalling has been linked to ER stress and mammalian target of rapamycin (mTOR) signaling, the relationship between cannabinoid signaling and amino acid metabolism remains unclear. mTOR is a serine/threonine protein kinase central to regulation amino acid metabolism and translation. THC, in a CB1 dependent fashion, stimulates mTOR in the hippocampus, but inhibits mTOR by stimulating ER stress in cancer cells(46, 47). In this study of hepatic tissue gene expression, IDFP caused a CB1 dependent decrease in the gene cassette involved in translation and amino acid metabolism. The direct effects of cannabinoid signaling on ER stress and mTOR activity in healthy liver will require further study.

As IDFP inhibits both MAGL and FAAH, the Cb1 dependent effects cannot be specifically ascribed to increases in either AEA or 2-AG levels. Future studies with specific chemical inhibitors or genetic manipulation of FAAH and/or MAGL will be necessary to confirm the relative contribution of each enzyme to the effects shown here. Though more specific than IDFP, the best available inhibitors of endocannabinoid breakdown still have off-target effects in the liver. Interestingly, the simultaneous elevation of AEA and 2-AG has been shown to have synergistic effects that are not recapitulated by raising levels of either endocannabinoid alone(48). Synthetic CB1 agonists may bind the receptor differently and produce differential downstream responses than the endocannabinoids. Nevertheless, the effects of such agonists on the IDFP-responsive genes whose effects were reversed by AM251 would be informative. The results support a causative role of CB1 signaling in the development of key features of the metabolic syndrome. Furthermore, the studies have identified novel genes responsive to IDFP in a CB1 dependent manner whose further study may add to our understanding pathways that are modulated by CB1 signaling. Future studies will validate the target genes and define their contribution to CB1 dependent alterations in metabolic parameters. The development of peripherally restricted Cb1 antagonists will be of importance in translating the findings from basic research, such as that presented here, to clinically meaningful solutions.

References

1. Lakka, H.M., Laaksonen, D.E., Lakka, T.A., Niskanen, L.K., Kumpusalo, E., Tuomilehto, J., and Salonen, J.T. 2002. The metabolic syndrome and total and cardiovascular disease mortality in middle-aged men. *Jama* 288:2709-2716.
2. Bluher, M., Engeli, S., Kloting, N., Berndt, J., Fasshauer, M., Batkai, S., Pacher, P., Schon, M.R., Jordan, J., and Stumvoll, M. 2006. Dysregulation of the peripheral and adipose tissue endocannabinoid system in human abdominal obesity. *Diabetes* 55:3053-3060.
3. Engeli, S., Bohnke, J., Feldpausch, M., Gorzelniak, K., Janke, J., Batkai, S., Pacher, P., Harvey-White, J., Luft, F.C., Sharma, A.M., et al. 2005. Activation of the peripheral endocannabinoid system in human obesity. *Diabetes* 54:2838-2843.
4. Sipe, J.C., Waalen, J., Gerber, A., and Beutler, E. 2005. Overweight and obesity associated with a missense polymorphism in fatty acid amide hydrolase (FAAH). *Int J Obes (Lond)* 29:755-759.
5. Despres, J.P., Golay, A., and Sjostrom, L. 2005. Effects of rimonabant on metabolic risk factors in overweight patients with dyslipidemia. *N Engl J Med* 353:2121-2134.
6. Pi-Sunyer, F.X., Aronne, L.J., Heshmati, H.M., Devin, J., and Rosenstock, J. 2006. Effect of rimonabant, a cannabinoid-1 receptor blocker, on weight and cardiometabolic risk factors in overweight or obese patients: RIO-North America: a randomized controlled trial. *Jama* 295:761-775.
7. Scheen, A.J., Finer, N., Hollander, P., Jensen, M.D., and Van Gaal, L.F. 2006. Efficacy and tolerability of rimonabant in overweight or obese patients with type 2 diabetes: a randomised controlled study. *Lancet* 368:1660-1672.
8. Van Gaal, L.F., Rissanen, A.M., Scheen, A.J., Ziegler, O., and Rossner, S. 2005. Effects of the cannabinoid-1 receptor blocker rimonabant on weight reduction and cardiovascular risk factors in overweight patients: 1-year experience from the RIO-Europe study. *Lancet* 365:1389-1397.
9. Van Gaal, L.F., Scheen, A.J., Rissanen, A.M., Rossner, S., Hanotin, C., and Ziegler, O. 2008. Long-term effect of CB1 blockade with rimonabant on cardiometabolic risk factors: two year results from the RIO-Europe Study. *Eur Heart J* 29:1761-1771.
10. Colombo, G., Agabio, R., Diaz, G., Lobina, C., Reali, R., and Gessa, G.L. 1998. Appetite suppression and weight loss after the cannabinoid antagonist SR 141716. *Life Sci* 63:PL113-117.
11. Cota, D., Marsicano, G., Tschop, M., Grubler, Y., Flachskamm, C., Schubert, M., Auer, D., Yassouridis, A., Thone-Reineke, C., Ortmann, S., et al. 2003. The endogenous cannabinoid system affects energy balance via central orexigenic drive and peripheral lipogenesis. *J Clin Invest* 112:423-431.
12. Di Marzo, V., Goparaju, S.K., Wang, L., Liu, J., Batkai, S., Jarai, Z., Fezza, F., Miura, G.I., Palmiter, R.D., Sugiura, T., et al. 2001. Leptin-regulated endocannabinoids are involved in maintaining food intake. *Nature* 410:822-825.
13. Jbilo, O., Ravinet-Trillou, C., Arnone, M., Buisson, I., Bribes, E., Peleraux, A., Penarier, G., Soubrie, P., Le Fur, G., Galiegue, S., et al. 2005. The CB1 receptor

antagonist rimonabant reverses the diet-induced obesity phenotype through the regulation of lipolysis and energy balance. *Faseb J* 19:1567-1569.
14. Ravinet Trillou, C., Arnone, M., Delgorge, C., Gonalons, N., Keane, P., Maffrand, J.P., and Soubrie, P. 2003. Anti-obesity effect of SR141716, a CB1 receptor antagonist, in diet-induced obese mice. *Am J Physiol Regul Integr Comp Physiol* 284:R345-353.
15. Ravinet Trillou, C., Delgorge, C., Menet, C., Arnone, M., and Soubrie, P. 2004. CB1 cannabinoid receptor knockout in mice leads to leanness, resistance to diet-induced obesity and enhanced leptin sensitivity. *Int J Obes Relat Metab Disord* 28:640-648.
16. Osei-Hyiaman, D., DePetrillo, M., Pacher, P., Liu, J., Radaeva, S., Batkai, S., Harvey-White, J., Mackie, K., Offertaler, L., Wang, L., et al. 2005. Endocannabinoid activation at hepatic CB1 receptors stimulates fatty acid synthesis and contributes to diet-induced obesity. *J Clin Invest* 115:1298-1305.
17. Jeong, W.I., Osei-Hyiaman, D., Park, O., Liu, J., Batkai, S., Mukhopadhyay, P., Horiguchi, N., Harvey-White, J., Marsicano, G., Lutz, B., et al. 2008. Paracrine activation of hepatic CB1 receptors by stellate cell-derived endocannabinoids mediates alcoholic fatty liver. *Cell Metab* 7:227-235.
18. Osei-Hyiaman, D., Liu, J., Zhou, L., Godlewski, G., Harvey-White, J., Jeong, W.I., Batkai, S., Marsicano, G., Lutz, B., Buettner, C., et al. 2008. Hepatic CB1 receptor is required for development of diet-induced steatosis, dyslipidemia, and insulin and leptin resistance in mice. *J Clin Invest* 118:3160-3169.
19. McAllister, S.D., and Glass, M. 2002. CB(1) and CB(2) receptor-mediated signalling: a focus on endocannabinoids. *Prostaglandins Leukot Essent Fatty Acids* 66:161-171.
20. Ahn, K., McKinney, M.K., and Cravatt, B.F. 2008. Enzymatic pathways that regulate endocannabinoid signaling in the nervous system. *Chem Rev* 108:1687-1707.
21. Smith, P.B., Compton, D.R., Welch, S.P., Razdan, R.K., Mechoulam, R., and Martin, B.R. 1994. The pharmacological activity of anandamide, a putative endogenous cannabinoid, in mice. *J Pharmacol Exp Ther* 270:219-227.
22. Nomura, D.K., Blankman, J.L., Simon, G.M., Fujioka, K., Issa, R.S., Ward, A.M., Cravatt, B.F., and Casida, J.E. 2008. Activation of the endocannabinoid system by organophosphorus nerve agents. *Nat Chem Biol* 4:373-378.
23. Ruby, M.A., Nomura, D.K., Hudak, C.S., Mangravite, L.M., Chiu, S., Casida, J.E., and Krauss, R.M. 2008. Overactive endocannabinoid signaling impairs apolipoprotein E-mediated clearance of triglyceride-rich lipoproteins. *Proc Natl Acad Sci U S A* 105:14561-14566.
24. Segall, Y., Quistad, G.B., Sparks, S.E., Nomura, D.K., and Casida, J.E. 2003. Toxicological and structural features of organophosphorus and organosulfur cannabinoid CB1 receptor ligands. *Toxicol Sci* 76:131-137.
25. Zimmer, A., Zimmer, A.M., Hohmann, A.G., Herkenham, M., and Bonner, T.I. 1999. Increased mortality, hypoactivity, and hypoalgesia in cannabinoid CB1 receptor knockout mice. *Proc Natl Acad Sci U S A* 96:5780-5785.

26. Smith, P.K., Krohn, R.I., Hermanson, G.T., Mallia, A.K., Gartner, F.H., Provenzano, M.D., Fujimoto, E.K., Goeke, N.M., Olson, B.J., and Klenk, D.C. 1985. Measurement of protein using bicinchoninic acid. *Anal Biochem* 150:76-85.
27. Van Gelder, R.N., von Zastrow, M.E., Yool, A., Dement, W.C., Barchas, J.D., and Eberwine, J.H. 1990. Amplified RNA synthesized from limited quantities of heterogeneous cDNA. *Proc Natl Acad Sci U S A* 87:1663-1667.
28. Llamas, B., Verdugo, R.A., Churchill, G.A., and Deschepper, C.F. 2009. Chromosome Y variants from different inbred mouse strains are linked to differences in the morphologic and molecular responses of cardiac cells to postpubertal testosterone. *BMC Genomics* 10:150.
29. Benjamini, Y., and Hochberg, Y. 1995. Controlling the False Discovery Rate - a Practical and Powerful Approach to Multiple Testing. *Journal of the Royal Statistical Society Series B-Methodological* 57:289-300.
30. Thomas, P.D., Kejariwal, A., Guo, N., Mi, H., Campbell, M.J., Muruganujan, A., and Lazareva-Ulitsky, B. 2006. Applications for protein sequence-function evolution data: mRNA/protein expression analysis and coding SNP scoring tools. *Nucleic Acids Res* 34:W645-650.
31. Berriz, G.F., King, O.D., Bryant, B., Sander, C., and Roth, F.P. 2003. Characterizing gene sets with FuncAssociate. *Bioinformatics* 19:2502-2504.
32. Yin, J.L., Shackel, N.A., Zekry, A., McGuinness, P.H., Richards, C., Putten, K.V., McCaughan, G.W., Eris, J.M., and Bishop, G.A. 2001. Real-time reverse transcriptase-polymerase chain reaction (RT-PCR) for measurement of cytokine and growth factor mRNA expression with fluorogenic probes or SYBR Green I. *Immunol Cell Biol* 79:213-221.
33. Alonzi, T., Maritano, D., Gorgoni, B., Rizzuto, G., Libert, C., and Poli, V. 2001. Essential role of STAT3 in the control of the acute-phase response as revealed by inducible gene inactivation [correction of activation] in the liver. *Mol Cell Biol* 21:1621-1632.
34. Buettner, C., Muse, E.D., Cheng, A., Chen, L., Scherer, T., Pocai, A., Su, K., Cheng, B., Li, X., Harvey-White, J., et al. 2008. Leptin controls adipose tissue lipogenesis via central, STAT3-independent mechanisms. *Nat Med* 14:667-675.
35. Lin, J., Yang, R., Tarr, P.T., Wu, P.H., Handschin, C., Li, S., Yang, W., Pei, L., Uldry, M., Tontonoz, P., et al. 2005. Hyperlipidemic effects of dietary saturated fats mediated through PGC-1beta coactivation of SREBP. *Cell* 120:261-273.
36. Li, L.O., Ellis, J.M., Paich, H.A., Wang, S., Gong, N., Altshuller, G., Thresher, R.J., Koves, T.R., Watkins, S.M., Muoio, D.M., et al. 2009. Liver-specific loss of long chain acyl-CoA synthetase-1 decreases triacylglycerol synthesis and beta-oxidation and alters phospholipid fatty acid composition. *J Biol Chem* 284:27816-27826.
37. Li, L.O., Mashek, D.G., An, J., Doughman, S.D., Newgard, C.B., and Coleman, R.A. 2006. Overexpression of rat long chain acyl-coa synthetase 1 alters fatty acid metabolism in rat primary hepatocytes. *J Biol Chem* 281:37246-37255.
38. Caraceni, P., Pertosa, A.M., Giannone, F., Domenicali, M., Grattagliano, I., Principe, A., Mastroleo, C., Perrelli, M.G., Cutrin, J., Trevisani, F., et al. 2009. Antagonism of the cannabinoid CB-1 receptor protects rat liver against ischaemia-reperfusion injury complicated by endotoxaemia. *Gut* 58:1135-1143.

39. Croci, T., Landi, M., Galzin, A.M., and Marini, P. 2003. Role of cannabinoid CB1 receptors and tumor necrosis factor-alpha in the gut and systemic anti-inflammatory activity of SR 141716 (rimonabant) in rodents. *Br J Pharmacol* 140:115-122.
40. Massa, F., Marsicano, G., Hermann, H., Cannich, A., Monory, K., Cravatt, B.F., Ferri, G.L., Sibaev, A., Storr, M., and Lutz, B. 2004. The endogenous cannabinoid system protects against colonic inflammation. *J Clin Invest* 113:1202-1209.
41. Richardson, J.D., Kilo, S., and Hargreaves, K.M. 1998. Cannabinoids reduce hyperalgesia and inflammation via interaction with peripheral CB1 receptors. *Pain* 75:111-119.
42. He, J.C., Gomes, I., Nguyen, T., Jayaram, G., Ram, P.T., Devi, L.A., and Iyengar, R. 2005. The G alpha(o/i)-coupled cannabinoid receptor-mediated neurite outgrowth involves Rap regulation of Src and Stat3. *J Biol Chem* 280:33426-33434.
43. Inoue, H., Ogawa, W., Ozaki, M., Haga, S., Matsumoto, M., Furukawa, K., Hashimoto, N., Kido, Y., Mori, T., Sakaue, H., et al. 2004. Role of STAT-3 in regulation of hepatic gluconeogenic genes and carbohydrate metabolism in vivo. *Nat Med* 10:168-174.
44. Ueki, K., Kondo, T., Tseng, Y.H., and Kahn, C.R. 2004. Central role of suppressors of cytokine signaling proteins in hepatic steatosis, insulin resistance, and the metabolic syndrome in the mouse. *Proc Natl Acad Sci U S A* 101:10422-10427.
45. Horiguchi, N., Wang, L., Mukhopadhyay, P., Park, O., Jeong, W.I., Lafdil, F., Osei-Hyiaman, D., Moh, A., Fu, X.Y., Pacher, P., et al. 2008. Cell type-dependent pro- and anti-inflammatory role of signal transducer and activator of transcription 3 in alcoholic liver injury. *Gastroenterology* 134:1148-1158.
46. Salazar, M., Carracedo, A., Salanueva, I.J., Hernandez-Tiedra, S., Lorente, M., Egia, A., Vazquez, P., Blazquez, C., Torres, S., Garcia, S., et al. 2009. Cannabinoid action induces autophagy-mediated cell death through stimulation of ER stress in human glioma cells. *J Clin Invest* 119:1359-1372.
47. Puighermanal, E., Marsicano, G., Busquets-Garcia, A., Lutz, B., Maldonado, R., and Ozaita, A. 2009. Cannabinoid modulation of hippocampal long-term memory is mediated by mTOR signaling. *Nat Neurosci* 12:1152-1158.
48. Long, J.Z., Nomura, D.K., Vann, R.E., Walentiny, D.M., Booker, L., Jin, X., Burston, J.J., Sim-Selley, L.J., Lichtman, A.H., Wiley, J.L., et al. 2009. Dual blockade of FAAH and MAGL identifies behavioral processes regulated by endocannabinoid crosstalk in vivo. *Proc Natl Acad Sci U S A* 106:20270-20275.

Tables

Table 1: PCR Primers

	Forward	Reverse
gusb	CAT GAG AGT GGT GTT GAG GAT CA	CCC ATT CAC CCA CAC AAC TG
orm2	TCA TGC TTG CCT TTG ACT TG	CAC GTG TGT GAC AGC CTT CT
psat1	AGC TCA GCT CCA TCA AAT CC	CAA AGC TTC GTC TCC TTT GG
eef1e1	AAA GGC AAT GGT TCA GCA GT	CGC CAG GGT GAT GTT ATG T
aars	TGG AGT GCA GAC AGA TTT GG	TCA CCC ATC TCC CAG AAG TT
rars	TTG CTG CTG CTC AGA TGA TT	CAT AAG GCG CAC AGT TTC AC
asns	GGG CAG AGA CAC CTA TGG AG	GAA GGA AGG GCTCCA CTT TT
acsl	CAG TTC ATC GGC CTC TTC TC	TCA GCT CCA AGG GTG TCA TA
pgc1b	GAG CTT TGA GGA GTC CCT GA	GGC TTG TAT GGA GGT GTG GT
ldlr	ACA GTG GCG TCA GTG ACA GT	CTC ATA CCA TGT GGC TGC TC
hmgcor	CTG GTG AGC TGT CCT TGA TG	GCG CTT CAG TTC AGT GTC AG
lbp	TCA CAC TAC CGG ACT TCA GC	GGA GCA GCT TCA GAG AGG AG
stat3	CCC GTA CCT GAA GAC CAA GT	GCA CCT TCA CCG TTA TTT CC
apcs	TGG ACA AGC TAC TGC TTT GG	GAT GTG GGA TCA GCT TCA CA
saa	GGG GAA CTA TGA TGC TGC TC	TGG TGT CCT CAT GTC CTC TG
insig1	CTG TAT TGC CGT GTT CGT TG	CTT CGG GAA CGA TCA AAT GT
lpin2	CTA TGC TGC CTT TGG AAA CC	CGA TGA TTT GTT CCC TTT GG

Table 2: Genes Significantly Altered by IDFP

Symbol	Entrez Gene ID	Fold Change		Nominal P-Values			Reversal (%)
		IDFP	AM251 /IDFP	DMSO vs. IDFP	IDFP vs. AM251/IDFP	DMSO vs. AM251/IDFP	
0610040J01Rik	76261	1.40	1.05	0.0033	0.0116	0.4560	87
1110002N22Rik	68550	0.61	0.82	0.0002	0.0128	0.0328	54
1190005F20Rik	98685	0.45	0.59	0.0000	0.0816	0.0031	26
1200014J11Rik	66874	0.72	0.74	0.0007	0.7028	0.0052	6
1300001I01Rik	74148	1.42	1.24	0.0001	0.1297	0.0646	43
1300007L22Rik	n/a	0.70	0.90	0.0074	0.1727	0.5277	66
1700030K09Rik	72254	0.41	0.46	0.0014	0.2304	0.0171	9
1700123O20Rik	58248	0.64	0.96	0.0000	0.0001	0.5039	88
1810008A18Rik	108707	0.60	0.69	0.0002	0.1440	0.0108	22
1810015C04Rik	66270	1.84	2.41	0.0009	0.0290	0.0001	-68
2010011I20Rik	67017	1.57	1.19	0.0021	0.0139	0.1920	67
2010305A19Rik	69893	0.33	0.58	0.0000	0.0013	0.0034	37
2210412D01Rik	70178	1.48	1.09	0.0067	0.0283	0.3647	81
2310016C08Rik	69573	2.82	1.48	0.0011	0.0253	0.0984	73
2310044G17Rik	217732	0.72	0.96	0.0056	0.0063	0.6385	85
2310065K24Rik	102122	0.60	0.82	0.0010	0.0014	0.1847	55
2410002O22Rik	66975	0.59	0.91	0.0000	0.0002	0.1297	77
2700097O09Rik	72658	0.58	1.03	0.0000	0.0000	0.6330	107
2810021B07Rik	66308	0.57	0.64	0.0002	0.3895	0.0040	16
2810403A07Rik	74200	0.59	0.76	0.0003	0.1108	0.0470	40
3110001A13Rik	66540	1.78	1.30	0.0012	0.0294	0.0981	62
3110037I16Rik	73172	0.55	0.62	0.0018	0.5287	0.0145	15
3300001P08Rik	67684	0.51	0.79	0.0000	0.0055	0.0673	56
4833426J09Rik	382051	1.37	1.37	0.0034	0.9701	0.0641	-2
4932442K08Rik	67544	0.31	0.61	0.0003	0.0478	0.0662	43
4933411K20Rik	66756	0.65	0.92	0.0003	0.0022	0.1615	77
4933428G20Rik	58996	1.38	1.16	0.0005	0.1196	0.2460	57
5730410E15Rik	319613	0.23	0.82	0.0001	0.0110	0.5222	77
5730449L18Rik	66637	0.47	0.60	0.0000	0.0111	0.0049	24
6430604K15Rik	269997	0.58	0.94	0.0007	0.0011	0.5278	85
9630015D15Rik	n/a	1.54	1.29	0.0010	0.0489	0.1580	47
AA415398	433752	0.63	0.63	0.0016	0.9293	0.0139	-2
Aars	234734	0.65	1.00	0.0010	0.0001	0.9958	100
Abcc3	76408	1.47	1.49	0.0053	0.9287	0.0617	-4
Abi3	n/a	0.39	0.69	0.0004	0.0010	0.0755	49
Acd	497652	0.72	0.75	0.0021	0.4997	0.0258	11
Acsl1	14081	1.79	1.05	0.0006	0.0016	0.7585	93
Actn4	60595	1.67	1.37	0.0006	0.0280	0.0557	44
Acvr2b	11481	0.67	0.71	0.0011	0.5634	0.0134	14
Adnp	11538	0.66	0.83	0.0001	0.0060	0.0243	51
Adrbk1	110355	0.63	0.66	0.0012	0.4819	0.0145	8
Aes	14797	1.60	1.35	0.0026	0.0665	0.0787	42
Agtr1a	11607	1.33	1.05	0.0018	0.0128	0.5043	83
Agxt2l1	71760	2.21	1.88	0.0028	0.4461	0.0149	27
AI132487	104910	1.36	1.23	0.0027	0.2532	0.0362	37
AI316807	102032	0.67	0.82	0.0014	0.1028	0.0978	43
AI451557	102084	0.39	1.06	0.0001	0.0002	0.4905	110

Akap12	83397	2.49	3.38	0.0025	0.3813	0.0489	-60
Aldoa	11674	1.62	0.94	0.0009	0.0008	0.5243	110
Ang	11727	0.66	1.04	0.0000	0.0003	0.6759	113
Ankzf1	52231	0.55	0.79	0.0001	0.0000	0.0740	54
Anxa6	11749	1.56	1.24	0.0053	0.0607	0.2303	56
Apcs	20219	0.48	1.06	0.0003	0.0014	0.7755	111
Apol9b	71898	1.66	1.02	0.0011	0.0032	0.9361	97
Arfl4	66182	2.52	1.74	0.0001	0.0161	0.0155	51
Arhgap18	73910	1.58	1.25	0.0011	0.0717	0.0515	56
Arhgap26	71302	8.47	4.03	0.0000	0.0092	0.0525	60
Arhgap30	226652	0.44	0.77	0.0004	0.0006	0.1630	59
Arhgef18	102098	0.64	0.80	0.0031	0.0373	0.1041	46
Arl16	70317	0.67	0.72	0.0004	0.4244	0.0191	14
Arl4a	11861	2.47	1.44	0.0000	0.0030	0.0171	70
Armcx1	78248	0.39	0.62	0.0000	0.0930	0.0154	37
Armcx3	71703	0.66	0.87	0.0006	0.0662	0.3248	63
Arrdc4	66412	1.82	1.27	0.0053	0.0793	0.1019	67
Asb3	65257	0.51	0.86	0.0000	0.0011	0.1047	71
Asns	27053	0.15	0.68	0.0000	0.0081	0.1654	62
Atf4	11911	0.71	0.92	0.0001	0.0372	0.4707	72
Atf7ip	54343	0.50	0.75	0.0004	0.0065	0.0497	50
Atxn1	20238	1.45	0.99	0.0079	0.0117	0.9053	102
Axin2	12006	0.49	0.78	0.0008	0.0508	0.2796	58
B230312A22Rik	230088	2.52	2.74	0.0007	0.6912	0.0068	-15
B230342M21Rik	100637	0.60	0.71	0.0011	0.3809	0.0266	28
B4galt3	57370	0.62	0.82	0.0000	0.0000	0.0218	54
Bap1	n/a	1.55	1.37	0.0006	0.1823	0.0063	33
BC002199	211556	0.63	0.85	0.0001	0.0008	0.1199	61
BC003236	n/a	2.12	1.43	0.0004	0.0186	0.0452	62
BC005537	79555	1.47	1.27	0.0000	0.0422	0.0052	43
BC017158	233913	0.71	0.70	0.0005	0.6648	0.0038	-4
BC017612	170748	0.61	0.70	0.0011	0.4524	0.0414	22
BC022224	192970	1.51	1.12	0.0006	0.0189	0.3783	77
BC026590	230234	0.60	0.61	0.0002	0.7012	0.0030	3
BC031353	235493	0.55	0.65	0.0061	0.5250	0.0711	22
BC037034	231807	0.65	0.66	0.0005	0.8537	0.0079	3
BC056474	414077	1.52	1.33	0.0079	0.3276	0.0430	36
Bcar1	12927	1.85	0.87	0.0032	0.0031	0.2851	116
Bcl2l1	12048	2.21	2.65	0.0001	0.2876	0.0035	-37
Bcl2l13	94044	1.39	1.22	0.0003	0.0875	0.0098	43
Bhlhb2	20893	1.98	0.92	0.0124	0.0150	0.4485	108
Brf2	66653	0.63	0.76	0.0001	0.0378	0.0030	36
Btbd12	52864	0.53	0.71	0.0006	0.0370	0.0483	39
Btg1	12226	1.36	1.14	0.0031	0.1868	0.3779	61
Bud13	215051	0.62	0.76	0.0020	0.0921	0.0846	35
C430004E15Rik	97031	2.41	1.27	0.0023	0.0142	0.1165	81
Casp1	12362	0.55	0.87	0.0012	0.0062	0.3831	71
Ccar1	n/a	0.65	1.11	0.0000	0.0000	0.2069	130
Ccdc120	54648	2.34	1.82	0.0136	0.3365	0.0248	39
Ccdc130	67736	0.41	0.69	0.0000	0.0009	0.0025	47
Ccdc131	216345	0.46	0.82	0.0000	0.0028	0.1567	66
Ccdc134	76457	0.35	0.66	0.0000	0.0425	0.0969	48
Ccnl1	56706	1.90	1.33	0.0029	0.0657	0.0399	63

Ccr5	12774	0.17	0.46	0.0000	0.0084	0.0126	35
Cd14	12475	3.06	3.93	0.0003	0.4732	0.0484	-42
Cd83	12522	6.86	1.96	0.0000	0.0001	0.2373	84
Cdc42bpb	217866	1.54	1.11	0.0028	0.0357	0.3891	79
Cdc42ep4	56699	1.50	1.23	0.0020	0.0161	0.1802	55
Cdc42ep5	58804	4.63	1.30	0.0048	0.0161	0.4133	92
Cdkn1a	12575	3.32	3.14	0.0004	0.8069	0.0119	8
Cebpb	12608	1.89	2.07	0.0001	0.1576	0.0008	-19
Chac1	69065	0.24	0.34	0.0000	0.0077	0.0011	14
Chchd8	68185	0.43	0.64	0.0001	0.0091	0.0165	36
Chkb	12651	1.81	1.26	0.0005	0.0151	0.0851	67
Chordc1	66917	0.61	0.83	0.0000	0.0364	0.1206	56
Chrd	12667	0.46	0.61	0.0001	0.0106	0.0110	28
Cirbp	12696	2.23	1.39	0.0000	0.0068	0.1263	68
Clk4	12750	0.87	1.12	0.0166	0.0001	0.0306	192
Clp1	98985	0.53	0.93	0.0000	0.0003	0.4819	84
Cml2	93673	0.52	0.84	0.0000	0.0028	0.0324	67
Cpeb2	231207	2.91	0.58	0.0045	0.0023	0.0231	122
Cpne8	66871	0.22	1.23	0.0001	0.0036	0.5340	130
Crcp	12909	1.67	2.02	0.0004	0.0137	0.0001	-53
Creb3l3	208677	1.44	1.24	0.0000	0.0849	0.0900	44
Cry2	12953	1.62	1.75	0.0043	0.6362	0.0111	-20
Cs	12974	1.40	1.26	0.0000	0.0430	0.0050	35
Csnk1d	104318	1.61	1.02	0.0010	0.0026	0.7489	96
Csnk1e	27373	1.93	1.30	0.0001	0.0055	0.0052	68
Ctsl	13039	2.03	2.75	0.0161	0.2423	0.0078	-70
Cttnbp2nl	80281	2.29	1.48	0.0014	0.0392	0.1084	63
Cxcl1	14825	0.38	0.96	0.0013	0.0130	0.8186	94
Cxcl4	56744	1.66	2.20	0.0014	0.4079	0.1316	-82
Cyp4f15	106648	1.38	1.50	0.0094	0.4543	0.0121	-33
D030074E01Rik	75964	2.31	1.04	0.0018	0.0035	0.7853	97
D11Wsu47e	276852	0.32	0.61	0.0000	0.0001	0.0089	43
D15Ertd682e	71919	0.51	0.89	0.0001	0.0006	0.3356	79
D6Wsu163e	28040	0.50	0.72	0.0000	0.0026	0.0012	44
D930015E06Rik	229473	2.61	0.89	0.0046	0.0061	0.6624	107
Dact2	240025	3.25	1.23	0.0072	0.0329	0.5637	90
Dgat2	67800	1.37	1.18	0.0056	0.0982	0.1029	53
Dhx30	72831	0.70	0.80	0.0008	0.0112	0.0343	34
Dnajb10	56812	0.63	0.72	0.0002	0.1252	0.0208	26
Dnajb9	27362	0.46	0.95	0.0000	0.0045	0.7878	91
Dnmbp	71972	6.94	3.64	0.0015	0.0656	0.0019	56
Dok3	27261	0.48	0.84	0.0001	0.0028	0.1955	70
Dom3z	112403	0.73	0.84	0.0002	0.0461	0.0476	40
Dot1l	208266	2.55	1.34	0.0002	0.0056	0.1598	78
Dph2	67728	0.52	0.97	0.0000	0.0000	0.7430	94
Dpp8	74388	0.64	0.84	0.0005	0.0012	0.1007	56
Dusp11	72102	0.72	0.97	0.0001	0.0001	0.5792	89
Dusp16	70686	1.76	1.59	0.0000	0.1980	0.0031	22
Dyrk2	69181	2.45	1.16	0.0003	0.0025	0.4973	89
E130012A19Rik	103551	2.07	2.12	0.0013	0.8838	0.0003	-5
Eef1e1	66143	0.57	1.14	0.0003	0.0001	0.0653	133
EG622320	622320	0.37	0.61	0.0001	0.0672	0.0175	38
Eif2ak2	19106	0.51	0.80	0.0000	0.0017	0.0733	59

Eif2b4	13667	0.73	0.95	0.0010	0.0005	0.5840	82
Eif4ebp1	13685	0.60	0.76	0.0002	0.0897	0.0181	40
Eif4ebp2	13688	1.44	0.96	0.0034	0.0006	0.7741	109
Ell	13716	0.65	0.92	0.0023	0.0076	0.4978	78
Eng	13805	1.47	1.20	0.0034	0.1104	0.0941	57
ENSMUSG00000053178	208595	0.44	0.64	0.0001	0.0127	0.0148	36
Eps8l2	98845	1.58	0.63	0.0012	0.0000	0.0005	164
Erdr1	170942	1.82	1.59	0.0045	0.4729	0.0544	28
Es22	13897	1.47	1.26	0.0048	0.1533	0.0395	44
Ets2	23872	1.73	1.58	0.0016	0.6055	0.0553	21
Ext1	14042	1.57	1.70	0.0004	0.4606	0.0054	-23
Extl1	56219	0.44	0.53	0.0011	0.2730	0.0130	16
F11r	16456	1.51	0.89	0.0001	0.0000	0.1863	122
Fadd	14082	0.67	0.61	0.0001	0.1722	0.0007	-18
Farsb	23874	0.74	0.96	0.0002	0.0031	0.5957	84
Fas	14102	0.69	1.03	0.0001	0.0013	0.7984	109
Fastkd5	380601	0.56	1.05	0.0000	0.0000	0.5685	112
Fbf1	217335	4.50	4.73	0.0020	0.8831	0.0285	-7
Fbxo21	231670	1.62	0.89	0.0001	0.0001	0.3711	118
Fbxo25	66822	0.64	0.64	0.0019	0.9652	0.0170	1
Fbxo30	71865	0.59	0.91	0.0004	0.0105	0.4410	78
Fbxo34	78938	1.73	1.65	0.0002	0.6224	0.0005	11
Fcgr3	14131	0.66	1.05	0.0002	0.0003	0.6106	114
Fem1b	14155	0.65	0.92	0.0000	0.0014	0.3568	78
Fermt2	218952	0.54	0.56	0.0020	0.8192	0.0158	3
Fgf21	56636	0.03	0.12	0.0000	0.0306	0.0007	9
Fgfrl1	116701	1.54	1.02	0.0007	0.0065	0.8933	96
Fgl1	234199	0.65	1.09	0.0004	0.0000	0.3263	125
Fkbp4	14228	1.69	0.96	0.0007	0.0005	0.7772	105
Flcn	216805	0.36	0.60	0.0000	0.0004	0.0103	38
Flot1	14251	0.50	0.99	0.0000	0.0000	0.9552	99
Flvcr2	217721	2.00	0.64	0.0043	0.0010	0.0493	136
Fndc3b	72007	0.55	1.32	0.0004	0.0004	0.1591	171
Foxa3	15377	0.74	0.70	0.0024	0.5906	0.0185	-17
Foxp1	108655	2.90	1.63	0.0000	0.0012	0.0213	67
Fpr2	14289	0.53	1.52	0.0003	0.0460	0.3430	211
Fst	14313	5.34	4.57	0.0016	0.6367	0.0214	18
G0s2	14373	0.29	0.16	0.0004	0.0745	0.0011	-18
G6pc	14377	2.64	1.31	0.0004	0.0066	0.2609	81
Gadd45b	17873	10.25	3.81	0.0001	0.0060	0.0159	70
Gamt	14431	0.68	0.70	0.0027	0.7534	0.0256	6
Gars	353172	0.65	0.85	0.0001	0.0186	0.0671	58
Gbl	56716	0.64	0.70	0.0003	0.1613	0.0118	17
Gck	103988	2.78	1.38	0.0008	0.0070	0.0700	78
Gfod2	70575	0.36	0.77	0.0001	0.0036	0.1197	64
Gimap9	317758	0.48	1.19	0.0013	0.0001	0.1981	137
Gja4	14612	2.49	2.15	0.0003	0.4454	0.0235	23
Gna12	14673	2.70	1.45	0.0000	0.0010	0.1579	74
Gnat1	14685	0.42	1.18	0.0010	0.0002	0.2488	131
Golga1	76899	0.52	0.68	0.0000	0.0547	0.0024	33
Golga3	269682	0.58	0.98	0.0000	0.0000	0.8176	96
Golph3l	229593	0.44	0.80	0.0001	0.0031	0.2321	64
Gpatch2	67769	0.61	0.95	0.0000	0.0002	0.2483	88

Gtf2e1	74197	0.62	1.03	0.0003	0.0001	0.7633	109
Gtf2h3	209357	0.62	0.70	0.0002	0.0596	0.0076	20
H3f3b	15081	2.06	1.95	0.0000	0.5370	0.0001	10
Hax1	23897	0.69	0.86	0.0000	0.0038	0.0354	55
Hdgfrp2	15193	0.74	0.74	0.0006	0.8648	0.0030	-2
Hdhd3	72748	0.69	0.57	0.0020	0.1943	0.0001	-39
Heatr1	217995	0.57	0.98	0.0001	0.0013	0.8485	94
Herpud1	64209	1.43	1.29	0.0014	0.1514	0.0597	34
Hhex	15242	0.40	0.73	0.0050	0.1665	0.2822	55
Hic2	58180	3.58	1.91	0.0005	0.0237	0.0678	65
Hist1h1c	50708	2.92	1.00	0.0000	0.0001	0.9855	100
Hist2h3b	319154	2.02	1.85	0.0001	0.4766	0.0007	16
Hist2h3c1	15077	2.02	1.81	0.0000	0.2801	0.0002	20
Hnrpl	15388	1.36	1.26	0.0001	0.1851	0.0301	28
Iars	105148	0.65	0.97	0.0001	0.0004	0.7385	93
Ibtk	n/a	0.68	0.88	0.0025	0.0094	0.3302	64
Icam1	15894	0.58	1.09	0.0000	0.0498	0.7575	121
Id2	15902	0.49	0.62	0.0008	0.0503	0.0251	26
Ifi47	15953	0.43	0.75	0.0008	0.0032	0.1946	56
Igfbp2	16008	1.53	1.56	0.0035	0.8322	0.0001	-7
Igtp	16145	0.66	0.79	0.0013	0.1542	0.0966	39
Iigp2	54396	0.56	0.81	0.0006	0.0305	0.2065	57
Il13ra1	16164	0.65	1.12	0.0016	0.0012	0.4318	134
Il15ra	16169	0.51	0.92	0.0000	0.0018	0.4202	84
Il16	16170	0.24	0.58	0.0015	0.0530	0.1856	45
Impact	16210	1.42	1.36	0.0026	0.6648	0.0001	13
Inhbe	16326	0.10	0.27	0.0000	0.0010	0.0004	19
Insc	233752	0.53	1.86	0.0016	0.0001	0.0094	285
Insig1	231070	1.90	1.08	0.0016	0.0057	0.6093	91
Ipmk	69718	1.53	1.04	0.0087	0.0383	0.7879	92
Irak3	73914	0.43	1.38	0.0003	0.0338	0.4535	166
Irf1	16362	0.50	0.57	0.0001	0.2113	0.0022	15
Irf2bp1	272359	0.59	0.60	0.0009	0.8987	0.0079	2
Itgb5	16419	1.33	0.88	0.0010	0.0000	0.2405	137
Jdp2	81703	3.82	2.13	0.0007	0.0191	0.0470	60
Jun	16476	1.69	1.81	0.0009	0.5974	0.0096	-17
Jund1	16478	3.17	1.50	0.0018	0.0129	0.1177	77
Kctd2	70382	0.47	0.45	0.0014	0.7387	0.0102	-3
Klb	83379	1.76	1.09	0.0001	0.0020	0.5108	89
Klf13	50794	1.56	1.82	0.0060	0.1901	0.0034	-47
Klf2	16598	1.97	2.07	0.0052	0.7692	0.0055	-10
Klf7	93691	1.47	1.13	0.0030	0.0412	0.4411	73
Krcc1	57896	0.74	0.80	0.0001	0.1696	0.0083	24
Krt10	16661	1.43	1.08	0.0006	0.0124	0.3558	81
Krt23	94179	1.84	0.54	0.0058	0.0005	0.0206	155
Krt8	16691	2.13	1.16	0.0055	0.0160	0.5518	86
Lars	107045	0.63	1.11	0.0000	0.0011	0.4374	129
Lcn2	16819	0.20	2.68	0.0028	0.0000	0.0007	311
Ldlr	16835	4.50	1.30	0.0000	0.0001	0.4476	92
Lhfpl2	218454	0.61	0.48	0.0049	0.2992	0.0011	-34
Litaf	56722	0.62	0.98	0.0001	0.0010	0.8448	94
Lmo4	16911	0.69	0.95	0.0045	0.0697	0.7649	84
Lnx2	140887	2.20	1.38	0.0114	0.0987	0.0128	68

LOC100041103	100041103	1.37	1.03	0.0015	0.0076	0.7494	92
LOC100044862	100044862	1.41	1.26	0.0000	0.0206	0.0015	38
LOC100045343	n/a	0.18	0.54	0.0000	0.0002	0.0305	44
LOC100045963	100045963	1.55	1.26	0.0001	0.0296	0.0879	52
LOC100046406	100046406	0.44	0.90	0.0006	0.0040	0.4710	81
LOC100046891	n/a	0.50	0.75	0.0000	0.0003	0.0145	51
LOC100047200	100047200	0.30	0.49	0.0003	0.0079	0.0167	26
LOC100047427	100047427	4.22	1.06	0.0001	0.0003	0.6144	98
LOC100047707	100047707	1.37	1.27	0.0004	0.1873	0.0366	27
LOC100047762	100047762	2.33	3.10	0.0004	0.0378	0.0000	-57
LOC100047834	100047834	0.69	0.79	0.0039	0.1913	0.0675	32
LOC100047911	100047911	0.49	0.59	0.0000	0.2808	0.0037	20
LOC100047934	100047934	0.27	0.69	0.0001	0.0063	0.1776	58
LOC100048105	100048105	1.46	1.06	0.0080	0.0372	0.4991	87
LOC216443	n/a	0.58	0.72	0.0001	0.0307	0.0054	34
LOC381302	n/a	0.43	0.57	0.0000	0.0662	0.0035	25
LOC382010	n/a	0.57	0.80	0.0006	0.0110	0.1617	55
Loh11cr2a	67776	0.71	0.86	0.0031	0.0785	0.1872	50
Lpgat1	226856	0.68	0.87	0.0056	0.0375	0.1943	61
Lpin2	n/a	3.22	1.70	0.0001	0.0069	0.1290	69
Lrfn3	233067	2.33	0.84	0.0073	0.0071	0.2294	112
Lrg1	76905	0.56	0.98	0.0000	0.0001	0.6464	96
Lrig1	16206	0.50	0.72	0.0001	0.0051	0.0146	44
Lrrc29	234684	0.17	0.60	0.0000	0.0001	0.0086	52
Lrrc3	237387	1.35	0.88	0.0022	0.0003	0.2183	134
Lypla3	192654	0.63	0.58	0.0001	0.1976	0.0006	-12
Lysmd4	75099	0.65	1.19	0.0011	0.0003	0.1053	155
Lztr1	66863	0.71	0.74	0.0016	0.4831	0.0306	12
Map3k1	26401	0.50	1.03	0.0019	0.0037	0.8088	105
Mapk6	50772	1.62	1.56	0.0001	0.6830	0.0008	9
Mapkapk2	17164	2.30	1.92	0.0015	0.3374	0.0024	29
Mbc2	23943	0.67	0.72	0.0007	0.3409	0.0064	16
Mbd3	17192	1.57	1.22	0.0007	0.0120	0.0675	61
Mboat5	14792	1.52	0.85	0.0000	0.0000	0.0953	128
Mcl1	17210	0.70	0.92	0.0017	0.0007	0.3423	72
Med31	67279	0.59	0.86	0.0000	0.0010	0.1385	66
Meis1	17268	0.57	0.62	0.0064	0.7070	0.0076	12
Mettl3	56335	0.47	0.61	0.0001	0.0586	0.0086	26
Mettl6	67011	0.43	1.02	0.0002	0.0000	0.8534	104
Mknk1	17346	0.63	0.84	0.0001	0.0140	0.0579	56
Mknk2	17347	2.02	1.78	0.0002	0.2976	0.0133	24
Mmp15	17388	1.96	1.01	0.0021	0.0138	0.9706	99

Mphosph6	68533	1.65	1.65	0.0065	0.9927	0.0045	0
Mrap	77037	1.43	1.90	0.0014	0.0439	0.0024	-113
Mreg	381269	1.41	0.86	0.0028	0.0001	0.2647	133
Mrm1	217038	0.45	0.61	0.0004	0.0586	0.0371	29
Mrpl50	28028	0.73	0.78	0.0005	0.0408	0.0125	16
Mtap7d1	245877	0.57	0.87	0.0000	0.0000	0.1030	70
Mterf	545725	0.42	0.70	0.0000	0.0005	0.0310	48
Mthfd2	17768	0.16	0.67	0.0000	0.0009	0.0885	61
Mtmr3	74302	2.08	1.42	0.0000	0.0041	0.0932	61
Mtnr1a	17773	2.00	0.88	0.0020	0.0004	0.6389	112
Myadm	50918	1.80	1.45	0.0003	0.1614	0.0717	44
Mycl1	16918	1.87	0.84	0.0020	0.0007	0.3935	119
Myd88	17874	0.54	1.15	0.0000	0.0002	0.2716	132
Narf	67608	0.55	1.04	0.0005	0.0001	0.7007	109
Ncbp2	68092	0.51	0.64	0.0003	0.2536	0.0343	28
Ncf4	17972	0.32	0.85	0.0011	0.0021	0.5671	78
Ncoa5	228869	0.57	0.81	0.0000	0.0002	0.0403	55
Ndrg1	17988	2.40	1.52	0.0009	0.0461	0.0537	63
Ndrl	n/a	2.27	1.61	0.0040	0.1439	0.0141	52
Nedd4l	83814	0.68	1.12	0.0017	0.0014	0.3578	137
Nfkbia	18035	1.98	1.87	0.0011	0.6242	0.0199	11
Nfkbib	n/a	3.26	2.62	0.0000	0.2077	0.0027	28
Nmd3	97112	1.53	1.42	0.0002	0.4758	0.0156	20
Nol10	217431	0.69	1.14	0.0007	0.0001	0.1108	145
Nola1	68147	0.67	0.91	0.0013	0.0129	0.4790	74
Nos3	18127	0.41	1.12	0.0016	0.0001	0.5277	120
Nploc4	217365	1.51	1.62	0.0004	0.3253	0.0006	-23
Nr1d1	217166	4.96	1.17	0.0001	0.0006	0.4059	96
Nr1h4	20186	0.51	0.62	0.0000	0.0211	0.0000	23
Nr2f6	13864	1.48	1.01	0.0026	0.0057	0.8921	98
Nsmce1	67711	0.69	0.75	0.0003	0.1461	0.0106	22
Nudt4	71207	1.38	1.21	0.0003	0.0955	0.0320	44
Nup62	18226	1.40	1.25	0.0072	0.2290	0.0371	37
Nupl2	231042	0.41	0.69	0.0000	0.0003	0.0018	49
Obfc2a	109019	0.60	0.74	0.0024	0.2133	0.0327	34
Optn	71648	1.35	1.08	0.0002	0.0074	0.2842	77
Oraov1	72284	0.40	0.49	0.0003	0.2439	0.0095	14
Orm1	18405	0.70	1.43	0.0076	0.0000	0.0021	246
Orm2	n/a	0.41	1.79	0.0020	0.0004	0.0543	233
Osmr	18414	0.60	1.43	0.0027	0.0529	0.3622	209
Ovca2	246257	0.64	0.71	0.0013	0.1092	0.0310	19
P2ry13	74191	0.22	0.51	0.0000	0.0071	0.0029	37
P2ry6	233571	0.42	0.60	0.0004	0.0041	0.0292	31
Pah	18478	1.52	1.51	0.0113	0.9595	0.0268	2
Parp16	214424	1.52	1.14	0.0021	0.0954	0.5736	73
Pdcl	67466	0.63	0.91	0.0006	0.0027	0.4792	76
Pelo	105083	0.64	0.91	0.0000	0.0017	0.3583	75
Per1	18626	2.67	2.46	0.0019	0.6952	0.0133	13
Pgpep1	66522	1.54	0.74	0.0008	0.0000	0.0509	148
Pgs1	74451	0.67	0.97	0.0001	0.0019	0.7464	91
Phactr4	100169	0.74	0.90	0.0002	0.0051	0.0827	63
Phf13	230936	1.70	1.05	0.0002	0.0007	0.6119	93
Phospho2	73373	0.73	0.93	0.0000	0.0065	0.2560	73

Pim3	n/a	2.15	1.58	0.0107	0.1822	0.0221	49
Pla2g6	53357	1.68	1.30	0.0005	0.0410	0.0290	55
Plekhf2	71801	1.51	1.19	0.0001	0.0103	0.0177	63
Plekhg5	269608	2.95	1.13	0.0006	0.0044	0.6486	93
Plrg1	53317	0.59	1.05	0.0000	0.0000	0.5487	113
Pls3	102866	0.63	0.93	0.0028	0.0086	0.6068	81
Pole4	66979	0.64	1.24	0.0034	0.0001	0.0659	169
Ppargc1a	19017	2.47	2.18	0.0059	0.5718	0.0104	20
Ppargc1b	170826	6.78	2.16	0.0000	0.0011	0.0509	80
Ppl	19041	2.06	1.45	0.0004	0.0551	0.0491	58
Ppp1r10	52040	0.33	0.89	0.0001	0.0001	0.3405	83
Ppp2r2d	52432	1.60	1.37	0.0001	0.0849	0.0014	39
Prdm4	72843	0.61	1.08	0.0001	0.0001	0.3931	119
Prmt3	71974	0.73	0.78	0.0022	0.3400	0.0132	20
Prox1	19130	0.56	0.71	0.0000	0.0915	0.0019	35
Prtn3	19152	0.26	0.31	0.0019	0.2944	0.0174	7
Psat1	107272	0.29	0.85	0.0010	0.0265	0.4430	79
Pscd3	19159	1.56	1.58	0.0002	0.9339	0.0244	-3
Pscdbp	227929	3.79	2.23	0.0000	0.0253	0.0318	56
Ptplad1	57874	0.70	0.81	0.0001	0.0260	0.0130	37
Ptpn1	19246	0.49	0.79	0.0001	0.0125	0.1403	58
Pus7l	78895	0.35	0.83	0.0000	0.0000	0.0352	74
Pvr	52118	2.40	2.12	0.0007	0.4515	0.0002	20
Pygo2	n/a	0.61	0.79	0.0000	0.0059	0.0293	45
Qrsl1	76563	0.63	0.70	0.0025	0.1078	0.0323	18
Rab40c	224624	0.73	0.84	0.0056	0.1304	0.0883	40
Rab43	69834	1.77	1.30	0.0001	0.0283	0.1327	61
Rabgef1	56715	1.57	0.97	0.0035	0.0045	0.6693	104
Rad1	19355	0.33	0.86	0.0002	0.0003	0.4313	79
Rars	104458	0.74	1.12	0.0001	0.0038	0.3418	147
Rars2	109093	0.62	0.87	0.0000	0.0003	0.0030	66
Rassf4	213391	0.43	0.64	0.0001	0.0037	0.0128	36
Rbm5	83486	0.46	0.71	0.0000	0.0001	0.0067	46
Rbms1	56878	1.35	1.18	0.0006	0.0526	0.0283	49
Rce1	19671	1.55	1.16	0.0028	0.0367	0.1723	72
Rcl1	59028	1.62	1.40	0.0000	0.0782	0.0100	35
Reep3	28193	1.35	1.48	0.0010	0.2282	0.0010	-37
Rell1	100532	2.92	1.11	0.0001	0.0004	0.5938	94
Rffl	67338	1.44	1.51	0.0009	0.5373	0.0014	-15
Rg9mtd1	52575	0.73	1.20	0.0003	0.0001	0.0294	175
Rgs1	50778	9.29	4.51	0.0001	0.0165	0.0085	58
Rhbdd1	76867	0.70	1.23	0.0033	0.0003	0.0949	177
Rhob	11852	1.65	1.64	0.0007	0.9427	0.0195	2
Rhou	69581	1.46	1.33	0.0006	0.3372	0.0146	29
Ribc1	66611	0.31	0.53	0.0001	0.0001	0.0142	32
Ripk4	72388	2.21	1.76	0.0000	0.0112	0.0024	38
Rnase4	58809	0.72	0.98	0.0000	0.0001	0.5132	91
Rnf113a1	69942	0.54	0.89	0.0003	0.0002	0.3876	76
Rnf135	71956	0.50	0.56	0.0000	0.0677	0.0009	13
Rnf185	193670	0.57	0.85	0.0000	0.0003	0.1032	65
Rogdi	66049	1.44	1.14	0.0011	0.0150	0.2098	68
Rora	19883	1.62	1.25	0.0011	0.0164	0.0928	59
rp9	55934	0.74	0.92	0.0008	0.0003	0.3285	71

Rpain	69723	0.55	1.03	0.0001	0.0003	0.8024	107
Rpp38	n/a	0.52	1.05	0.0010	0.0001	0.7117	111
Rtn3	20168	1.60	1.00	0.0017	0.0020	0.9698	99
Rtp3	235636	0.46	0.86	0.0001	0.0052	0.2295	74
S100a10	20194	1.49	1.00	0.0010	0.0026	0.9713	101
Saa2	20209	0.25	1.30	0.0034	0.0000	0.2739	139
Saa4	20211	0.51	1.11	0.0053	0.0026	0.5097	123
Sdc1	20969	1.75	1.76	0.0004	0.9384	0.0018	-1
Sema4a	20351	0.60	0.61	0.0003	0.8042	0.0033	2
Sephs2	20768	1.48	1.29	0.0011	0.1111	0.0257	41
Sept9	53860	1.80	1.02	0.0083	0.0175	0.8471	97
Sergef	27414	0.62	0.71	0.0007	0.3173	0.0177	23
Serpina10	217847	0.51	0.79	0.0000	0.0000	0.0212	58
Serpina3k	20714	1.56	1.36	0.0028	0.1531	0.0230	35
Serpinh1	12406	2.02	1.20	0.0041	0.0347	0.2826	81
Sesn1	140742	2.17	1.22	0.0005	0.0049	0.0318	81
Setd1a	233904	1.47	1.33	0.0028	0.3574	0.0458	31
Setdb2	239122	3.00	1.78	0.0033	0.0788	0.0113	61
Sf3a3	75062	0.72	0.88	0.0001	0.0029	0.1348	58
Sfrs1	110809	0.66	0.96	0.0000	0.0022	0.6800	89
Sfrs3	20383	0.62	0.99	0.0002	0.0005	0.9612	99
Sfrs4	57317	1.52	1.48	0.0013	0.7423	0.0166	8
Sfrs7	225027	0.39	0.58	0.0000	0.0100	0.0007	30
Sgk2	27219	1.76	1.31	0.0001	0.0601	0.1874	59
Sgms2	74442	2.00	0.60	0.0015	0.0001	0.0522	140
Sgpl1	20397	1.62	1.19	0.0008	0.0138	0.0839	70
Sh3bp5l	79566	0.45	0.67	0.0000	0.0021	0.0016	39
Sh3yl1	24057	0.59	0.57	0.0014	0.7464	0.0067	-4
Siah2	20439	0.62	0.72	0.0019	0.2606	0.0503	27
Sidt2	214597	1.44	1.45	0.0041	0.9524	0.0374	-3
Skap2	54353	0.60	0.94	0.0000	0.0000	0.4750	86
Slc15a4	100561	2.00	1.75	0.0000	0.2414	0.0011	25
Slc20a1	20515	2.09	1.56	0.0058	0.1412	0.0173	48
Slc25a15	18408	1.55	2.26	0.0009	0.0001	0.0000	-128
Slc25a33	70556	1.43	1.30	0.0013	0.2662	0.0047	31
Slc25a42	73095	1.60	1.04	0.0080	0.0442	0.8024	93
Slc25a45	107375	0.68	0.66	0.0017	0.7774	0.0024	-6
Slc30a1	22782	1.57	0.88	0.0000	0.0000	0.3395	122
Slc30a5	69048	0.60	1.21	0.0001	0.0000	0.0879	152
Slc37a1	224674	0.15	0.86	0.0002	0.0001	0.4805	84
Slc41a2	338365	0.35	1.82	0.0004	0.0003	0.0503	225
Slc6a6	21366	1.45	1.07	0.0012	0.0010	0.5951	85
Slc6a9	14664	0.60	0.88	0.0019	0.0388	0.1274	70
Slc9a1	20544	0.63	0.60	0.0017	0.6373	0.0053	-7
Slco2a1	24059	1.50	1.16	0.0069	0.0516	0.2262	67
Smarcad1	13990	0.60	0.94	0.0002	0.0024	0.3329	85
Smarcc2	68094	1.65	1.09	0.0030	0.0263	0.6210	86
Smarcd2	83796	0.70	0.57	0.0012	0.0127	0.0014	-43
Smek2	104570	0.64	0.87	0.0006	0.0003	0.2223	64
Snip1	76793	0.55	1.02	0.0000	0.0001	0.8433	104
Snupn	66069	0.64	0.64	0.0019	0.9827	0.0050	0
Snx10	71982	0.43	1.43	0.0002	0.0000	0.0250	176
Snx11	74479	0.52	0.81	0.0002	0.0013	0.0687	61

Snx18	170625	1.47	1.11	0.0001	0.0019	0.2028	78
Snx24	69226	1.43	1.12	0.0000	0.0006	0.0207	72
Soat2	223920	0.57	0.82	0.0003	0.0077	0.1422	59
Spnb3	20743	1.41	0.97	0.0005	0.0024	0.7884	108
Sppl3	74585	0.72	0.74	0.0026	0.6448	0.0188	8
Spsb1	74646	2.16	1.98	0.0013	0.7541	0.1405	16
Srfbp1	67222	0.30	0.74	0.0001	0.0001	0.0847	63
Stat1	20846	0.59	0.84	0.0000	0.0019	0.0612	61
Stat2	20847	0.51	1.14	0.0000	0.0000	0.1704	128
Stat3	20848	0.52	1.01	0.0000	0.0000	0.9316	102
Stip1	20867	1.46	1.38	0.0025	0.5266	0.0122	18
Stk11	20869	1.36	1.14	0.0037	0.0524	0.1824	60
Stk24	n/a	1.40	1.06	0.0001	0.0008	0.3371	85
Stk38l	232533	0.58	0.62	0.0001	0.5889	0.0023	10
Stx18	71116	0.66	1.12	0.0006	0.0226	0.5811	135
Stx5a	56389	0.62	0.87	0.0000	0.0006	0.1051	65
Syvn1	74126	0.72	1.01	0.0002	0.0148	0.9573	102
Tapt1	231225	0.64	0.86	0.0000	0.0005	0.0899	62
Tatdn2	381801	1.66	1.69	0.0016	0.8397	0.0059	-5
Tbc1d13	70296	1.50	0.89	0.0056	0.0017	0.5081	123
Tbp	21374	0.56	0.98	0.0000	0.0000	0.7221	96
Tbx3	21386	0.37	0.59	0.0001	0.0067	0.0153	35
Tfb1m	224481	0.61	0.56	0.0024	0.4657	0.0072	-12
Tfrc	22042	1.96	2.98	0.0004	0.0348	0.0024	-106
Tgm1	21816	0.51	0.90	0.0002	0.0029	0.4478	79
Tha1	71776	0.45	0.61	0.0001	0.0012	0.0083	29
Tlcd1	68385	0.65	0.62	0.0002	0.6664	0.0018	-9
Tmem185b	226351	0.54	0.66	0.0001	0.0277	0.0052	26
Tmem186	66690	0.33	0.68	0.0000	0.0004	0.0141	52
Tmem199	195040	0.54	0.68	0.0001	0.0341	0.0187	31
Tmem39a	67846	0.55	1.16	0.0034	0.0014	0.4897	135
Tmprss2	50528	2.03	1.86	0.0009	0.5180	0.0025	16
Tmprss6	n/a	1.49	1.22	0.0013	0.0110	0.1192	55
Tnfrsf12a	27279	1.89	2.00	0.0071	0.7570	0.0099	-13
Tob1	22057	2.13	1.19	0.0117	0.0696	0.4825	83
Tpm4	326618	1.53	1.34	0.0043	0.4674	0.2051	36
Trak1	67095	1.37	1.40	0.0035	0.8453	0.0323	-9
Trfp	56771	0.41	0.65	0.0000	0.0017	0.0197	41
Trim39	79263	0.57	1.19	0.0000	0.0002	0.2421	143
Trim56	384309	0.58	0.80	0.0003	0.0271	0.0302	52
Trp53bp2	209456	1.95	1.72	0.0001	0.2248	0.0002	25
Trp53inp1	60599	3.43	2.71	0.0002	0.1753	0.0002	30
Tut1	70044	0.46	0.81	0.0000	0.0000	0.0253	64
Ube2m	22192	1.49	1.54	0.0036	0.7838	0.0093	-9
Ugt2b34	100727	1.42	1.23	0.0063	0.2413	0.0739	45
Upf2	326622	0.58	0.81	0.0001	0.0003	0.0910	54
Uvrag	78610	1.86	1.27	0.0000	0.0009	0.1611	68
Vmo1	327956	0.65	0.74	0.0008	0.4172	0.0165	24
Vps37b	330192	1.77	1.11	0.0010	0.0064	0.1440	85
Vrk3	101568	0.62	0.75	0.0001	0.0036	0.0167	33
Wdr20a	69641	0.63	0.98	0.0005	0.0033	0.8368	95
Whsc2	24116	0.56	0.80	0.0001	0.0090	0.0995	55
Wwc2	52357	0.67	0.83	0.0003	0.0376	0.0103	48

X99384	27355	1.51	1.10	0.0000	0.0013	0.2257	79
Xbp1	22433	0.43	0.75	0.0000	0.0003	0.0455	57
Ythdf1	228994	0.72	1.02	0.0007	0.0004	0.8258	107
Zbtb24	268294	0.63	0.77	0.0014	0.1877	0.0164	36
Zc3h7a	106205	0.70	1.24	0.0002	0.0000	0.0431	181
Zfp207	22680	0.65	1.04	0.0000	0.0026	0.7115	112
Zfp263	74120	0.74	0.91	0.0001	0.0019	0.1746	66
Zfp282	101095	0.50	0.73	0.0004	0.0166	0.0250	45
Zfp36	22695	2.24	1.87	0.0009	0.2900	0.0105	30
Zfp46	22704	0.46	0.75	0.0001	0.0009	0.0507	53
Zfp574	232976	0.67	0.71	0.0028	0.4405	0.0219	12
Zfp597	71063	0.55	0.94	0.0001	0.0012	0.5281	86
Zfp60	22718	0.24	0.85	0.0000	0.0000	0.2449	80
Zfp672	319475	0.52	0.72	0.0003	0.0027	0.0378	42
Zfp825	235956	0.58	0.85	0.0000	0.0032	0.1331	65
Zfp94	22756	0.18	0.44	0.0000	0.0308	0.0066	32
Zfx	22764	0.65	0.94	0.0001	0.0005	0.2258	82
Zhx3	320799	1.53	1.20	0.0001	0.0246	0.0796	63
Zranb1	360216	1.43	1.51	0.0001	0.5130	0.0058	-19
Zswim4	212168	1.96	1.77	0.0001	0.2252	0.0002	21

Table 3: Panther Biological Process Analysis

Biological Process	number	±	P value
DMSO vs. IDFP			
Cell adhesion	175	+	0.00003
Biological process unclassified	2524	-	0.00005
Cell structure and motility	389	+	0.00181
Homeostasis	80	+	0.00315
Lipid, fatty acid and steroid metabolism	401	+	0.00354
Extracellular matrix protein-mediated signaling	30	+	0.00551
Sulfur metabolism	42	+	0.01200
Cell communication	318	+	0.01750
Fatty acid metabolism	109	+	0.04710
Growth factor homeostasis	7	+	0.04810
IDFP vs. IDFP/Am251			
rRNA metabolism	45	+	0.00281
Lipid, fatty acid and steriod metabolism	401	+	0.00471

Table 4: FuncAssocaite 2.0 Analysis of Genes Decreased by IDFP in a CB1 Dependent Manner

Attribute name	Attribute ID	N	X	LOD	P_adj
acute-phase response	GO:0006953	5	28	1.37	0.008
aminoacyl-tRNA ligase activity	GO:0004812	8	45	1.37	<0.001
ligase activity, forming carbon-oxygen bonds	GO:0016875	8	45	1.37	<0.001
ligase activity, forming aminoacyl-tRNA and related compounds	GO:0016876	8	45	1.37	<0.001
tRNA aminoacylation for protein translation	GO:0006418	7	42	1.33	<0.001
amino acid activation	GO:0043038	7	42	1.33	<0.001
tRNA aminoacylation	GO:0043039	7	42	1.33	<0.001
acute inflammatory response	GO:0002526	6	40	1.28	0.001
tRNA metabolic process	GO:0006399	11	107	1.09	<0.001
ncRNA metabolic process	GO:0034660	11	180	0.85	0.001
translation	GO:0006412	12	252	0.73	0.008
RNA metabolic process	GO:0016070	20	544	0.62	0

Table 5: Altered CB1 Dependent Genes Represented within the Enriched Pathways

	Fold Change		Nominal P-Value			Reversal (%)
	IDFP	AM251	DMSO vs IDFP	IDFP vs. AM251	AM251 vs. DMSO	
Acute Phase Response						
orm1	0.70	1.43	0.008	0.000	0.002	246
orm2	0.41	1.79	0.002	0.000	0.054	233
saa2	0.25	1.30	0.003	0.000	0.274	139
saa4	0.51	1.11	0.005	0.003	0.510	123
stat3	0.52	1.01	0.000	0.000	0.932	102
Amino Acid metabolism & Translation						
rars	0.74	1.12	0.000	0.004	0.342	147
lars	0.63	1.11	0.000	0.001	0.437	129
aars	0.65	1.00	0.001	0.000	0.996	100
iars	0.65	0.97	0.000	0.000	0.739	93
farsb	0.74	0.96	0.000	0.003	0.596	84
rars2	0.62	0.87	0.000	0.000	0.003	66
gars	0.65	0.85	0.000	0.019	0.067	58
ncoa5	0.57	0.81	0.000	0.000	0.040	55
eef1e1	0.57	1.14	0.000	0.000	0.065	133
eif2b4	0.73	0.95	0.001	0.001	0.584	82
psat1	0.29	0.85	0.001	0.026	0.443	79
pelo	0.64	0.91	0.000	0.002	0.358	75
asns	0.15	0.68	0.000	0.008	0.165	62
eif2ak2	0.51	0.80	0.000	0.002	0.073	59
Lipid, Fatty acid, and Steroid Metabolism						
sgms2	2.00	0.60	0.001	0.000	0.052	140
pgc1β	6.78	2.16	0.000	0.001	0.051	80
pla2g6	1.68	1.30	0.000	0.041	0.029	55
mtmr3	2.08	1.42	0.000	0.004	0.093	61
lpin2	3.22	1.70	0.000	0.007	0.129	69
insig1	1.90	1.08	0.002	0.006	0.609	91
chkb	1.81	1.26	0.000	0.015	0.085	67
apol9b	1.66	1.02	0.001	0.003	0.936	97
acsl1	1.79	1.05	0.001	0.002	0.758	93
ldlr	4.50	1.30	0.000	0.000	0.448	92

Table 6: Expression of Genes involved in Stat3 signaling and Lipid Metabolism in WT and CB1 -/- Mice [a]

Gene	WT DMSO	WT IDFP	CB1 -/- DMSO	CB1 -/- IDFP
Stat3 Signaling				
stat3	1.00 ± 0.15	0.43 ± 0.02	0.96 ± 0.29	0.84 ± 0.14
lbp	1.00 ± 0.12	0.78 ± 0.13	1.00 ± 0.28	1.11 ± 0.13
apcs	1.00 ± 0.19	0.61 ± 0.16	0.69 ± 0.27	0.64 ± 0.11
Lipid Metabolism				
acsl1	1.00 ± 0.09^{ab}	1.61 ± 0.34^{a}	1.04 ± 0.16^{ab}	0.73 ± 0.10^{b}
insig1	1.00 ± 0.16^{a}	2.35 ± 0.41^{b}	0.81 ± 0.19^{a}	0.81 ± 0.16^{a}
pgc1b	1.00 ± 0.14^{a}	4.28 ± 0.25^{b}	1.28 ± 0.29^{a}	2.34 ± 0.37^{c}
ldlr	1.00 ± 0.23^{a}	1.50 ± 0.32^{b}	1.05 ± 0.49^{a}	0.81 ± 0.18^{a}
lpin2	1.00 ± 0.27	1.72 ± 0.25	1.03 ± 0.10	1.64 ± 0.24
hmgcr	1.00 ± 0.04	2.17 ± 0.56	1.09 ± .026	1.21 ± 0.45

[a]Groups not sharing a common superscript letter are significantly different ($p<0.05$).

Figure 1

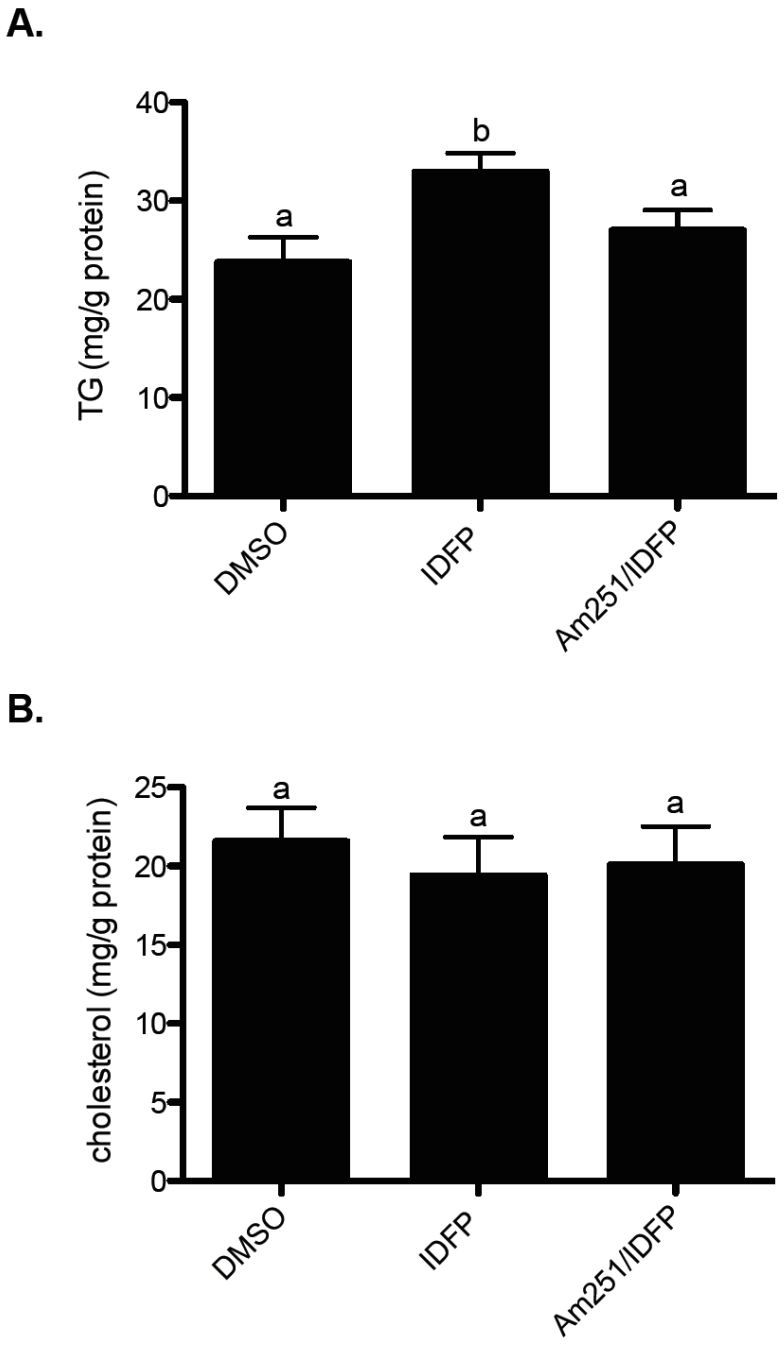

Figure 1: CB1-dependent effects of IDFP on hepatic TG (A) and cholesterol (B) levels. Mice were treated with DMSO or IDFP (10 mg/kg, ip, 4 h) alone or 15 min following AM251 (10 mg/kg, ip). n=13-15.

Figure 2

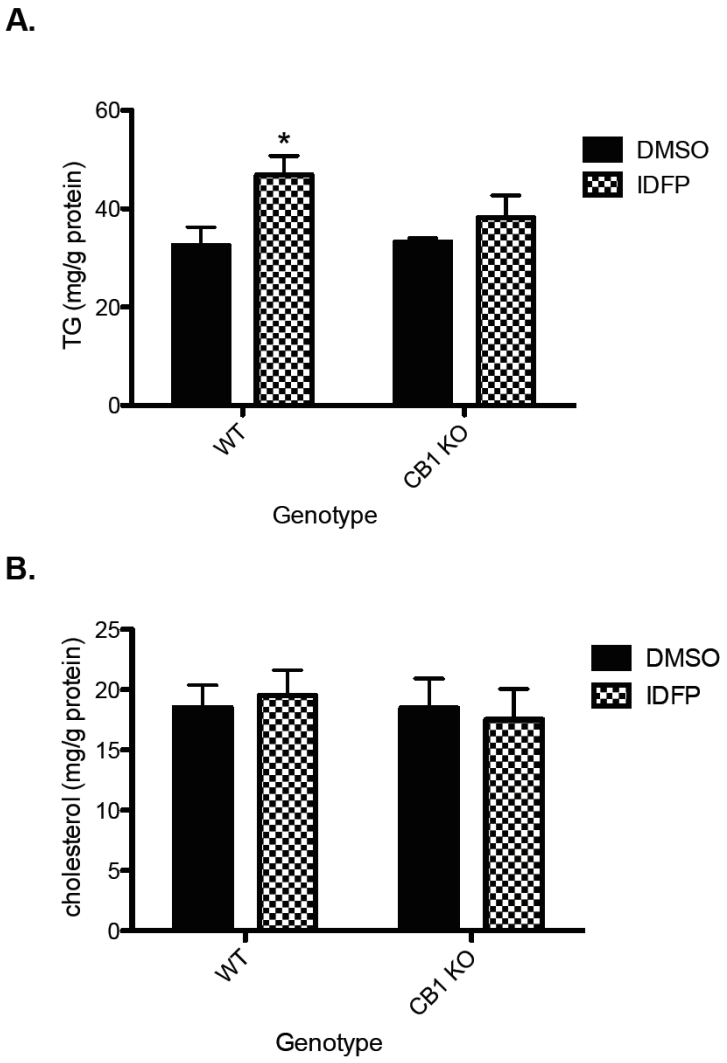

Figure 2: CB1-dependent effects of IDFP on hepatic TG (A) and cholesterol (B) levels. Wild-type and CB1 -/- mice were treated with DMSO or IDFP (10 mg/kg, ip, 4 h) alone or 15 min following AM251 (10 mg/kg, ip). n=5-6.

Figure 3.

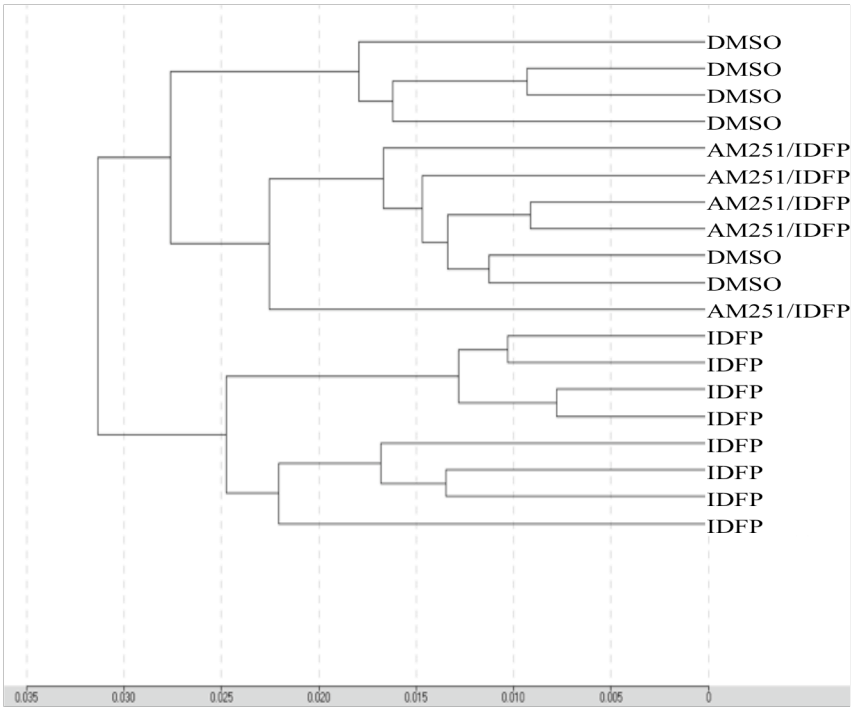

Figure 3: Hierarchical clustering of the transcriptome of individual mice.
Dendrogram representation of cluster analysis from BeadStudio software 3.2 (Illumina).

Figure 4

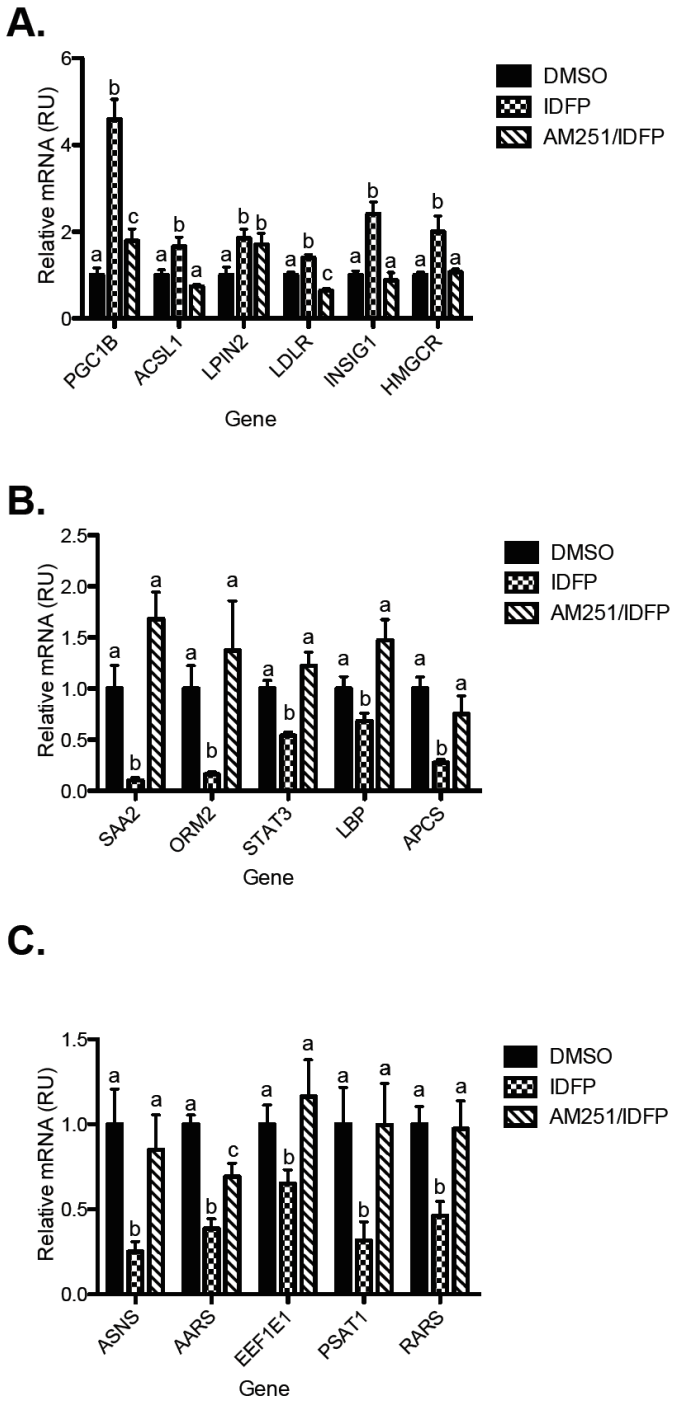

Figure 4: CB1-dependent effects of IDFP on hepatic expression of lipid metabolism (A), inflammatory (B), and amino acid metabolism genes (C). RNA was isolated from the mice used for the experiment in Fig. 1. n=17-18.

CHAPTER 5
Conclusions & Future Directions

PPAR α is a transactional nodal point in the regulation of lipid metabolism activated by endogenous lipids and hypolipidemic agents. While fibrates are weak PPAR α ligands, pharmaceutical companies are pursuing stronger PPAR α ligands to maximize hypolipidemic potential. However, the utility of these stronger ligands has been hampered by side effects. Understanding the endogenous ligation of PPAR α may be key to achieving optimal results by pharmacological intervention. My work supports the role of lipoprotein-derived fatty acids as PPAR α ligands. Taken together with the work of Daniel Kelly's laboratory, my data strongly suggests that the route of fatty acid uptake influences its ability to stimulate PPAR α. To determine if CD36 represents the saturable process of fatty acid uptake that fails to stimulate PPAR α, it would be interesting to determine the relationship between fatty acid uptake and PPAR α activation in the setting of altered CD36 expression. Together the data suggest that an "overflow" pathway of fatty acid uptake becomes active in the lipolytic microenvironment and is responsible for the delivery of PPAR α ligands. The existence and nature of this pathway warrants further study.

My work with IDFP successfully demonstrated direct regulation of lipid metabolism by endocannabioids through CB1. IDFP induced apoE-dependent hypertriglyceridemia associated with apoE depleted VLDL and enriched HDL. This suggests that apoE distribution regulates triglyceride-rich lipoprotein metabolism. Indeed, work in the 1980s generated a wealth of information about apoE distribution, including the observation that patients with hypertriglyceridemia had a greater proportion of apoE free VLDL. While recent tracer studies have confirmed that the presence of apoE directs traffic of TG-rich lipoproteins and remnants towards whole particle uptake, little is known about the signals regulating apoE distribution. My work shows that CB1 stimulation alters apoE distribution by inhibiting the transfer of apoE from HDL to TG-rich lipoproteins in mice. These effects should be confirmed in settings of CB1 activation in humans. Additionally, the ability of rimonabant to influence the allocation of apoE among lipoproteins would be of great interest. More broadly, the prevalence of aberrant apoE distribution as a cause of hypertriglyceridemia requires further study. If the mechanisms regulating allocation of apoE can be understood, it may be possible to pharmacologically shift apoE to TG-rich lipoproteins and decrease their plasma levels. The necessity of apoE for chylomicron clearance combined with the newly recognized prognostic value of post-prandial triglyceride measurements underscore the potential therapeutic value of manipulating apoE levels and distribution.

IDFP administration generated hypertriglyceridemia and hepatic steatosis in fasted animals. A key unanswered question is the location of the CB1 responsible for IFDP observed effects. The use of tissue specific knockout models will be necessary to address this issue. This is of particular interest as the adverse psychological effects associated with rimonabant, and other centrally active CB1 antagonists, prevent their clinical use. However, disassociation of feeding behavior and alterations in peripheral metabolism, such as those demonstrated here and by the work of George Kunos, suggest that blockade of peripheral CB1 may be effective in treating metabolic disease while limiting adverse side effects. Thus, the discovery of peripherally restricted CB1 antagonists is a necessary next step, though one likely to be completed outside of academia.

The contrasting origins of fibrates and rimonabant illustrate the current state of affairs in pharmacometabolic research. The first fibrate was discovered after screening over 400 branched chain fatty acid analogous for hypolipidemic effects in rats, almost four decades before the discovery of PPAR α. Conversely, rimonabant emerged only after CB1 had been cloned and molecularly characterized. However, no amount of molecular detail could have predicted the outcome of the clinical trials, since assessing the mental health of cultured cells and rodents remains a difficult task. It is the fibrates, discovered by a simple chemical screen, rather than rimonabant, which was targeted to a specific receptor, that are still used today. This is not an isolated example as many of the current treatments for metabolic disease predate knowledge of their molecular mechanism. While no one doubts the power of molecular biology, its ability to deliver better treatments for metabolic disease may require better understanding of how individual pathways are integrated in the control of whole body physiology. Hopefully, the work presented here serves as a tiny step in the effort to bring mechanistic insight, and the promise that it carries, from the bench to the bedside.